

Comparative analysis of a two-dimensional and three-dimensional model of BT-20 triple negative breast carcinoma cells in response to an antiproliferative agent

by

Jie Wang

A dissertation submitted in fulfilment of the requirements for the degree

Master of Science

in

Pharmacology

in

Faculty of Health Sciences

at

University of Pretoria

Supervisor: Dr Werner Cordier¹

Co-supervisor: Prof Duncan Cromarty¹; Dr Iman van den Bout^{2,3}

1. Department of Pharmacology, School of Medicine, Faculty of Health Sciences, University of Pretoria
2. Department of Physiology, School of Medicine, Faculty of Health Sciences, University of Pretoria
3. Centre for Neuroendocrinology, School of Medicine, Faculty of Health Sciences, University of Pretoria

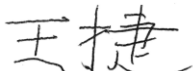
Declaration

I: **Jie Wang**

Student number: **15336213**

Thesis title: **Comparative analysis of a two-dimensional and three-dimensional model of BT-20 triple negative breast carcinoma cells in response to an antiproliferative agent**

1. Understand what plagiarism entail and am of the University's policy in this regard.
2. I declare that this dissertation is of my own original work. Where someone else's work was used (whether from a printed source, the internet or any other source), this has been properly acknowledged and referenced in accordance with departmental requirements.
3. I did not use another student's previous work and submitted it as my own.
4. I did not allow and will not allow anyone to copy my work with the intention of presenting it as his or her own work

Signature: 

Date: 29 November 2018

Turnitin report

208/2019

Turnitin

Document Viewer

Turnitin Originality Report

Processed on: 26-Feb-2019 15:28 SAST
 ID: 671205667
 Word Count: 23805
 Submitted: 2

Jie By W (Werner) Cordier

Similarity Index

21%

Similarity by Source

Internet Sources:	18%
Publications:	15%
Student Papers:	N/A

[Include quoted](#) [Include bibliography](#) [excluding matches < 10 words](#) [download](#) [print](#)
 mode: quickview (classic) report

1% match (Internet from 08-Feb-2019)	https://repository.up.ac.za/handle/2263/63048/Lepide_Assessment_2017.pdf?isAllowed=y&sequence=1
1% match (Internet from 07-Feb-2019)	https://repository.up.ac.za/handle/2263/56955/Cordier_Vitro_2016.pdf?isAllowed=y&sequence=1
1% match (Internet from 22-Jun-2016)	http://www.intechopen.com
1% match (Internet from 08-Feb-2019)	https://repository.up.ac.za/handle/2263/63830/Cordier_Bulb_2018.pdf?isAllowed=y&sequence=1
1% match (Internet from 03-Sep-2016)	https://en.wikipedia.org/wiki/Breast_carcinoma
<1% match (Internet from 08-Feb-2019)	https://repository.up.ac.za/handle/2263/67044/Naude_Dynamic_2018.pdf?isAllowed=y&sequence=1
<1% match (Internet from 06-Sep-2010)	http://jnl.oxfordjournals.org
<1% match (Internet from 04-Dec-2010)	http://home.histec.or.th
<1% match (Internet from 26-Nov-2012)	http://www.ncbi.nlm.nih.gov
<1% match (Internet from 08-Feb-2010)	http://king@sb.coastal.edu
<1% match (publications)	Hui Yao, Guoqun He, Shichao Yao, Chan Chen, Jijiang Song, Thomas J. Rosol, Xiyun Deng, "Tijole-negative breast cancer: is there a treatment on the horizon?", Oncotarget, 2016
<1% match (Internet from 17-Feb-2018)	http://www.cansa.org.za
<1% match (Internet from 23-Sep-2018)	http://www.stem-art.com
<1% match (Internet from 24-Jun-2010)	http://www.jci.org
<1% match (Internet from 29-May-2018)	https://www.dovepress.com/getfile.php?fileID=42156
<1% match (Internet from 08-Feb-2019)	

https://api.turnitin.com/hwreport_classic.asp?lang=en_us&id=671205667&n=1&bypass_cv=1

1/34

Dedication

To my mom and girlfriend, Jing Wang and Lingling Ye, for the support and confidence that you transmitted to me throughout my study abroad and for helping me overcome loneliness.

Acknowledgements

“Stay Hungry, Stay Foolish”

Steve Jobs

I would like to give my sincere gratitude to the following people and organizations:

To my supervisor, Dr Werner Cordier:

Thank you for the continuous support, advice and for building up my lab skills from zero. Without your help, I could not finish my research abroad. I hope to work with you again in the future.

To my co-supervisor, Prof Duncan Cromarty:

Thank you for teaching me all academic knowledge and training me in the lab. Without your continued support and patience, I could not finish my four-year study in South Africa.

To my co-supervisor, Dr Iman van den Bout:

Thank you for the guidance, training, patience and assistance in this project. I really appreciate your precise attitude in the research.

To Prof Vanessa Steenkamp:

Thank you for your constant motivation, training and advice and for leading me into the scientific world.

To my uncle, cousin and sister in law:

Thank you for your unconditional love, care and support. Without your help, I wouldn't have the opportunity to study in South Africa. There is no bond stronger than family.

To my friends, Kea and Hafiza:

Thank you for encouraging me to move on when I fell into loneliness and helplessness. I am missing the work with you in the lab during the weekend.

To Department of Pharmacology at University of Pretoria:

Thanks to all the staffs in our department for your constant motivation and support. You made me feel at home and helped me overcome my fears.

Abstract

Triple-negative breast cancer (TNBC) lacks the expression of estrogen receptor- α , progesterone receptor and human epidermal growth factor receptor 2 (HER2). The lack of dependence on estrogen by TNBC cells makes anti-estrogen chemotherapy ineffective. Compounding this, within solid tumors, differential blood supply creates an oxygen and nutrient gradient, providing cells close to the vasculature with a more hospitable environment, while those in the core are deprived. In the search for treatments that may display efficacy against such tumours, it is necessary to make use of *in vitro* systems that accurately depict the clinical setting. Traditional two-dimensional (2D) culturing fails to replicate this environment, however, they are commonly used when assessing biological activity of new chemical entities. Three-dimensional (3D) cultures, in the form of spheroids, should enact a similar gradient which includes the proliferative outer layer, a quiescent inner zone and a necrotic center. The aim of the study is to compare the growth characteristics of BT-20 triple-negative breast carcinoma cells in a traditional 2D culture to a 3D model established by the Department of Physiology, University of Pretoria.

BT-20 spheroids (40 000 cells/well) were grown using traditional culturing and the liquid overlay method for monolayer (2D) and spheroid (3D) cultures, respectively. Spheroid volume was assessed using light microscopy, while viability was visualized by live-dead staining. Metabolic capacity was determined using the resazurin cleavage assay. Protein content was determined using the bicinchoninic acid assay. Cytotoxicity of doxorubicin was determined in monolayers by sulforhodamine B staining after 72 h. Monolayer cultures and spheroids (day 4) were exposed to the IC_{25} , IC_{50} and IC_{75} of doxorubicin for 72 h, after which protein content and acid phosphatase (APH) activity were determined using spectrophotometry, cellular kinetics by flow cytometry, and p53 expression detected by Western blot analysis.

BT-20 spheroids displayed structural integrity and viability over the growth period, with decreasing size and increasing numbers of membrane compromised cells (suggestive of necrosis) at Day 4. No necrosis was observed at Days 7 or 10. Due to spheroids compaction and lack of resorufin formation, metabolic activity could not be assessed accurately, highlighting the density of the spheroid as a potential contributor to reduced drug susceptibility. Neither spheroid protein content nor APH activity changed throughout the culturing period, while the monolayer cultures presented with higher values. Doxorubicin displayed an IC_{25} , IC_{50} and IC_{75} of 1.4 μ M, 3.6 μ M and 11.75 μ M respectively in monolayer cultures. Spheroid size, protein content and APH activity was affected only at the IC_{75} , accompanied by an increase in the percentage of sub-G1-phase cells linked to a

reduction in G1-phase cells. Lower doxorubicin concentrations resulted in increased spheroid size, protein content and APH activity. Expression of p53 was non-significantly increased after exposure to the IC₂₅ of doxorubicin in both models, however, expression was lower in spheroids than in monolayers. Non-significant alterations to cell cycle kinetics was evident, with decreased G0/G1-phase cells, increased G2/M-phase cells and increased p53 expression, which suggest that a late cell cycle blockade was induced. In addition, the non-significant lower expression of p53 in treated spheroids suggests that the 3D-conformation exhibited reduced chemosensitivity to doxorubicin.

Cultured 3D spheroids presented with higher resistance to doxorubicin compared to monolayer cultures. Given the nature of *in vivo* tumours, a 3D model as platform for drug screening may present as a more representative model during drug development studies.

Study outputs

Conference proceedings

Poster presentations

- Wang J, Cromarty AD, van den Bout I, Cordier W. Comparative analysis of a two-dimensional and three-dimensional model of BT-20 triple negative breast carcinoma cells in response to an antiproliferative agent. Health Sciences Faculty Day, University of Pretoria, South Africa, 22 Aug 2017.
- Wang J, Cromarty AD, van den Bout I, Cordier W. Comparative analysis of a two-dimensional and three-dimensional model of BT-20 triple negative breast carcinoma cells in response to an antiproliferative agent. 18th World Congress of Basic and Clinical Pharmacology, Kyoto, Japan 1-6 Jul 2018.

Table of Contents

Declaration	i
Turnitin report	ii
Dedication	iii
Acknowledgements	iv
Abstract	vi
Study outputs	viii
List of Figures	xiii
List of Tables	xvi
List of Abbreviations	xvii
Chapter 1: Introduction	1
1.1. Cancer	1
1.1.1. Introduction.....	1
1.1.2. Hallmarks of cancer	2
1.1.2.1. Sustained proliferative signalling.....	3
1.1.2.2. Evading growth suppressors.....	3
1.1.2.3. Resisting cell death.....	3
1.1.2.4. Enable replicative immortality.....	4
1.1.2.5. Inducing angiogenesis.....	4
1.1.2.6. Activating invasion and metastasis.....	5
1.1.2.7. Inflammatory microenvironment.....	5
1.2. The cell cycle	5
1.2.1. Introduction.....	5

1.2.2. Cell cycle regulatory component	7
1.3. Breast cancer	8
1.3.1. Introduction.....	8
1.3.2. Diagnosis.....	9
1.3.2.1. Histopathological examination.....	9
1.3.2.2. Grading breast cancer cells	9
1.3.2.3. Staging breast cancer	9
1.3.2.4. Receptor status	9
1.3.3. Management.....	11
1.3.3.1. Hormone blocking therapy	11
1.3.3.2. Chemotherapy	11
1.3.3.3. Monoclonal antibodies.....	12
1.4. Triple-negative breast cancer.....	12
1.4.1. Introduction.....	12
1.4.2. Treatment modalities.....	12
1.4.3. Doxorubicin	15
1.5. The solid tumour microenvironment.....	18
1.5.1. Disadvantages of traditional drug screening platforms	18
1.5.2. Multicellular tumour spheroids.....	19
1.6. Aim.....	21
1.7. Objectives	21
Chapter 2: Materials and methods	22
2.1. Culture protocol of the BT-20 cell line	22
2.2. Seeding of cells as monolayer and spheroid culture	22

2.3. Microscopic evaluation of spheroid size and volume	23
2.4. Fluorometric determination of metabolic capacity of monolayer and spheroids cultures	23
2.5. Spectrophotometric determination of protein content of monolayer and spheroids cultures	24
2.6. Determination of viability status of cells in monolayer and spheroids cultures.....	24
2.7. Flow cytometric determination of cell cycle of monolayer and spheroid cultures.....	25
2.8. Analysis the cytotoxic effect of doxorubicin on BT-20 cells in monolayer and spheroid cultures.....	25
2.8.1. Measurement monolayer culture cellular density.....	25
2.8.2. Exposure of monolayer and spheroid cultures to doxorubicin	26
2.8.3. Alteration to acid phosphatase activity of exposed monolayer and spheroid cultures.....	26
2.8.4. p53 expression of exposed monolayer cultures and spheroids	27
2.9. Statistics.....	28
Chapter 3: Results	29
3.1. Growth characteristics of BT-20 spheroids	29
3.1.1. Spheroid structure, size and volume	29
3.1.2. Metabolic capacity of spheroids	30
3.1.3. Viability staining of spheroids.....	31
3.1.4. Protein content and acid phosphatase activity of spheroids.....	32
3.1.5. Cellular kinetics of spheroids	34

3.2. Comparison of the effect of doxorubicin in the monolayer and spheroid culture models.....	35
3.2.1. Doxorubicin reduced monolayer cell density	35
3.2.2. Doxorubicin incurs cytotoxic morphological changes in monolayers at low concentrations, but requires higher concentrations in spheroids	35
3.2.3. Doxorubicin visibly decreases cell viability in spheroids, however, does permeate the spheroid.....	37
3.2.4. Doxorubicin reduces protein content at higher concentrations	38
3.2.5. Doxorubicin decreases acid phosphatase activity at higher concentrations	38
3.2.6. Doxorubicin blocks cells in the G2/M-phase in spheroid cultures, with associated DNA damage, due to p53-mediated activity	39
Chapter 4: Discussion.....	43
Chapter 5: Conclusion	50
5.1. Summarisation	50
5.2. Limitations and recommendations of the study	51
References.....	53
Appendix I: Ethical approvals	66
Appendix II: Reagent preparation.....	68

List of Figures

Figure 1. The original six hallmarks of cancer, highlighting molecular differences from healthy cells that contribute to cancer formation.(9).....	3
Figure 2. A graphical representation of cellular cycling.(27)	6
Figure 3. Cell cycle regulatory components determined to be altered in human cancers.(34)	7
Figure 4. Potential agents for treatment of triple negative breast cancer.(87).....	13
Figure 5. Chemical structure of doxorubicin.....	16
Figure 6. A graphical representation of candidate genes involved the pharmacodynamics of doxorubicin in cancer cells.(109)	17
Figure 7. The relation between the tumour microenvironment and blood vessels. (A) Diagrammatic representation of tumour cells and the extracellular matrix (ECM) surrounding a capillary. (B) Schematic representation of the gradient of oxygen concentration (pO_2 : dashed line) and of pH (dotted line) in relation to the nearest tumour blood vessel.(83)	18
Figure 8. Cellular growth in the two-dimensional model.	19
Figure 9. The structure and microenviroment of multicellular tumour spheroid.	20
Figure 10. The formation of multicellular spheroids.....	20
Figure 11. Resazurin is converted by metabolically active cells to the fluorescent product, resorufin.(134)	23
Figure 12. Representation of the cytosolic APH catalysed reaction.(89).....	27
Figure 13. Representative images about morphology of cells grown as a monolayer culture and spheroids (5X objective). A) Monolayer culture 24 h post-seeding; spheroids at B) four, C) seven and D) ten days post-seeding.....	29
Figure 14. Volume of spheroids over the 10-day culturing period.	30
Figure 15. Metabolic capacity of monolayer culture and spheroids measured as	

relative fluorescence intensity of 4-day, 7-day and 10-day spheroids.30

Figure 16. A representative image of spheroid exposed to resazurin indicating localisation and lack of release of resorufin (5X objective).....31

Figure 17. Representative images about viability of cells grown as a monolayer culture and spheroids using fluorescein diacetate-propidium iodide live-dead staining (5X objective). A) Monolayer culture 24 h post-seeding; spheroids at B) 4-, C) 7- and D) 10-days post-seeding.....32

Figure 18. Protein content of cells grown in monolayer culture and spheroid model.....33

Figure 19. Acid phosphatase activity of cells grown as a monolayer culture and spheroids.....33

Figure 20. Cellular kinetics of cells grown as a monolayer culture and spheroids. Significance is based on comparisons between G₀/G₁ phase and the rest of phases in each group34

Figure 21. The effect of doxorubicin on cell density of cells grown in a monolayer culture after 72 h. A) Controls used during the assay, and B) dose-response curve of doxorubicin over a range of concentrations; Significant difference relative to the cell density of the negative control.....35

Figure 22. Representative images about morphology of monolayer cells treated by doxorubicin for 72 h and negative control (5X objective). A) Negative control; spheroids treated at B) IC₂₅, C) IC₅₀ and D) IC₇₅ concentration36

Figure 23. Representative images about morphology of spheroids treated by doxorubicin for 72 h and negative control (5X objective). A) Negative control; spheroids treated at B) IC₂₅, C) IC₅₀ and D) IC₇₅ concentration36

Figure 24. Volume of spheroids treated with doxorubicin after 72 h37

Figure 25. Representative images of spheroids exposed to doxorubicin at IC₂₅ for 72 h (5X objective). A) Spheroid stained by FDA-PI; B) unstained spheroid displaying doxorubicin fluorescence.....37

Figure 26. Protein content of cells cultured as a monolayer and spheroids after exposure to doxorubicin for 72 h.....38

Figure 27. Acid phosphatase activity of monolayer culture and after 72 h exposure39

Figure 28. Cell cycle phase of cells treated by doxorubicin at IC₂₅, IC₅₀ and IC₇₅ in

monolayer culture. A) Sub-G1 phase; B) G0/G1-, S- and G2/M-phase.....40

Figure 29. Cell cycle phase of cells treated by doxorubicin at IC₂₅, IC₅₀ and IC₇₅ in spheroids. A) Sub-G1 phase; B) G0/G1-, S- and G2/M-phase41

Figure 30. A representative image about expression of p53 in monolayer and spheroid cultures as measured by western blot.....42

Figure 31. Expression of p53 in monolayer and spheroid cultures after exposure to doxorubicin for 72 h as measured by quantitation42

List of Tables

Table 1. The top ten most common cancers in males in South Africa in 2014	2
Table 2. The top ten most common cancers in females in South Africa in 2014....	2
Table 3. The therapeutic options of triple-negative breast cancer	13
Table 4. Percentage of cells in each phase of the cell cycle in the monolayer culture and spheroids.....	34
Table 5. Protein content of cells after exposure to doxorubicin at IC ₂₅ , IC ₅₀ and IC ₇₅ in the monolayer culture and spheroids.....	38
Table 6. Acid phosphatase activity of cells after exposure to doxorubicin at IC ₂₅ , IC ₅₀ and IC ₇₅ in the monolayer culture and spheroids	39
Table 7. Percentage of cells in the sub-G1 phase after exposure to doxorubicin for 72h.....	40
Table 8. Percentage of cells in the G ₀ /G ₁ -, S- and G ₂ /M-phases after exposure to doxorubicin for 72 h	41
Table 9. Percentage of cells in the sub-G1 phase after exposure to doxorubicin for 72 h.....	41
Table 10. Percentage of cells in the G ₀ /G ₁ -, S- and G ₂ /M-phases after exposure to doxorubicin for 72 h	41
Table 11. Expression of p53 in monolayer culture and spheroids after exposure to doxorubicin at IC ₂₅ for 72 h.....	42

List of Abbreviations

Symbols and numerical indicators

°C	Degree centigrade
%	Percentage
µg	Microgram
µL	Microliter
µm	Micrometer
µM	Micromolar
µg/mL	Microgram per milliliter
2D	Two-dimensional
3D	Three-dimensional
2N	Diploid
4N	Tetraploid
A	
ABCC1	ATP binding cassette subfamily C member 1
ABCC2	ATP binding cassette subfamily C member 2
ABCB1	ATP binding cassette subfamily B member 1
ABCG2	ATP binding cassette subfamily G member 2
ATCC	American Type Culture Collection
ACSL4	Acyl-CoA synthetase 4
ADP	Adenosine diphosphate
APH	Acid phosphatase
ATP	Adenosine triphosphate
B	
Bax	Bcl-2-associated X protein

BCA	Bicinchoninic acid
Bcl	B-cell lymphoma
BH3	Bcl-2 homologous
BSA	Bovine serum albumin
C	
C	Concentration
CAT	Chloramphenicol acetyl transferase
CDK	Cyclin-dependent kinase
CKI	Cyclin-dependent kinase inhibitor
cm ²	Centimeter squared
CO ₂	Carbon dioxide
Cu ²⁺	Copper ions
D	
d	Diameter
DEME	Dulbecco's Modified Eagle's Medium
DMSO	Dimethyl sulfoxide
DNA	Deoxyribonucleic acid
DNase	Deoxyribonuclease
E	
EGFR	Epidermal growth factor receptor
EGTA	Ethylene glycol-bis(2-aminoethylether)-N,N,N',N'-tetraacetic acid
ER	Estrogen receptor
ERCC	Excision repair cross-complementing rodent repair deficiency, complementation group 2
ECM	Extracellular matrix
F	
FCS	Foetal calf serum
FDA	Fluorescein diacetate
FL3	FL3 channel
G	
<i>g</i>	Centrifugal force
G0-phase	Quiescent stage
G1-phase	Post-mitotic gap phase

G2-phase	Pre-mitotic gap phase
G2-phase	Pre-mitotic gap phase
GPX1	Glutathione peroxidase 1
H	
h	Hour
Ham's F12	Ham's Nutrient Mixture F12
HER2	Human epidermal growth factor receptor 2
HMG-CoA	3-Hydroxy-3-methylglutary-coenzyme
I	
IC ₂₅	Concentration which inhibits 25% cell growth
IC ₅₀	Concentration which inhibits 50% cell growth
IC ₇₅	Concentration which inhibits 75% cell growth
L	
LDH	Lactate dehydrogenase
M	
Mdm2	Murine double minute 2
mg	Milligram
min	Minute
mL	Milliliter
mM	Millimolar
MLH1	MutL homolog 1
M-phase	Mitosis phase
MSL2	MutS homolog
mTOR	Mammalian target of rapamycin
N	
NCR	National Cancer Registry
NFKB1	Nuclear factor kappa subunit 1
nm	Nanometer
nm	Nanometer
NQO1	NAD(P)H dehydrogenase (quinone) 1
P	
p53	Tumor protein p53
PARA	Poly (ADP-ribose) polymerase
PBS	Phosphate-buffered saline
pH	Log hydronium ion concentration
PDVF	Polyvinylidene fluoride

PI	Propidium iodide
PI3K	Phosphatidylinositol-4,5-bisphosphate 3-kinase
PR	Progesterone receptor
R	
RALBP1	RalA binding protein 1
RB	Retinoblastoma-associated
RFI	Relative fluorescence intensity
RIPA	Radio-immunoprecipitation assay
RGD	Tripeptide Arg-Gly-Asp
RNase	Ribonuclease
ROS	Reactive oxygen species
S	
SEM	Standard error of the mean
SDS-PAGE	Sodium dodecyl sulfate polyacrylamide gel electrophoresis
SLC22A16	Solute carrier family 22 member 16
S-phase	DNA synthesis phase
SOD2	Superoxide dismutase 2
SR	Steroid hormone receptors
SRB	Sulforhodamine B
T	
TBS	Tris-buffered saline
TBST	Tris-buffered saline Tween-20
TCA	Trichloroacetic acid
TKs	Tyrosine kinases
TNBC	Triple-negative breast cancer
TNM system	T: the size of tumour; N: whether or not cancer has spread lymph nodes; M: whether or not cancer has metastasized
TOP2A	DNA topoisomerase 2-alpha
Tris	2-Amino-2-(hydroxymethyl)propane-1,3-diol hydrochloride
U	
U/mL	Units per milliliter
USA	United State
V	
VEGF	Vascular endothelial growth factor
W	
w/v	Weight to volume
X	

XDH

Xanthine dehydrogenase

Chapter 1

Introduction

1.1. Cancer

1.1.1. Introduction

Cancer is a disease where cellular proliferation is no longer under normal physiological growth control. Cancerous cells thus continue to proliferate, and may in turn become malignant.(1) When such cancerous cells accumulate, they may form a mass or lump with associated symptoms, such as abnormal bleeding, prolonged coughing and unexplained weight loss, to mention but a few.(2) Cancer occurs worldwide; by 2020, approximately 15 million new cancer diagnoses are expected.(3) In the United States of America, 23% of deaths are due to cancer; it is currently the second most common reason for death after heart disease.(4)

Numerous factors have been implicated in carcinogenesis, which includes internal (inherited mutations, hormones and immune conditions) and environmental or acquired factors (tobacco, diet, radiation and infections). Approximately 5-10% of all cancers are caused by genetic defects, allowing for the unchecked proliferation of damaged cells. However, environment and lifestyle choices contribute to approximately 90-95% of cancer. (5) For example, tobacco is a large contributor of cancer-related deaths (between 25 to 30%). Diet is estimated to contribute 20-35% to carcinogenesis, while infection accounts for 15-20%. Other external factors include radiation, stress, physical activity, and environment pollutants.(5)

There are more than a hundred categories of cancer depending on their molecular typing and origin, which includes that of the lung, prostate, colon, rectum, stomach and breast.(6)(7) In South Africa, one of the most important sources of cancer statistics is the National Cancer Registry (NCR), which is the organization that assesses the data of all cancers diagnosed at all national pathology laboratories (Table 1).(8)

Table 1. The top ten most common cancers in males in South Africa in 2014.

Type of cancer	Number of cases	Estimated lifetime risk	Percentage of all cancers
Prostate cancer	7 057	1:19	19.18%
Colorectal cancer	1 943	1:79	5.28%
Lung cancer	1 791	1:80	4.87%
Cancer of unknown primary*	1 740	1:91	4.73%
Kaposi sarcoma	978	1:320	2.66%
Cancer of the bladder	942	1:152	2.56%
Non-Hodgkin's lymphoma	932	1:221	2.53%
Malignant melanoma	869	1:187	2.36%
Oesophageal Cancer	848	1:178	2.31%
Cancer of the stomach	767	1:204	2.08%

* Origin of cancer in the body is unknown.

Table 2. The top ten most common cancers in females in South Africa in 2014.

Type of cancer	Number of cases	Estimated lifetime risk	Percentage of all cancers
Breast cancer	8 230	1:27	21.78%
Cervical cancer	5 735	1:42	15.17%
Cancer of unknown primary*	1 691	1:124	4.47%
Colorectal cancer	1 620	1:134	4.29%
Cancer of the uterus	1 256	1:145	3.32%
Lung cancer	936	1:195	2.48%
Non-Hodgkin's lymphoma	870	1:296	2.30%
Malignant melanoma	755	1:311	1.00%
Kaposi sarcoma	669	1:555	1.77%
Cancer of the oesophagus	650	1:326	1.72%

* Origin of cancer in the body is unknown.

1.1.2. Hallmarks of cancer

Cancer is characterized by unique hallmarks when compared to normal, healthy cells (Figure 1). These include, amongst others, uncontrolled replicative potential, evasion of death signals, altered metabolic status, invasiveness and increased mutation frequency.(9)

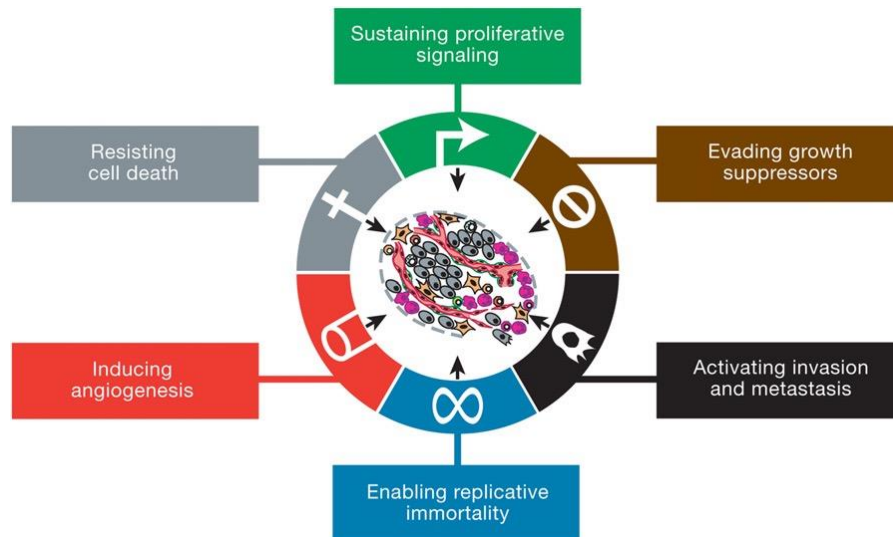


Figure 1. The original six hallmarks of cancer, highlighting molecular differences from healthy cells that contribute to cancer formation.(9)

1.1.2.1. Sustained proliferative signalling

One of the most fundamental traits of cancer is its ability to maintain proliferative capabilities. In healthy tissue, the production and release of growth-promoting signals are regulated carefully, which control entry into and progression through the cell growth and division cycle. This process guarantees a homeostasis of cell number to maintain normal tissue architecture and function. However, in cancerous cells, such signals are dysfunctional, which give cells the ability to grow unchecked. Large parts of enabling signals are delivered by growth factors, which combine with cell-surface receptors to activate proliferation and growth.(10)

1.1.2.2. Evading growth suppressors

To assist with indefinite proliferation, cancer cells evade anti-growth signals that decrease proliferative capacity. In such a way, tumour suppressor genes are rendered dysfunctional or poorly expressed. Many tumor suppressor genes have been identified by their characteristic inactivation in animal and human cancer models, which work in various ways to prevent cell growth and proliferation. For example, the retinoblastoma-associated (RB) and p53 proteins are encoded by two prototypical tumor suppressor genes, which are central control nodes moderated by two key complementary cellular regulatory circuits to mediate proliferation, senescence and apoptosis.(11)

1.1.2.3. Resisting cell death

Cancer cells further possess the ability to avoid cell death mechanisms when detected. Apoptosis includes both upstream regulators and downstream

effectors. The upstream regulators are divided into two major pathways (the intrinsic program and extrinsic program).(12) Both can stimulate the activation of inactive pro-caspases 8 and 9, which induce cell death via effector caspases. Effector caspases oversee the execution phase of apoptosis. Signals are controlled by pro- and anti-apoptotic proteins (Bcl-2 family). Typically, Bcl-2, Bcl-x_L, Bcl-w, Mcl-1 and A1 inhibit apoptosis through the binding to and suppression of two pro-apoptotic triggering proteins (Bax and Bak), which prevent the mitochondrial release of cytochrome *c*. Cytochrome *c* in turn activates caspases to induce apoptosis. Bax and Bak have protein-protein domains (BH3 motifs) that share similarity with those on some Bcl-2-like proteins. The activities of proteins (BH3-only protein) of the Bcl-2 subfamily, which contains a single BH3 motif, are connected to the cellular-abnormality sensor.(12, 13) A DNA damage sensor acts with the p53 tumour suppressor protein, which stimulates expression of the Noxa and Puma BH3-only protein to increase the level of DNA breaks. If survival signals are not enough, it can induce apoptosis by BH3-only protein (Bim). Cancer cells evade cell death pathways using such strategies. Cancerous cells can decrease expression or function of p53 suppressor genes, thus preventing removal of the cell after DNA damage has occurred. They can also increase the expression of anti-apoptotic regulators or survival signals, and inhibit extrinsic ligand-induced death circuits.(14, 15)

1.1.2.4. Enabling replicative immortality

Normal cells die after a certain number of divisions. Cancer cells bypass this restriction and thus indefinitely replicate. This restriction is caused by two observed barriers to proliferation: senescence (cells are non-proliferative but viable) and crisis (cell death). During cell proliferation, repeated division leads to senescence and then, for those cells that succeed in avoiding senescence, to crisis phase. Cells that obtain the ability to indefinitely proliferate are said to undergo immortalisation. Telomeres, which are multiple tandem hexanucleotide repeats, are used to protect chromosomes during division, and shorten as cells proliferate. At such times, chromosomes become unstable and cell death is induced. The number of cellular generations is decided by the length of telomeric DNA. When telomeres lose their capacity for protection, it triggers cells to enter into crisis. Cancer cells obtain the capacity to maintain enough of the telomere's length to avert triggering senescence or apoptosis, which is induced by increasing the expression of telomerase or obtaining an alternative recombination-based telomere.(16, 17)

1.1.2.5. Inducing angiogenesis

During embryogenesis, vasculature develops in two ways. Firstly, vasculogenesis is the birth of new endothelial cells, which can assemble into tubes. Secondly, angiogenesis allows for the sprouting of new vessels from the original. Normally the vasculature remains largely quiescent. However, angiogenesis is activated

transiently during wound healing and female reproductive cycling in adults. Cancer cells induce angiogenesis and keep it active for large periods of time to continuously form new blood vessels for the supply of oxygen and nutrients, and to remove metabolic waste and carbon dioxide.(18)

1.1.2.6. Activating invasion and metastasis

Cancer cells can relocate to other organs or invade neighbouring tissues through a process called metastasis. The associated cancer cells appear altered in their shape and in their attachment to other cells and the extracellular matrix. One of the most significant alternations is the loss of E-cadherin expression, which is the key adhesion molecule for cell-cell adhesion. E-cadherin allows for assembly of epithelial cell sheets which induces quiescence through establishing adherent junction with adjacent epithelial cells. In cancer cells, E-cadherin is typically down-regulated, allowing for metastasis.(19, 20) The process of invasion and metastasis is summarized as a series of individual steps. The process arises from local invasion into adjoining stromal tissue. Cancer cells upon arrival at a arteriole can intravasate into blood or lymphatic vessels, and transit through the lymphatic and hematogenous system before escaping from the lumen of vessels into other tissues (extravasation). Cancer cells can remain dormant in this tissue (micrometastases). Finally, the micrometastatic lesions can be activated to proliferate and grow into macroscopic tissue (colonization).(21, 22)

1.1.2.7. Inflammatory microenvironment

An inflammatory component is present in the microenvironment of most neoplastic tissues. Key characteristics of cancer related inflammation include the infiltration of white blood cells, presence of tumor-associated macrophages, the presence of polypeptide messengers of inflammation, and the occurrence of tissue remodelling and angiogenesis.(23)

The ability of cancerous cells to mediate their own proliferation remains a characteristic problem when dealing with treatment. Such proliferation occurs due to alterations of, among others, the cell cycle.

1.2. The cell cycle

1.2.1. Introduction

The cell cycle is a continuous and discrete process whereby cells grow, and ultimately divide into two identical daughter cells. The cell cycle is categorized into the interphase, mitosis, and cytokinesis (Figure 2). The interphase is divided into three phases, namely the gap 1 (G1)-, synthesis- and gap 2-phase.(24) During the G1-phase, diploid (2N) cells grow and synthesize proteins required for DNA synthesis. Chromosomes replicate and divide during the S-phase to form

identical sister chromatids held together by a centromere. During the G₂-phase, tetraploid cells (4N) continue to grow and produce proteins necessary for cellular division. Upon completion of the G₂-phase, cells transition to the mitosis phase (M-phase). The latter is further divided into four phases: prophase, metaphase, anaphase, and the telophase. In prophase, chromosomes condense and the nuclear membrane disappears. Centrioles separate and take position at opposite poles of the cell, while spindle fibers form and radiate toward the center of the cell.(25) In metaphase, spindle fibers connect the centromere of each sister chromatid to the opposite poles of the cell.(26) During anaphase, sister chromatids separate to opposite sides of the cells, while in telophase, chromosomes uncoil. A nuclear envelope forms around the chromosomes at each pole of the cell and spindle fibers dissolve. Cytokinesis generally follows the end of the M-phase to divide cells with a membranous cleavage furrow to create two identical daughter cells.(25)

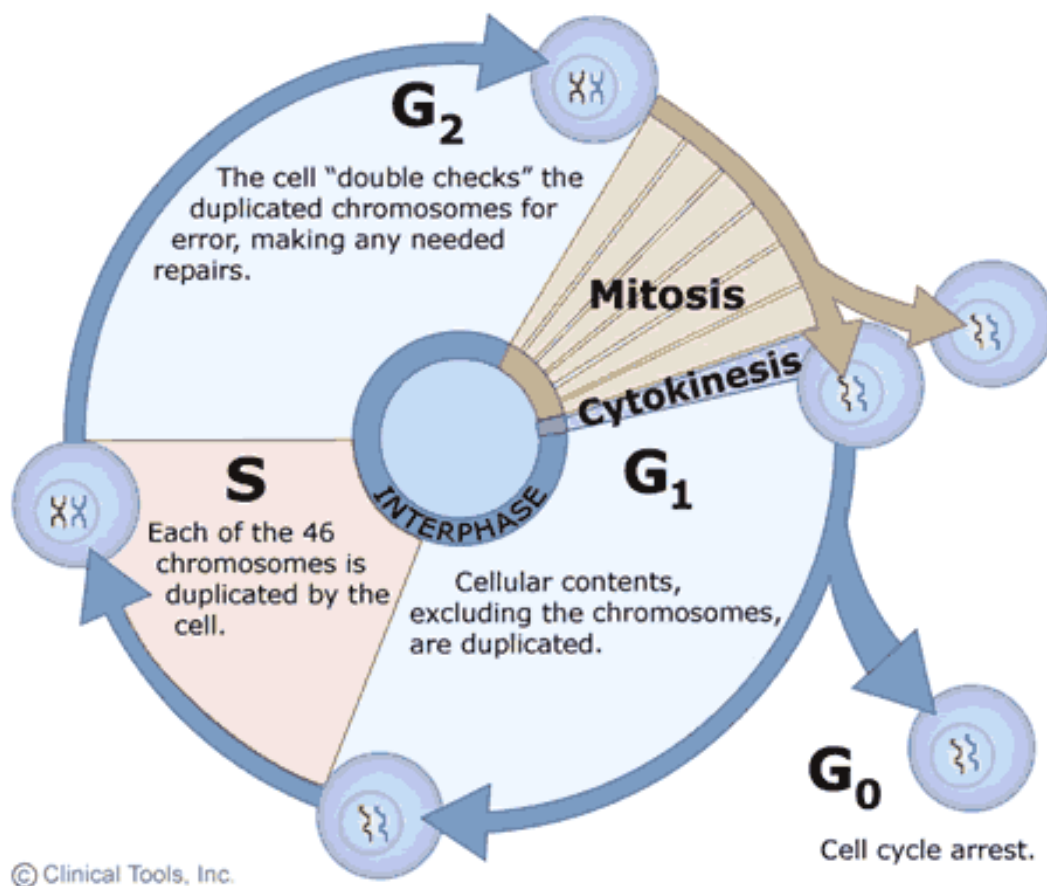


Figure 2. A graphical representation of cellular cycling.(27)

Cells may at times exit the cell cycle into a quiescent, gap 0 (G₀)-phase. During the G₀-phase, cells are metabolically active, but do not replicate. If required, cells may re-enter the cell cycle to continue their proliferation, such as when damage has occurred to an organ system.(24) Each specific phase of the cell cycle is tightly controlled by a variety of different factors to ensure that all processes are

finished before the next phase is commenced, such as cyclin-dependent kinase (CDK) regulation, restriction points and checkpoints.(28)

1.2.2. Cell cycle regulatory components

The cell cycle is a tightly regulated discrete system, in which systematic progression is controlled by various factors and checkpoints. Cyclins are a family of proteins that regulate the progression of the cell cycle by activating cyclin-dependent kinases (CDKs) upon complexation. These complexes are critical in the induction of active cycling factors. Cyclin-dependent kinases activate cycling factors on serine or threonine using adenosine triphosphate (ATP) as a phosphate donor.(29) Each phase is under control by different cyclin/CDK pairs (Figure 3).(30) There are at least nine CDKs and more than twelve cyclin families described. The most prominent cyclin/CDK complexes are cyclin D/CDK4(6), cyclin E/CDK2, cyclin A/CDK2, and cyclin B/CDK1 (cdc2). Cyclin D1, D2, and D3 cooperate with CDK4 and CDK6, and are critical for progression through the early G1 phase. Cyclin D/CDKs work in collaboration with cyclin E/CDK2 to allow for transition into the S phase. At this junction cells reach a restriction point,(31) which assesses whether cells have all requirements for further progression.(32) Cyclin E/CDK2 controls progression into the S-phase, after which cyclin A/CDK2 promotes the completion thereof. Further cellular cycling is dependent on CDK1 in association with cyclin A and B, which allows for G2-phase transition and completion of the mitosis and cytokinesis phases. Cyclin-dependent kinase inhibitors (CKIs) bind and inactivate Cdk/cyclin-pairs, which serve as brakes to halt cell cycle progression under unfavorable conditions.(33)

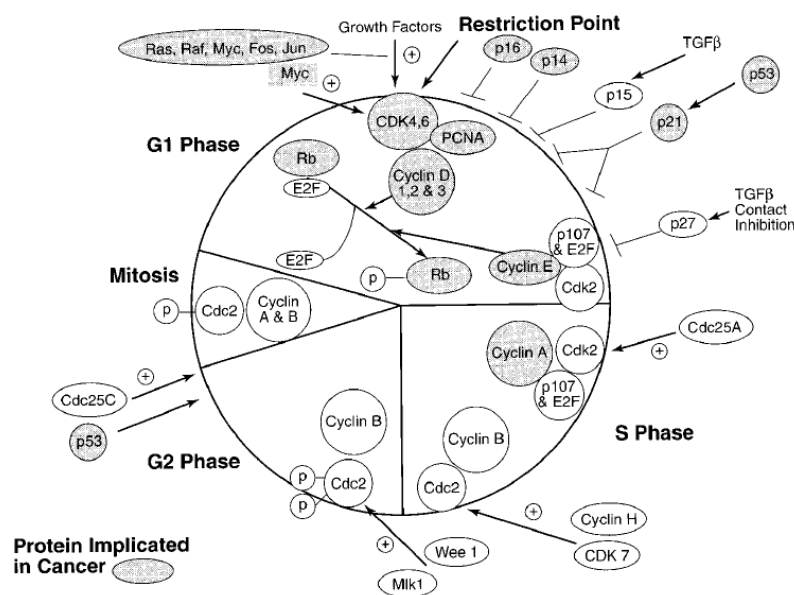


Figure 3. Cell cycle regulatory components determined to be altered in human cancers.(34)

Cyclin-dependent kinase inhibitors are divided into two groups based on their structures and CDKs specificity. The Ink4 family members, such as p16 (Cdkn2a), p15 (Cdkn2b), p18 (Cdkn2c) and p19 (Cdkn2d), reduce activity of CDK4 and CDK6. The Cip/Kip family members, such as p21 (Cdkn1a), p27 (Cdkn1b) and p57 (Cdkn1c), broadly regulate the activity of cyclin D-, E-, A- and B-dependent kinase pairs.(35) Cyclin-dependent kinases, cyclin and CKI family members regulate transcription, DNA damage repair, proteolytic degradation, epigenetic regulation, metabolism, stem cell self-renewal, neuronal functions and spermatogenesis.(36)

p53, also known as TP53 or tumor protein 53, is the protein that manages the cell cycle and suppresses tumor formation. p53 protects cellular stability by inhibiting genome mutation. The name originates from its molecular mass: 53 kilodalton fraction of cell protein.(37) The p53 protein was identified in 1979 by co-immunoprecipitation of p53 with T-antigen in SV40-transformed cells.(38) There are three functions for p53: growth arrest, DNA repair and apoptosis. Activation of p53, which in turn promotes apoptosis of tumour cells, is considered to be a key mechanism of action of several chemotherapeutics (such as doxorubicin) and DNA repair proteins. When DNA gets damaged, p53 binds DNA, which can in turn activates the expression of genes encoding for p21. In such a way, p21 interacts with a cell division-stimulating protein (Cdk2 and Cdc 2) and arrests cells in the G0/G1 and G2/M phase for DNA repair proteins to rectify damage. If DNA damage is irreparable, p53 will initiate apoptosis.(39) p53 cannot bind to DNA effectively after mutation, thus the p21 protein is not expressed by genes to act as an anti-growth signal. Therefore, cell division goes uncontrolled and tumours are formed.(40)

1.3. Breast cancer

1.3.1. Introduction

Breast cancer, as the name suggest, is a cancer originating from breast tissue.(41) The signs of breast cancer include a lump in the breast, a change in breast shape, dimpling of the skin, fluid secretions from the nipple and a scaly patch of skin.(42) Breast cancer has become one of most aggressive cancer in the world, which occurs in 22.9% of female cancer cases. Breast cancer leads to 458,503 cancer deaths worldwide, which includes 13.7% of cancer deaths in women and 6% of cancer deaths for both male and female in 2008.(43) In 2012, 1.68 million cancer case and 552,000 deaths were due to breast cancer.(44) Breast cancer is heavily linked to age. Only 5% of all breast cancer cases are diagnosed in women under 40 years old. The factors of breast cancer development involve female sex, obesity, lack of physical exercise, drinking alcohol, hormone replacement therapy, ionizing radiation, old age and family history. The two methods by which breast cancer is diagnosed include biopsies and the presence of a lump. If the cancer has spread into other tissues, further tests are used(45). Fortunately survival rates of

breast cancer are as high as 80% in the UK and 90% in the US, with a survival rate of more than five years.(46)(47)

1.3.2. Diagnosis

1.3.2.1. Histopathological examination

Histopathological examination is the primary method to classify breast cancer. Based on whether the cancer arises in the epithelial lining, ducts or lobules, breast cancer may be defined as ductal and lobular carcinoma. Based on the invasion of the carcinoma, breast cancer is further classified as carcinoma *in situ* or invasive.(48)

1.3.2.2. Grading of breast cancer cells

Cellular differentiation is an important process that allows to differentiate their shape, cellular characteristics and function for various organ systems. Cancer cells lose differentiation during transformation and immortalization. Classification includes well differentiated (low grade), moderately differentiated (intermediate grade) and poorly differentiated (high grade).(49)

1.3.2.3. Staging breast cancer

The approach to staging breast cancer relies on the TNM system (T: the size of tumour; N: whether or not cancer has spread into lymph nodes; M: whether or not cancer has metastasized). Stage 0 refers to pre-carcinoma or marker conditions such as ductal carcinoma *in situ* or lobular carcinoma *in situ*. Stage 1 to 3 includes cancer within breast or regional nodes, while stage 4 refers to cancer that has spread into the bloodstream and metastasized, as well as presents with a less favorable prognosis.(50)

1.3.2.4. Receptor status

Diagnosis using receptor status depends on whether breast cancer cells express estrogen receptor (ER), progesterone receptor (PR) and human epidermal growth factor receptor 2 (HER2). Breast cancer lacking any of these receptors is referred to as triple-negative breast cancer (TNBC).(51)

The ER are nuclear receptors that are activated by estrogen.(52) Estrogen-activation of the ER receptor may result in signal transduction via two pathways: “genomic” and “nongenomic”. In the genomic pathway, estrogens permeate into the cell and bind to nuclear ER. The nuclear estrogen-ER complex binds to the estrogen response element sequences directly or with protein-protein interaction by activator protein 1 or SP1 sites in the promoter region of estrogen-responsive genes, which leads to recruitment of coregulatory

proteins (such as, coactivators and co-repressors). This action regulates the mRNA level and subsequent protein production and physiological responses.(53) The non-genomic pathway is faster, and takes seconds or minutes in comparison to the genomic pathway's hours for signal transduction. The non-genomic pathway targets ER located in the plasma membrane or adjacent to the membrane, or through other non-ER membrane associated estrogen-binding proteins. Activation increases Ca^{2+} or nitric oxide levels, and promotes kinase function.(54)

The PR is a ligand-activated transcription factor member of the steroid hormone receptors (SR) subfamily of nuclear receptors. PR includes two main isoforms (A and B), which are created from the same gene through alternate translational start sites (PR-B includes full-length, however, PR-A is an N-terminally truncated version). Once progesterone binds to the PR, dimerization occurs, leading to DNA binding and subsequent transcription.(55)

HER2 is a member of the epidermal growth factor receptor family, which has tyrosine kinase activity. After dimerization occurs upon ligand binding, transphosphorylation of the intracellular tyrosine residues take place, and initiates a variety of signalling pathways (e.g. proliferation).(56)

The ER, PR and HER2 play a role in the growth of breast tissue (and ultimately cancer). These receptors generally promote the growth of cancerous tumors; most types of breast cancer show positive expression for one or more receptors. Contrary to other types of breast cancer, such as ER-positive subtypes, TNBC lack these receptors and therefore treatment is more problematic. Chemotherapeutic drugs can block attachment of hormones to their respective receptors to block proliferative signals, but this cannot be done in TNBC.(57) Estrogen is implicated in the development of breast cancer due to accumulation in the epithelium.(58) Stimulation of the ER by estrogen leads to proliferation of mammary cells. The increase in cell division and DNA synthesis leads to the risk for replication errors and detrimental mutations, which disturb the standard cellular processes such as apoptosis, cellular proliferation and DNA repair. Alternatively, estrogen metabolism results in the generation of genotoxic by-products, which can destroy DNA and leads to point mutations. Research indicates that estrogen might initiate and promote breast cancer through both a proliferative- and metabolite-based mechanism.(59) Even though progesterone also plays an important role in breast tumorigenesis, anti-estrogen therapy has become the standard treatment to treat ER-positive cancer.(60) Most HER2-based research has been done in breast cancer, which was found to promote mammary carcinogenesis *in vitro* and *in vivo*.(61, 62) The HER2 receptor belongs to the epidermal growth factor receptor (EGFR) family, which main four members: HER1 (EGFR, ErbB1), HER3 (ErbB3) and HER4 (ErbB4), respectively. Each of these receptors include an extracellular bind domain, a single transmembrane-spanning domain and a long cytoplasmic tyrosine kinase

domain.(63) The HER receptor is monomer on the cell surface. Generally, binding of ligands to their extracellular domains induce receptor dimerization and transphosphorylation of their intracellular domains. The HER2 receptor has no identified ligand and prefers entering an activated state constitutively or a heterodimer formation with other HER members, such as HER1 and HER3. Receptor homo- or heterodimerization leads to the activation of downstream signalling pathways associated with the autophosphorylation of tyrosine residues within the cytoplasmic domain. These signalling pathways include the mitogen-activated protein kinase (MAPK) pathway, phosphatidylinositol-4,5-bisphosphate 3-kinase (PI3K), and protein kinase C (PKC) pathway, which results in cell proliferation, survival, differentiation, angiogenesis and invasion.(64) The HER signalling pathways normally regulate cellular programs during development and post-natal life. However, its deregulation is relative to pathogenesis of several human tumours. Overexpression of HER2, enhancing and prolonging signals that trigger cell transformation and proliferation, has a causal role in the promotion of carcinogenesis. The absence of the auto-inhibited conformation explains, at least in part, this HER2 transforming potential. Amplification and/or overexpression of HER2 have been reported in malignancies, such as breast, ovarian, prostate, colorectal, pancreatic and gastric cancers.(65)

1.3.3. Management

The therapeutic approach for treating breast cancer is based on several factors, including those of the patient and molecular typing of the cancer itself. Surgical resection of the primary tumor along with associated chemotherapy, radiation therapy or both is currently the standard of care for the treatment of hormone receptor-positive cancers. For metastatic and advanced stages of breast cancer, monoclonal antibodies (such as trastuzumab and pertuzumab against HER2) and other immune-modulating therapies are applied.(66) There are three main categories of drugs for adjuvant breast cancer treatment after surgery.

1.3.3.1. Hormone blocking therapy

Estrogen acts as a growth factor in ER-positive breast cancer which means that estrogenic blocking drugs are effective in inhibiting cancer cell growth. These agents function by i) directly bind to the ER (such as tamoxifen), prevent stimulation of the receptor, or ii) by decreasing the production of estrogen (e.g. aromatase inhibitors such as anastrozole or letrozole).(67) Aromatase inhibitors are only used for female patients after menopause. Active aromatase in postmenopausal women is different from the normal structure in premenopausal women, thus these agents don't inhibit the predominant aromatase in premenopausal women.(68)

1.3.3.2. Chemotherapy

Chemotherapy is commonly used to treat progressive breast cancer (stage 2-4) or ER-negative tumours. Such treatments are often provided as combinations for 3-6 months. One of the most prevalent combinations is cyclophosphamide and doxorubicin (a.k.a. AC).(69) Taxane drugs such as docetaxel are sometimes added (a.k.a. CAT) to this treatment. Otherwise, CMF is used, consisting of cyclophosphamide, methotrexate and fluorouracil. The main mechanism by which these drugs work is to reduce proliferation via the induction of DNA damage and blockage of the cell cycle. These treatments target highly proliferative cells.(70)

1.3.3.3. Monoclonal antibodies

The HER2 receptor initiates cellular growth and division after stimulation by growth factors such as epidermal growth factor. Trastuzumab, a monoclonal antibody that binds to HER2, blocks its stimulation resulting in decreased growth of breast cancer cells. However, the disadvantages of trastuzumab are its high cost and the presence of serious side effects such as heart damage.(71)

1.4. Triple-negative breast cancer

1.4.1. Introduction

Triple-negative breast cancer (TNBC) is a subtype of breast cancer characterized by cells lacking ER, PR and HER2 expression. About 10-20% of breast cancers are found to be triple-negative. Most TNBCs exhibit a basal-like phenotype. Within African-American and Hispanic women below the age of 50, TNBC is more common than in other groups.(72) About 80-90% of TNBC are defined as invasive ductal carcinomas while the rest are apocrine, lobular, adenoid cystic, medullary, or metaplastic.(73, 74) TNBC patients have an increased risk of lymphocytic infiltrations and present with higher grades and larger tumours. Furthermore, there is a four-fold increase in the incidence of distant metastases, which is associated with a shortened survival frequency for patients.(75) Metastases often occur in the lung and central nervous system. Approximately 15-30% of patients with TNBC are diagnosed with brain metastases.(76, 77) There is a strong underlying genetic aetiology for TNBC, where 15% of cases are linked to mutations in *BCR1* and *BCR2*.(57)

Prognosis is poor due to the aggressive nature of TNBC, and the lack of targeted therapy due to the inability to target the three aforementioned receptors.(78, 79) Currently, no specific markers have been identified that distinguish these tumours and therefore no targeted therapy is available.(57)

1.4.2. Treatment modalities

Treatment of patients with TNBC includes surgery and radiotherapy (first-line option), as well as chemotherapy, or a mixture thereof.(80) Therapy targeting receptors such as ER, PR and HER2 are ineffective, however, some cytotoxic agents (Figure 4) display efficacy against TNBC, such as anthracyclines e.g. doxorubicin or epirubicin, and taxanes.(81)

As stated before, cancer cells sustain proliferative growth. Normally, the major target of cytostatic drugs is the cell cycle, which prevents further cycling and thus reduces proliferation. Such cytostatic therapies target cancer growth by selective interference with proliferative pathways, however, do not necessarily cause direct cytotoxicity.(82) Resistance to chemotherapy is an ever-present risk and has become the main factor of failure in patients with advanced and inoperable cancer. One of the most prominent reasons for this occurrence is the selectivity of cytostatic antineoplastic drugs against proliferative cells. Due to this, cancerous cells that remain dormant are not targeted, and thus may re-enter the cell cycle after treatment.(34, 83-85) There are currently no optimal treatments for TNBC, however, some studies have addressed chemotherapy before surgery, referred to as neoadjuvant therapy, which may be an option.(86)

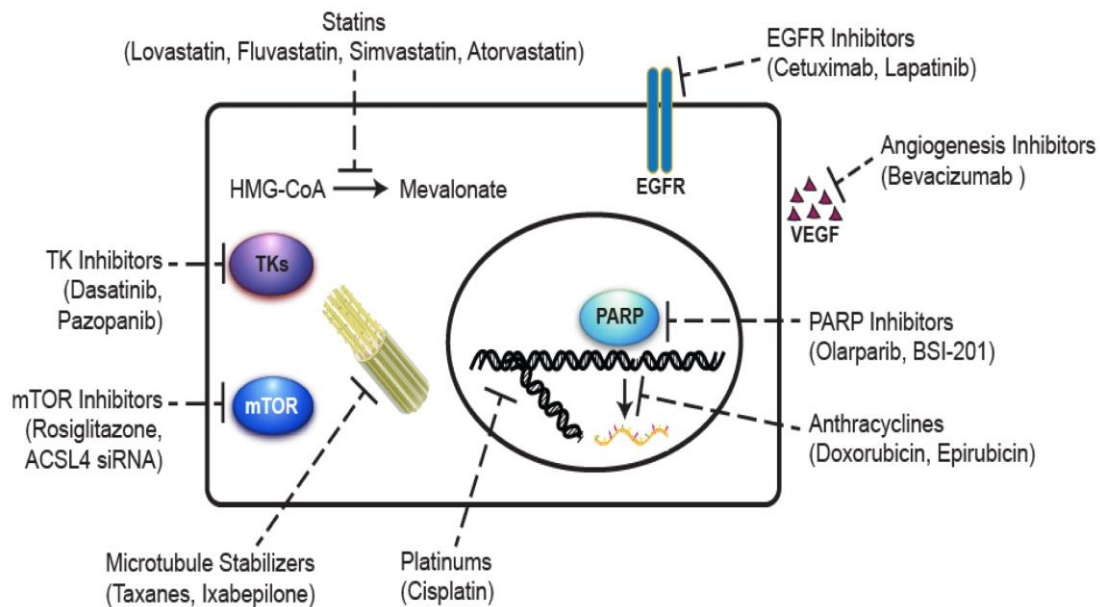


Figure 4. Potential agents for treatment of triple negative breast cancer.(87)

Table 3. The therapeutic options for treatment of triple-negative breast cancer.

Name	Classification	Mechanism of action	Examples
Microtubule stabilizers	Cytotoxic chemotherapy	Microtubule stabilizers polymerize tubulin in the microtubule to inhibit cell division.(88)	Taxanes and ixabepilone

Name	Classification	Mechanism of action	Examples
Anthracyclines		Anthracyclines prevent RNA synthesis through insertion between base pairs of the DNA/RNA strand, thus inhibiting proliferation.(89)	Doxorubicin and epirubicin
Platinums		Platinum agents create inter- or intra-strand double-stranded DNA crosslinks to inhibit the appearance of the replication fork, inhibiting proliferation.(90)	Cisplatin
Poly (ADP-ribose) polymerase (PARA) inhibitors		PARA repairs single-stranded DNA breaks that occurred during the cell cycle.(91) The PARA inhibitors inhibit the repair of single-strand breaks in the cell cycle.(90)	Olarparib and BSI-201
Angiogenesis inhibitors	Targeted therapy	Vascular endothelial growth factors (VEGF) are expressed to a higher degree in TNBC than in non-TNBC.(92) Angiogenesis inhibitors prevent the formation of new blood vessels by deterring VEGF activity.(90)	Bevacizumab
Epidermal growth factor receptor inhibitors		EGFR is highly expressed in TNBC, which links to a poor prognosis and response to chemotherapy.(93-95) The EGFR inhibitors prevent cancer cell division.	Cetuximab and lapatinib
Tyrosine kinases (TKs) inhibitors		TKs (including the Src and Abl family and c-Kit) appear over-expressed, and affect breast cancer metastasis. The TK inhibitors prevent cellular division by blocking intracellular TK activity.(90)	Dasatinib and pazopanib

Name	Classification	Mechanism of action	Examples
Mammalian target of rapamycin (mTOR) inhibitors		mTOR plays an important role during the phosphatidylinositol-4,5-bisphosphate 3-kinase (PI3K)-protein kinase B (Akt)-mTOR pathway, which is directly related to cellular quiescence and proliferation. The overexpression of Acyl-CoA synthetase 4 (ACSL4), which is a protein encoded by <i>ACSL4</i> , regulates arachidonic acid metabolism and can lead to overactivity of the PI3K-Akt-mTOR pathway in breast cancer. Such mTOR inhibitors prevent cellular proliferation and growth by inhibiting <i>ACSL4</i> expression, thus reducing PI3K-Akt-mTOR activation.(96, 97)	Rosiglitazone and ACSL 4 siRNA
Statins		Statins inhibit the conversion of 3-hydroxy-3-methylglutaryl-coenzyme (HMG-CoA) to mevalonate through the cholesterol synthesis pathway, which has been found to have a beneficial effect against cancer proliferation.(87)	Lovastatin, fluvastatin, simvastatin and atorvastatin

1.4.3. Doxorubicin

Doxorubicin (Figure 5) belongs to the anthracycline class of antibiotics and is one of the first compounds developed for alternative tumour treatment. Compared to other anthracyclines, doxorubicin has a higher efficacy against solid tumours, especially breast cancer.(98) Due to its stable structure and high treatment potential, doxorubicin is considered one of the most effective agents against cancer by the Food and Drug Administration.(99) Doxorubicin limits cell division, resulting in slower disease development. However, cardiotoxicity is a limiting side effect for its use.(100) Doxorubicin can intercalate with DNA to inhibit both DNA and RNA polymerase, thus reducing DNA replication and RNA transcription.(101)

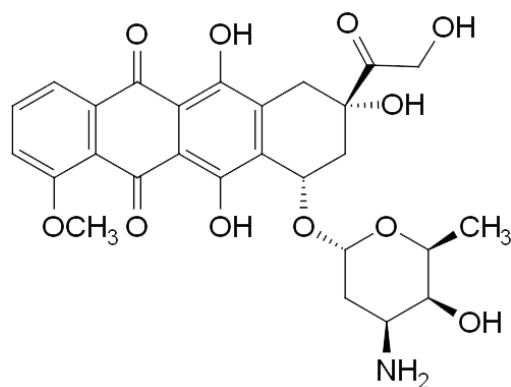


Figure 5. Chemical structure of doxorubicin.(102)

Additionally, it has been shown to bind to topoisomerase enzymes I and II. By stabilizing the topoisomerase II complex, resealing of the DNA double helix after unwinding during replication is inhibited, which halts replication.(103) Blocking of cells in the G1- and G2-phases of the cell cycle will eventually lead to apoptosis if DNA damage cannot be repaired.(104) These mechanisms are controlled by pharmacogenes that regulate DNA repair mechanisms and the cell cycle (TOP2A, MLH1, MSH2, TP53, and ERCC2 genes), and thus are good candidates for anticancer lead development. (105)

Doxorubicin may also generate free radicals, which promote damage to cellular membranes, DNA and protein (Figure 6).(103) As doxorubicin is oxidized, semiquinone, an unstable metabolite, is formed. Semiquinone is converted back to doxorubicin during a reaction that releases reactive oxygen species, which promotes the oxidation of cellular constituents, induces oxidative stress, and triggers apoptosis.(106) The candidate pharmacogenes to regulate this pathway include those regulating oxidation such as NADH dehydrogenases, nitric oxide synthases, xanthine oxidase, and those capable of deactivating the free radicals i.e. glutathione peroxidase, catalase, and superoxide dismutase.(107, 108)

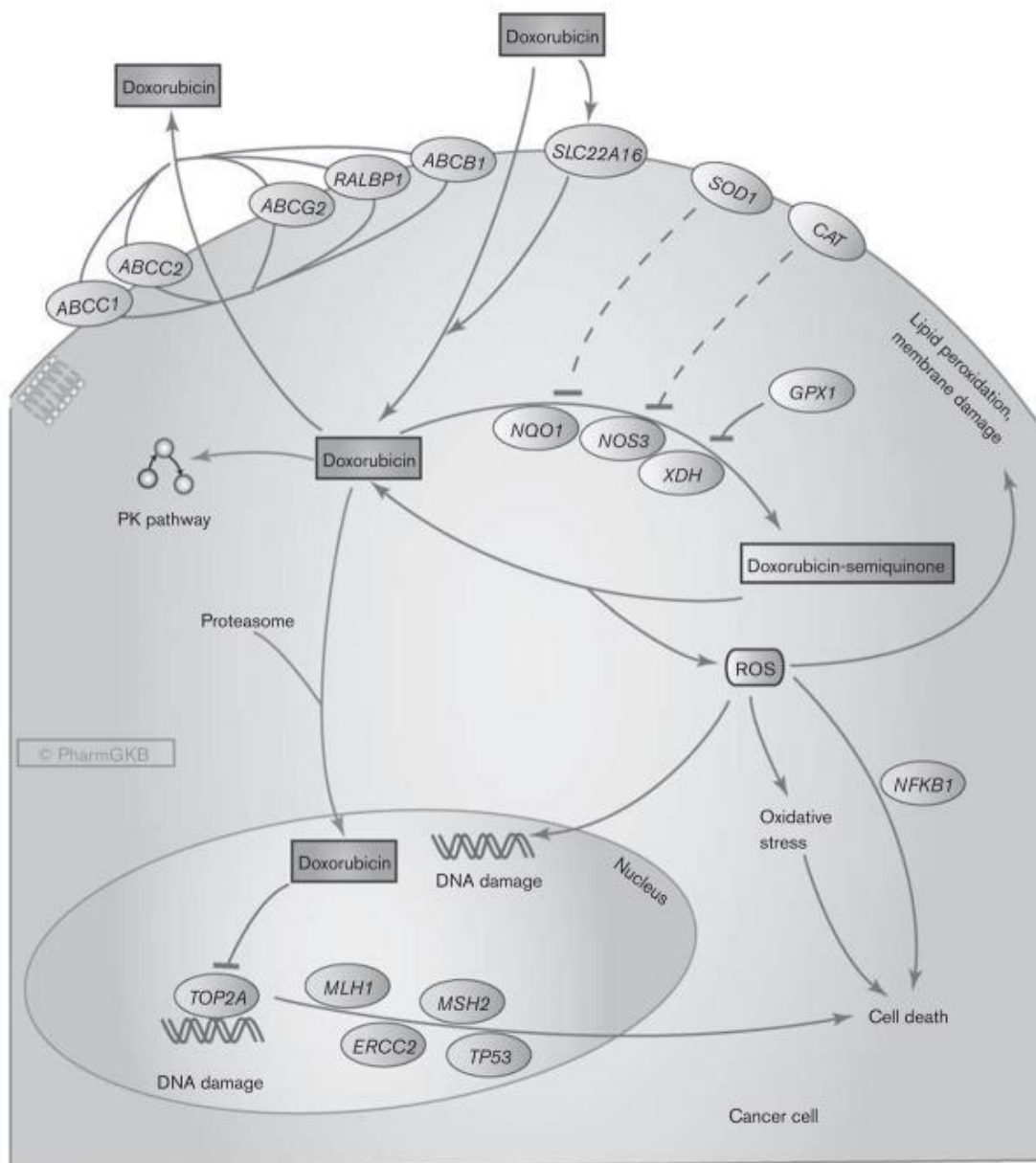


Figure 6. A graphical representation of candidate genes involved the pharmacodynamics of doxorubicin in cancer cells.(109) Abbreviations: ABCB1 - ATP binding cassette subfamily B member 1; ABCG2 - ATP binding cassette subfamily G member 2; ABCC1 - ATP binding cassette subfamily C member 1; ABCC2 - ATP binding cassette subfamily C member 2; ABCB1 - ATP binding cassette subfamily B member 1; ABCG2 - ATP binding cassette subfamily G member 2; CAT - chloramphenicol acetyl transferase; ERCC2 - excision repair cross-complementing rodent repair deficiency, complementation group 2; GPX1 - glutathione peroxidase 1; MLH1 - MutL homolog 1; MSH2 - MutS homolog; NFKB1 - nuclear factor kappa subunit 1; NOS3 - nitric oxide synthase 3; NQO1 - NAD(P)H dehydrogenase (quinone) 1; RALBP1 - RalA binding protein 1; ROS - reactive oxygen species; SLC22A16 - solute carrier family 22 member 16; SOD2 - superoxide dismutase 2; TOP2A - DNA topoisomerase 2-alpha; TP53 - tumor protein p53; XDH - xanthine dehydrogenase.

1.5. The solid tumour microenvironment

In epithelial tumours, cells are contained within a three-dimensional (3D) space in close contact with one another. In these tumours, the homeostatic regulation and growth of blood vessels are impaired in the core of the tumour, generating a gradient of nutritional and oxygen supply. To grow in these poorly vascularized tumour areas, cells adapt to this unsuitable metabolic microenvironment (Figure 7B).(110) Cells in these poorly vascularised regions are more likely to be dormant or exhibit reduced growth rates when compared to cells located in close proximity to blood vessels.(9, 111)

This differential environment within a tumour is poorly reconstituted in the standard two-dimensional (2D) culture platforms used in primary anticancer drug screening assays. This results in a poor correlation between efficacy in pre-clinical screening and ultimate effectiveness of drugs in *in vivo* settings.

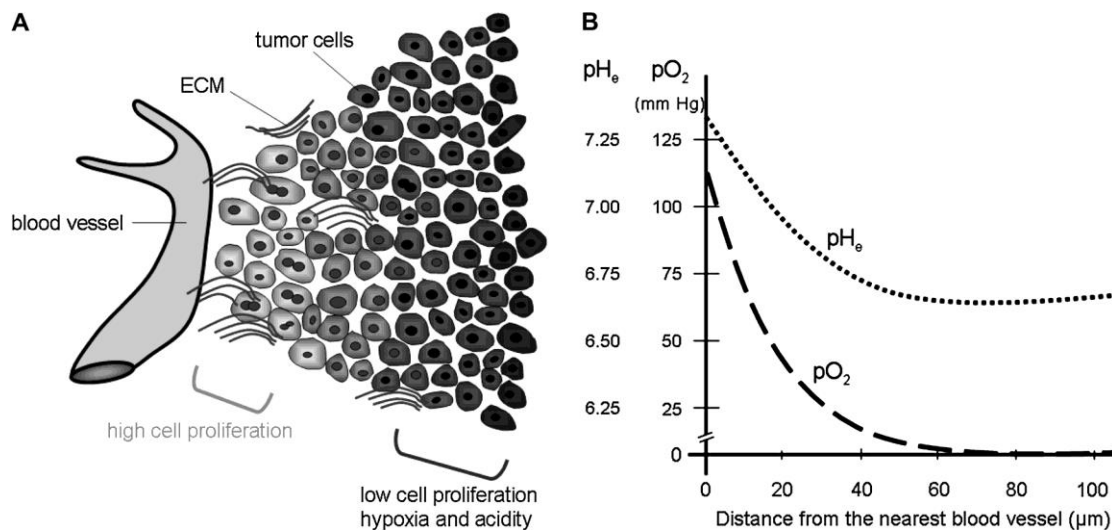


Figure 7. The relation between the tumour microenvironment and blood vessels. (A) Diagrammatic representation of tumour cells and the extracellular matrix (ECM) surrounding a capillary. (B) Schematic representation of the gradient of oxygen concentration (pO_2 : dashed line) and of pH (dotted line) in relation to the nearest tumour blood vessel.(83)

1.5.1. Disadvantages of traditional drug screening platforms

Two dimensional monolayer cultures have been used for decades in high-throughput drug screening assays (Figure 8).(112) Unfortunately, these *in vitro* results generally do not translate well into an *in vivo* or clinical system, leading to inaccurate predictions of clinical effects. The standard pathway for drug development currently starts with screening of candidate compounds in a 2D culture-based assay, further *in vitro* evaluation, preclinical testing in model organisms and eventual clinical trials in human subjects. Using this methodology, a success rate of less than 10% is achieved, with many compounds not passing

phase III clinical trials, resulting in loss of investments.(113, 114) To ameliorate this financial and time loss, more representative initial cell models need to be developed to more accurately predict compound efficacy at an early stage. The reason for this failure of early prediction of clinically-relevant molecules lies in the cell culture method employed in most screening assays. Most assays are based on liquid overlay cultures on a flat surface. Cells use cytoskeletal adjustments to adapt to this environment, which leads to abnormal polarity, cell metabolism and protein expression. Furthermore, they lack the characteristic extracellular matrix of these cell types in an *in vivo* setting.(115) As such, 2D models cannot mimic the complex and dynamic microenvironment of *in vivo* structures due to the lack of proper cell-cell and cell-matrix interactions. Thus they lose tissue architecture which is responsible for mechanical and chemical cues. It is therefore essential to develop cell culture models that can accurately represent tumours. This will allow for a more representative milieu of the cancerous environment with better prediction of drug efficacy in preclinical assessments.(116)

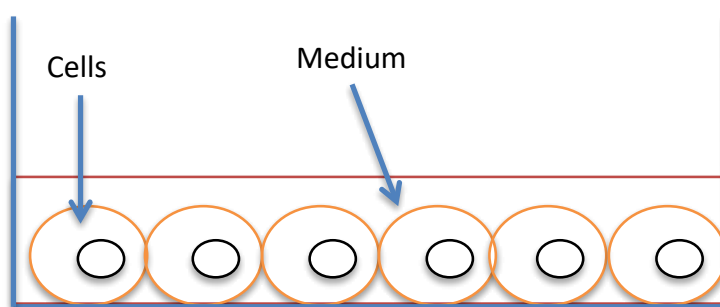


Figure 8. Cellular growth in the two-dimensional model.

1.5.2. Multicellular tumour spheroids

Three-dimensional cancer cell cultures imitate the organization of native tumour tissues *in vivo*. In 3D systems, cells are induced to aggregate by adhering to one another using cell-cell adhesion.(117) Gradients of nutrient delivery, oxygen transfer, waste removal and proliferation are evident in multicellular tumour spheroids (MCTS).(34, 85) Large multicellular tumour spheroids (MCTS; >200 μm in diameter) display three distinct regions, including a proliferative periphery region, a viable but quiescent intermediate region, and necrotic core (Figure 9).(82, 117) The process of MCTS formation includes three steps: (i) separated cells move closer to constitute the loose aggregates due to long chain ECM fibres with multiple RGD (tripeptide Arg-Gly-Asp) motifs, which can combine with the integrin on the cell membrane; (ii) expression of cadherin increases on the cellular membrane due to the cell-cell interaction; (iii) cells move together to form solid aggregates and constitute MCTS because of homotypic cadherin-cadherin binding (Figure 10).(118) Multicellular tumour spheroids have been used as models for various experimental studies on

radiotherapy, chemotherapy, radioimmunotherapy, cell- and antibody-based immunotherapy, hyperthermia, gene therapy, and photodynamic treatment. Multicellular tumour spheroids serve as the basis for the microenvironmental regulation of proliferation, viability, energy metabolism, nutrient metabolism, invasion, cell-cell interaction, and extracellular matrix composition.(92)

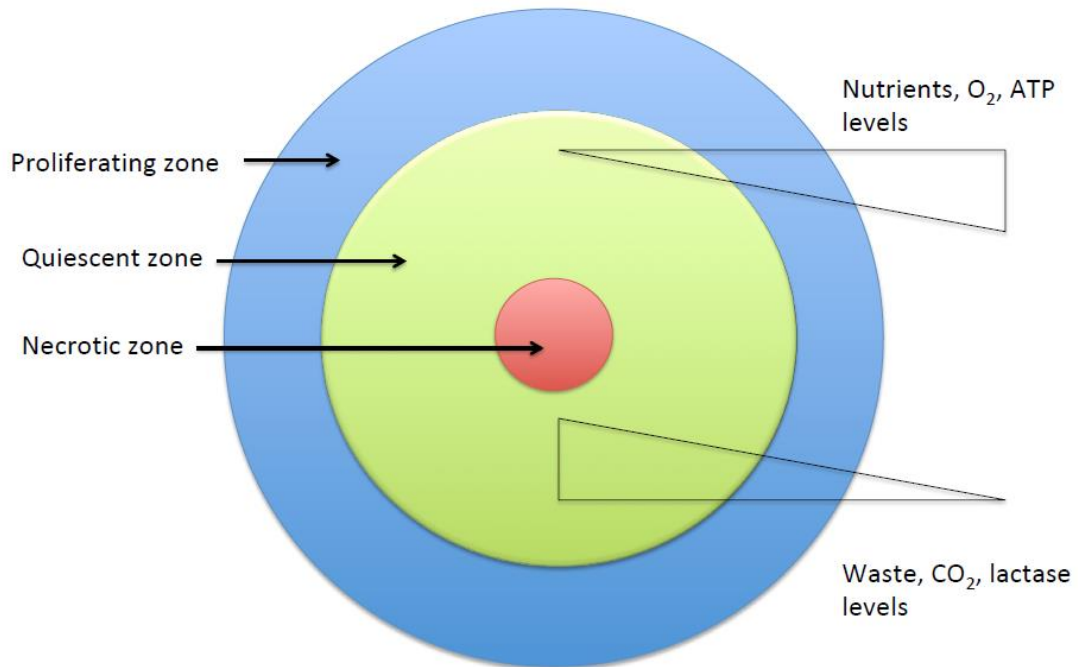


Figure 9. The structure and microenvironment of multicellular tumour spheroid.

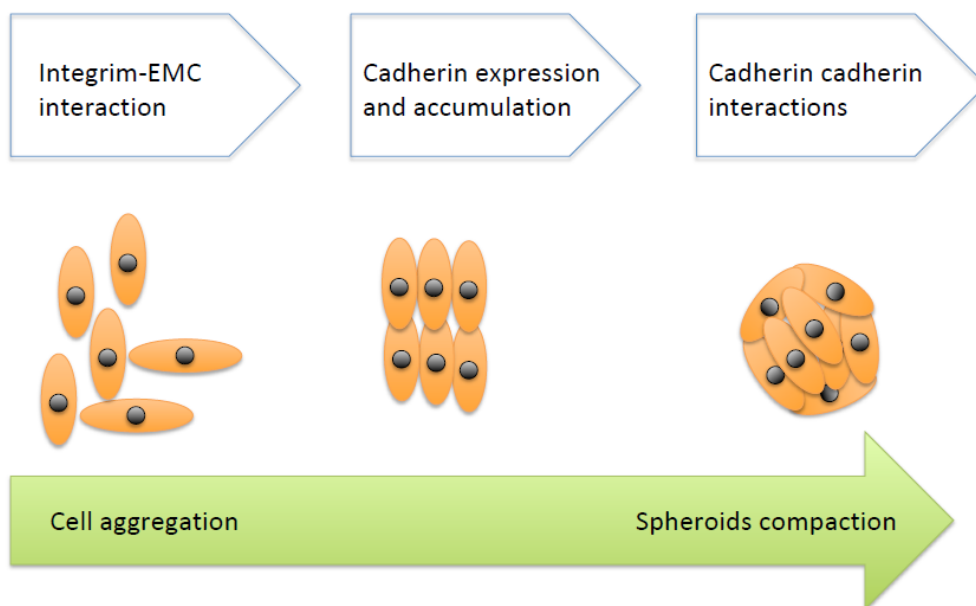


Figure 10. The formation of multicellular spheroids.

Multicellular tumour spheroids have important advantages for chemotherapeutic assessments. MCTS recreate the morphological and functional features of the tumour *in vivo* so that they may serve as more representative models.(112, 119-122) The intricate micromilieu that has been shown to exist in tumours and MCTS is mostly absent in monolayer cultures. These spheroids create gradients of oxygen, nutrients, metabolites, and soluble signals. Due to the differential availability of such factors, heterogeneous cell populations arise (necrotic, quiescent and proliferative cells) with a well-defined geometry and physiological cell-cell and cell-extracellular matrix interactions in the spheroids.(90, 123, 124) To further improve the spheroid system, co-cultures with cell types regularly found in *in vivo* tumour environments can be done to generate more complex, but physiologically relevant, cultures.(125, 126)

1.6. Aim

The aim of the study was to investigate the potential use of a 3D culture system for future compound screening by investigating the effect of the known anticancer compound (doxorubicin) on the cell cycle of BT-20 triple-negative breast carcinoma cells in a 2D and 3D model of cell growth.

1.7. Objectives

The objectives of the study are:

- To establish reproducible BT-20 spheroids.
- To compare the basal growth characteristics of BT-20 cells grown in both monolayer and spheroid culture systems in terms of: morphology, live-dead status, protein content, cellular conversion, acid phosphatase activity, and cell cycle kinetics.
- To determine the effect of doxorubicin on growth characteristics of BT-20 cells grown in monolayer and spheroid cultures with reference to: morphology, live-dead status, protein content, acid phosphatase activity, cell cycle kinetics and p53 expression

Chapter 2

Materials and methods

For this study, ethical clearance was obtained from the Research Ethics Committee of the Faculty of Health Sciences, University of Pretoria (Appendix I; REC 214/2017). All reagents used, as well as the preparation thereof and relevant recipes, are listed in Appendix II.

2.1. Culture protocol of the BT-20 cell line

The BT-20 triple-negative breast carcinoma cell line (ATCC® HTB-19™) was gifted by the Department of Physiology, University of Pretoria (originally obtained from Cellonex, Johannesburg, South Africa). Cells were cultured in 75 cm² cell culture flasks and maintained in a 1:1 mixture of Dulbecco's Modified Eagle's Medium (DMEM) and Ham's F12 nutrient medium supplemented with 1% nonessential amino acids, 1% L-glutamine, 100 U/mL penicillin, 100 U/mL streptomycin and 10% heat-inactivated foetal calf serum (FCS). Cells were grown at 37°C in a humidified atmosphere with 5% CO₂. Cells were grown to 70% confluence, washed with sterile phosphate-buffered saline (PBS) and harvested using trypsinisation. Detached cells were centrifuged (Beckman Allegra X-14/R Series Benchtop Centrifuge, Beckman Coulter) at 200 *g* for 5 min, and the cell pellet was resuspended in 1 mL 10% FCS-fortified medium. The cellular concentration was determined using the trypan blue (0.1% w/v) exclusion assay and a haemocytometer. Cells were diluted to 4 x 10⁵ cells/mL in 10% FCS-supplemented medium.

2.2. Seeding of cells as monolayer and spheroid cultures

The liquid overlay technique is a simple and cost-effective technique to culture MCTS.(127) By creating a low-attachment surface with agarose, cells cannot attach to the culture surface, and thus rather attach to one another. This allows for self-assembly into a 3D structure (128, 129) with individual assessment possible due to isolated growth.(130)

Cellular monolayers were cultured by seeding 4 x 10⁴ cells (100 µL cells/well) into sterile 96-well plates. Plates were incubated overnight to allow for attachment to the surface of the plate.

Spheroids were cultured using a modified version of the liquid overlay technique as described previously.(127) Standard operating procedures were optimized by the Department of Physiology as part of an ongoing study, and were replicated in this study with an increased cell number. Prior to seeding of cells, 70 µL sterile 1%

agarose (w/v in medium) was pipetted into 96-well plates while rotating the plate gently to allow for proper coverage. Plates were allowed to cool down so that an agarose plug was formed at the bottom of the plate. Cells (100 μ L) were pipetted onto the agarose plugs to achieve 4×10^4 cells/well, with an additional aliquot of 100 μ L 10% FCS-supplemented medium added to each well. Plates were incubated for four days, after which 100 μ L medium was exchanged daily with fresh medium. Spheroids were cultured for ten days. To assess spheroid characteristics, the following endpoints were assessed: size and volume, protein content, metabolic activity and viability.

2.3. Microscopic evaluation of spheroid size and volume

Spheroids were observed by phase contrast microscopy using an AxioVision phase contrast light microscope (Zeiss, Jena, Germany) on days 4, 7 and 10 using a 5X objective. The diameter of each spheroid was measured in ImageJ (National Institute of Health and the Laboratory for Optical and Computational Instrumentation).(131) The volume calculated using the following formula (132):

$$Volume = \frac{4}{3} \pi \frac{1}{8} d^3, \text{ where } d \text{ is the diameter of the spheroid.}$$

2.4. Fluorometric determination of metabolic capacity of monolayer and spheroids cultures

Resazurin conversion is a simple, efficient and reliable method to test cellular metabolic capacity as a surrogate for viability. The dye is not cytotoxic, thus cells can be used for further experiments post-analysis. Resazurin is a blue, weakly fluorescent molecule, however, when reduced to resorufin by viable cells in cytoplasm, it is converted to a pink, highly fluorescent molecule (Figure 11), which is the irreversible reaction and mediated by intracellular diaphorase enzymes.(133)

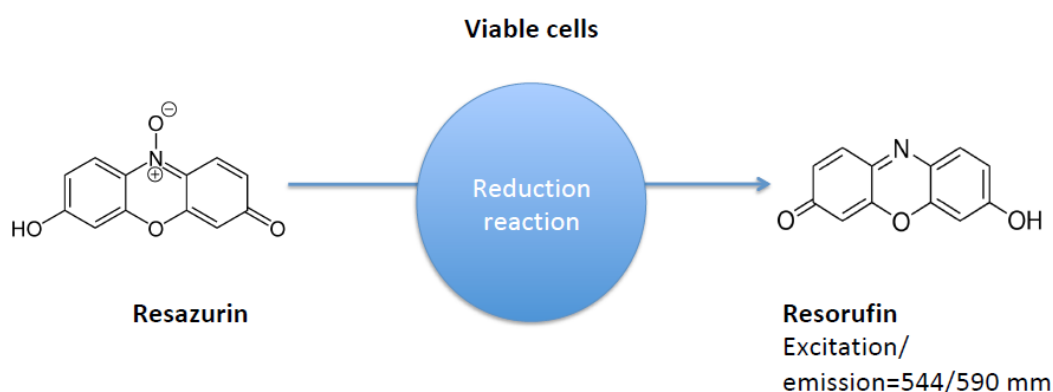


Figure 11. Resazurin is converted by metabolically active cells to the fluorescent product, resorufin.(134)

An aliquot of medium (100 μ L) of monolayer and spheroid cultures was replaced with 100 μ L resazurin (60 μ M; diluted in PBS), and the plate incubated for 2 h. Blanks contained resazurin alone. A 100 μ L aliquot of the supernatant of each well was transferred to a white microtiter plate, and the intensity measured at an excitation and emission wavelength of 544 nm and 590 nm, respectively, using a FLUOstar Optima fluorometer (BMG Labtech, Heidelberg, Germany).

2.5. Spectrophotometric determination of protein content of monolayer and spheroids cultures

The bicinchoninic acid (BCA) protein assay is one of the most widely used methods to assess protein content. Copper ions (Cu^{2+}) in an alkaline medium are reduced to Cu^+ by proteins, which then react with two BCA molecules to form a purple complex.(135)

Monolayer cultures were washed twice with 100 μ L PBS and collected through trypsinisation. Spheroids (N = 5-8) were harvested using a pipette tip, combined and washed twice with 1% FCS-supplemented PBS. Collected cells and spheroids were lysed in 50 μ L radio-immunoprecipitation assay (RIPA) buffer for 30 min in a sonicator (40 KHz; Branson 52, Branson Cleaning Equipment Co.) with ice. Lysates were stored at -80°C until needed.

Reagent A (50 parts, containing 0.1% [w/v] sodium bicinchoninate, 2% [w/v] sodium carbonate decahydrate, 0.16% [w/v] sodium tartrate dihydrate, 4% [w/v] sodium hydroxide and 0.95% [w/v] sodium bicarbonate, pH = 11.25) and reagent B (1 part, 4% [w/v] copper sulfate pentahydrate) were mixed prior to experimentation. Lysates were centrifuged (Beckman Allegra X-14/R Series Benchtop Centrifuge, Beckman Coulter) at 16 000 g for 10 min. Into 96-well plates, 5 μ L sample and 195 μ L BCA working solution was added. Samples were either PBS (blank), bovine serum albumin (BSA) standard (five half-dilutions of a 1 000 $\mu\text{g}/\text{mL}$), or lysate. Plates were covered with film and incubated for 30 min at 37°C . The absorbance was measured at 562 nm with an ELX800 microplate reader (Bio-Tek Industries, Inc).

2.6. Determination of viability status of cells in monolayer and spheroids cultures

Cell viability assessment was performed by using a dual staining method staining viable and deceased cells. Fluorescein diacetate (3'6'-diacetyl-fluorescein) (FDA) (excitation/emission=493/510 nm) is a colourless compound which enters viable cells where it is hydrolysed to the highly fluorescent compound, fluorescein.(86) Propidium iodide (PI) (excitation/emission=540/625 nm) is a

membrane impermeant dye that is excluded from viable cells, but can enter cells with compromised cell membranes; as such, PI enters apoptotic or necrotic cells where it binds to double-stranded DNA by intercalating between base pairs.(136) Therefore, viable cells will fluoresce at 488 nm while non-viable cells will fluoresce at 562 nm.(137)

Monolayer cultures were seeded into 6-well plates at 1×10^6 cells/well and allowed to attach overnight. Spheroids (4, 7 and 10 days) were washed with 1 mL PBS and transferred to a 24-well plate. Monolayer and spheroid cultures were washed twice with 1 mL PBS, and stained with 1 mL staining solution (4 $\mu\text{g}/\text{mL}$ FDA; 3 $\mu\text{g}/\text{mL}$ PI) for 4 min at 37°C . Samples were washed twice with PBS and observed using a fluorescence microscope (Zeiss, Jena, Germany) in 1 mL PBS. The filter sets for FDA and PI are FITC and Taxe filters.

2.7. Flow cytometric determination of cell cycle of monolayer and spheroid cultures

Cellular monolayers were cultured in 6-well plates for 24 h. Attached cells were collected through trypsinisation and centrifuged at $200 g$ for 5 min.

Spheroids were transferred to a 1.5 mL tube, washed with PBS and dissociated by trypsinisation (5 min) and aspiration with a pipette. Monolayer cells and dissociated spheroids were washed twice with 1 mL PBS supplemented with 1% FCS. Cells were fixed by adding 3 mL cold 70% ethanol drop-wise under agitation. Fixed cells were incubated overnight at 4°C , after which they were centrifuged at $200 g$ for 5 min and the supernatant discarded. Cells were stained with 1 mL PI staining solution (containing 40 $\mu\text{g}/\text{mL}$ PI, 100 $\mu\text{g}/\text{mL}$ DNA-free RNase and 0.1% Triton X-100) for 40 min and analyzed flow cytometrically (Beckman FC500 flow cytometer, Beckman Coulter) using FL3 (excitation: 488 nm, emission: 620 nm).

2.8. Analysis of the cytotoxic effect of doxorubicin on BT-20 cells in monolayer and spheroid cultures

2.8.1. Measurement of monolayer cell density

The effect of doxorubicin on cell density was determined using the sulforhodamine B (SRB) staining assay according to Voigt *et al.* (2005). The SRB assay is a widely used method for *in vitro* cytotoxicity screening. The assay relies on the ability of SRB to bind protein components of cells that have been fixed to tissue-culture plates by trichloroacetic acid (TCA). Sulforhodamine B is a bright-pink aminoxanthene dye with two sulfonic groups that bind to basic amino-acid residues under mild acidic conditions, while dissociating under basic conditions. As the binding of SRB is stoichiometric, the amount of dye extracted from stained cells is directly proportional to the cell mass.(138)

Monolayer cultures (as seeded in Section 2.2) were treated with 100 μ L negative control (medium), vehicle control (0.2% dimethyl sulfoxide [DMSO]), positive control (1% saponin) or doxorubicin (half-log dilutions of 40 μ M) prepared in FCS-free medium. Blanks containing 200 μ L medium alone (5%-FCS supplemented) were used to account for background noise. Plates were incubated for 72 h, after which cell density was determined. Cells were fixed with 50 μ L cold 50% TCA overnight at 4°C. Plates were rinsed with running tap water, and 100 μ L SRB solution (0.057% [w/v] in 1% acetic acid) added to each well for 30 min. Plates were washed three times with 100 μ L acetic acid (1% [v/v]) and allowed to dry at 40°C. Bound dye was dissolved in 200 μ L Tris buffer (10 mM, pH 10.5). The optical density was measured by using an ELX800UV microplate reader (Bio-Tek) at 540 nm (reference 630 nm). All values were blank subtracted, and the cell density expressed as a percentage of the negative control. The inhibitory concentrations reducing 25% (IC₂₅), 50% (IC₅₀) and 75% (IC₇₅) of growth were calculated using non-linear regression.

2.8.2. Exposure of monolayer and spheroid cultures to doxorubicin

Spheroids (day 4) were exposed to the IC₂₅ (1.4 μ M), IC₅₀ (3.6 μ M) and IC₇₅ (11.75 μ M) of doxorubicin as determined in 2D for 72 h, and assessed for changes in size and volume (Section 2.3.), metabolic activity (Section 2.4.), acid phosphatase activity (APH; Section 2.8.3.), protein content (Section 2.5.), cell viability staining (Section 2.6), cell cycle kinetics (Section 2.7.) and p53 expression (Section 2.8.4.). Monolayers were exposed and measured similarly for comparison.

2.8.3. Alteration to acid phosphatase activity of exposed monolayer and spheroid cultures

Various cytotoxicity assays are available for the investigation of a drug's effect on cell cultures,(139-142) however, the APH assay has been described to be a low labour alternative for spheroid assessments. The APH assay has been used in both monolayer and spheroid studies, where the product absorption is proportional to the viable cell number in the range of 10³ to 10⁵ monolayer cells(143) and offers high linearity.(144) During the resazurin reduction assay, the fluorescence of resorufin wasn't detected in spheroid cultures, thus the APH assay was used as a surrogate to measure cell viability. The APH assay is based on the quantification of intracellular APH activity. Cytosolic APH in viable cells hydrolyses *p*-nitrophenyl phosphate to *p*-nitrophenol, of which absorption is proportional to the viability of cells (Figure 12).(89)

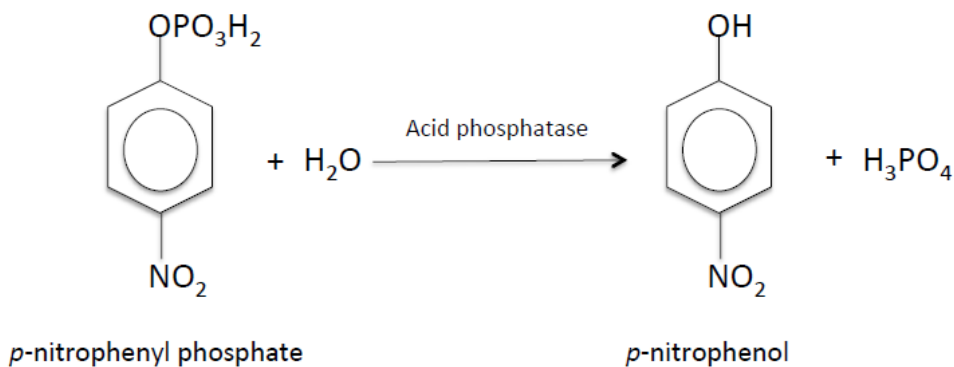


Figure 12. Representation of the cytosolic APH catalysed reaction.(89)

Monolayer and spheroid cultures were washed with 100 μ L PBS. Spheroids were transferred to clear 96-well plates in 100 μ L PBS. An aliquot of assay buffer (100 μ L; 0.1 M sodium acetate, 0.1% Triton-X-100 and 0.2% p-nitrophenyl phosphate) was added to each well, and incubated for 90 min at 37°C. After incubation, 10 μ L of 1 M sodium hydroxide was pipetted into each well to stop the reaction. The absorption was measured at 405 nm using an ELX800UV microplate reader (Bio-Tek).

2.8.4. p53 expression of exposed monolayer cultures and spheroids

Sodium dodecyl sulfate polyacrylamide gel electrophoresis (SDS-PAGE) and Western blotting are widely used to assess protein expression levels. Protein lysates are separated by gel electrophoresis based on molecular weight. Separated proteins are transferred to a membrane. Antibodies targeting p53 are added to visualise only p53 protein using chemiluminescence.(145)

Laemmli sample buffer (50 μ L) was added to 50 μ L lysate, after which it was heated for 5 min at 100°C. A Criterion TXG Stain-Free gel (Bio-Rad Laboratories, Johannesburg, South Africa) was placed inside an electrophoresis chamber, which was filled with running buffer. Lysate (10 μ g protein as determined by BCA assay) or 5 μ L stain-free standards were pipetted into wells. The gel was initially developed at 60 V and then at 200 V until the dye front reached the bottom of the gel. The gel was removed from the electrophoresis chamber and washed with deionized water to remove SDS. The image of the gel was observed with a ChemiDoc MP (Bio-Rad, California, USA). Proteins were blotted onto polyvinylidene fluoride (PDVF) membranes using a Trans-Blot Turbo Instrument (Bio-Rad, California, USA). The gel was placed on top of the membrane and covered with the top pad. The sandwich was rolled to remove air bubbles, the lid placed on the cassette, and the instrument locked. The cassette was placed into the Trans-Bolt Turbo Instrument, and the transfer was performed for 7 min. After transfer, the membrane was blocked with 3% BSA in Tris-buffered saline

Tween-20 (TBST) for 30 min. The mouse anti-p53 antibody (Celtic Diagnostics, South Africa) was diluted (1:1000) in 15 mL blocking buffer. The membrane was incubated with the primary antibody overnight at 4°C on a shaker. The membrane was washed five times with 20 mL TBST for 5 min. A secondary antibody conjugated to horseradish peroxidase (goat anti-mouse) (Celtic Diagnostics, South Africa) diluted in 15 mL blocking buffer (1:5000) was added to the membrane and incubated for 1 h. The membrane was washed five times. The membrane was placed into a ChemiDoc MP, and 800 µL Clarity Western ECL substrate added onto it. The reaction was developed for 5 min. After visualisation of the protein bands, the membrane was washed with 20 mL TBST five times and stained for β-actin (mouse; Bio-Rad, California, USA) as above. p53 expression was expressed as fold difference relative to β-actin expression.

2.9. Statistics

Data is stored in the Department of Pharmacology for a minimum of 15 years on at least two digital mediums. All experiments were conducted with intra- and inter- triplicates. Data was compiled in Microsoft Excel (Word 2010) and the result expressed as the mean ± standard error of the mean (SEM). Statistical analysis was done using GraphPad Prism 5.0 (Prism Software). Kruskal-Wallis, with a post-hoc Dunn's test was used to assess differences between concentrations. Histogram plots of propidium iodide distribution were divided into regions for sub-G1, G0/G1, S and G2/M using CXP Analysis. Western blot results were analysed using Image Lab. Flow cytometric and Western blot results were compared using two-way ANOVA. A $p < 0.05$ was considered significant.

Chapter 3

Results

3.1. Growth characteristics of BT-20 spheroids

3.1.1. Spheroid structure, size and volume

The spheroid model established by Dr Iman van den Bout in the Department of Physiology (University of Pretoria) was adjusted slightly in terms of cell number used. The BT-20 cell line displays a long doubling time of 51 h,(146) thus 40 000 cells per well were used to establish a sufficiently large spheroid to be used within the experimental time. Monolayer cultures attached to the plate surface after overnight culturing. Morphological assessment using both light microscopy and cell viability staining indicated no observable detriments to cell growth, and thus cultures were considered healthy for downstream biological assessments. BT-20 cells were successfully grown both as monolayer (Figure 13A) and spheroid cultures (Figure 13B-D). BT-20 cells grew unhindered on agarose for four days, which led to the formation of reproducible, compact spheroids (Figure 12B). At seven and ten days after plating, spheroids decreased in size but their shape remained consistent (Figure 13C, D). An increase in loose cells and cellular debris was observed over the ten days of culturing. In comparison to the spheroids obtained on day 4 (volume = 0.36 mm³), the volume decreased to 0.27 mm³ at day 7, and 0.23 mm³ at day 10 (Figure 14).

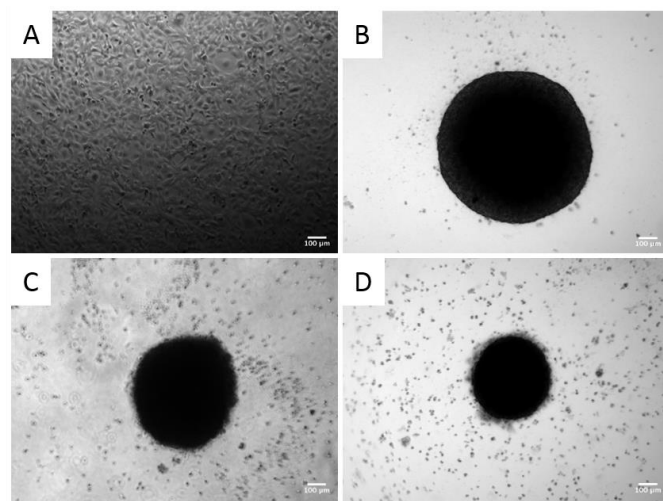


Figure 13. Representative images about the morphology of cells grown as a monolayer culture and spheroids (5X objective). A) Monolayer culture 24 h post-seeding; spheroids at B) 4-, C) 7- and D) 10-day post-seeding.

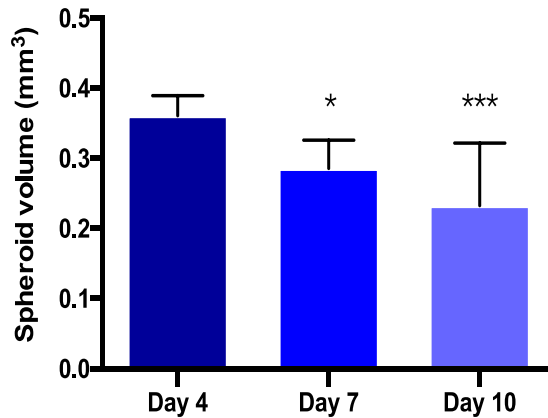


Figure 14. Volume of spheroids over the 10-day culturing period. Day 4 = $0.36 \pm 0.03 \text{ mm}^3$; day 7 = $0.29 \pm 0.04 \text{ mm}^3$; day 10 = $0.23 \pm 0.09 \text{ mm}^3$. Significance is based on comparisons between day 4 and other culturing days. * $p < 0.05$, *** $p < 0.001$ (N = 9).

3.1.2. Metabolic capacity of spheroids

The conversion of resazurin to resorufin was used to measure cell viability with cellular metabolism as surrogate marker. Although an increase in resorufin fluorescence was detected in monolayer cultures (relative fluorescence intensity [RFI]: 1234), little fluorescence was observed for spheroids throughout the culture period (RFI: 11.82 to 29.45) (Figure 15). Given the lack of fluorescence, suspicions of lack of permeation of resazurin into the spheroid or lack of conversion to resorufin was assessed using fluorescence microscopy. Spheroids exposed to resazurin were observed to fluoresce under microscopy (Figure 16).

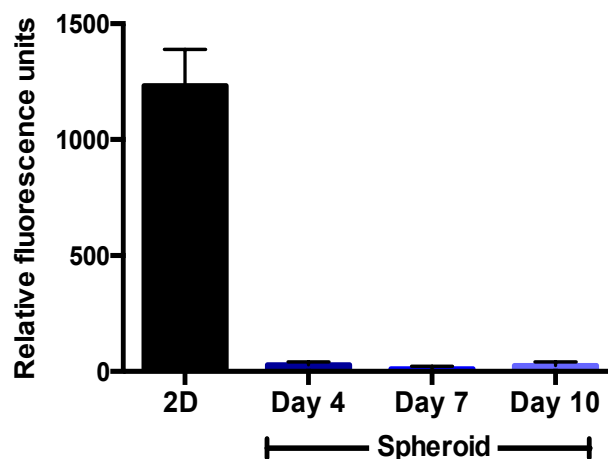


Figure 15. Metabolic capacity of monolayer and spheroid cultures measured as relative fluorescence intensity of 2D (1234 ± 156.3), 4-day (29.45 ± 11.98), 7-day (11.82 ± 10.9) and 10-day (25.5 ± 16.09) spheroids (N=12).

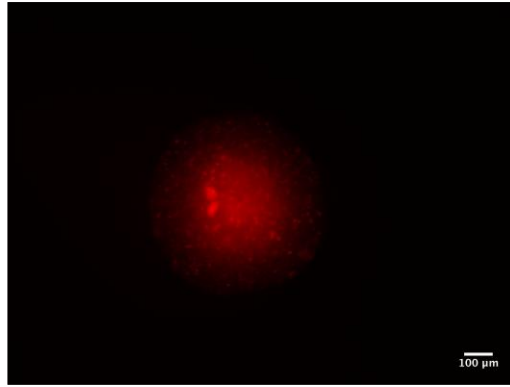


Figure 16. A representative image of spheroid exposed to resazurin indicating localisation and lack resorufin release into surrounding media (5X objective).

3.1.3. Viability staining of spheroids

Fluorescein diacetate (green fluorescence) and PI (red fluorescence) staining was used to determine the viability of spheroids. Cells grown as a monolayer culture did not display noticeable signs of PI staining, while strong fluorescein staining was observed (Figure 17A). Spheroids grown for four days displayed a broad outer layer of intense green fluorescence, while the central core was devoid of fluorescence (Figure 17B). At the same time, PI staining was absent in the broad outer region positive for fluorescein, but intense staining was confined to the central spheroid core. Surprisingly, spheroids grown for seven and ten days no longer had a central core displaying PI fluorescence. Instead, a gradient of fluorescein was present throughout the spheroid with a thin outer layer most fluorescent and the rest of the spheroid displaying lower but visible fluorescence (Figure 17C,D).

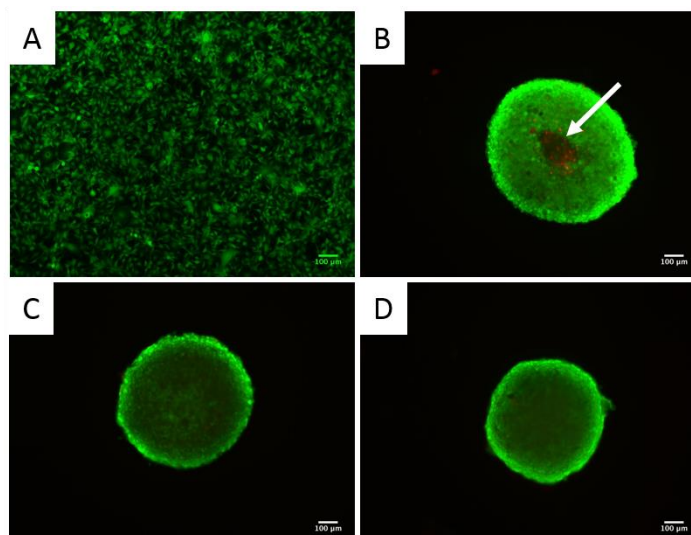


Figure 17. Representative images about viability of cells grown as a monolayer culture and spheroids using fluorescein diacetate-propidium iodide live-dead staining (5X objective). A) Monolayer culture 24 h post-seeding; spheroids at B) 4-, C) 7- and D) 10-day post-seeding. The white arrow indicates increase propidium iodide staining in the spheroid, suggesting a necrotic core.

3.1.4. Protein content and acid phosphatase activity of spheroids

Protein content is an important parameter to monitor the growth of cells over a period of time, and thus is seen as a surrogate for viability. In the traditional 2D drug screening, cells are seeded for 24 h to allow for attachment to the plate surface prior to treatment. For the purposes of the study, spheroids were grown for four days prior to exposure. As such, baseline characteristics of the culturing environment prior to exposure were determined.

Comparison was done between the baseline pre-exposure culture periods for both models. Monolayer cultures were lysed and protein content measured as 16.90 $\mu\text{g}/\text{well}$. Protein contents of spheroids from day 4 to day 10 were 9.60, 9.86 and 10.03 $\mu\text{g}/\text{well}$ (Figure 18). Although spheroid protein content increased by ~ 0.43 $\mu\text{g}/\text{spheroid}$ over the six days of culturing, this was not a significant increase.

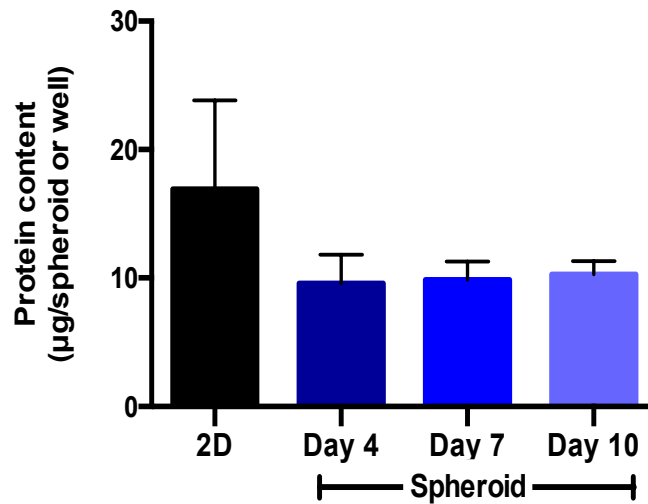


Figure 18. Protein content of cells grown in monolayer culture and spheroid model. 2D = 16.90 ± 6.93 µg/well; day 4 = 9.60 ± 2.22 µg/spheroid; day 7 = 9.86 ± 1.14 µg/spheroid; day 10 = 10.03 ± 1.02 µg/spheroid; N=9.

Acid phosphatase activity of spheroids did not change significantly during the culturing period (Figure 19).

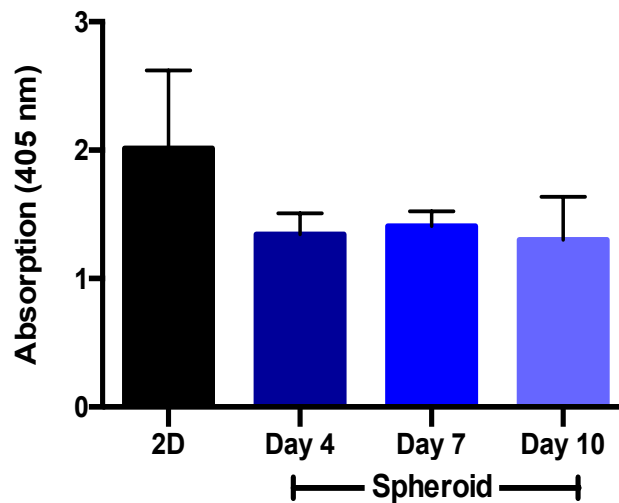


Figure 19. Acid phosphatase activity of cells grown as a monolayer culture and spheroids. 2D = 2.01 ± 0.61 ; day 4 = 1.34 ± 0.17 ; day 7 = 1.41 ± 0.11 ; day 10 = 1.3 ± 0.34 ; N=9.

When APH activity is normalised to protein content of each culturing environment, no significant difference is seen between any of the samples (2D: 0.12 absorption/µg; day 4: 0.14 absorption/µg; day 7: 0.14 absorption/µg; day 10: 0.13 absorption/µg).

3.1.5. Cellular kinetics of spheroids

The majority of cells collected at day 0 as a monolayer culture were in the G0/G1-phase (81.65%) (Figure 20, Table 4). Percentages of G0/G1-phase in monolayer and spheroids were significantly higher than other phases ($p < 0.05$). During growth as spheroids, a similar trend was observed for cells in the S- and G2/M-phase (~4 and ~7%, respectively), however, the G0/G1-phase cells decreased slightly as the sub-G1 phase increased. In comparison to day 4 of culture (12.50%), day 10 presented with 20.55% cells in the sub-G1 phase (Figure 20, Table 4).

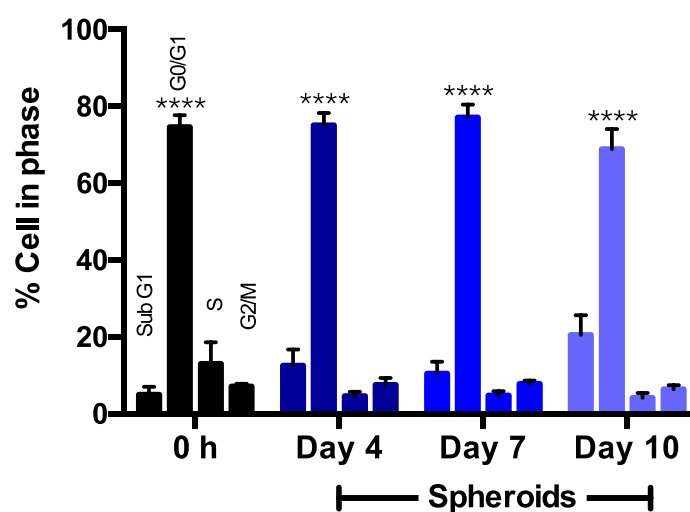


Figure 20. Cellular kinetics of cells grown as a monolayer culture and spheroids. Significance is based on comparisons between G0/G1 phase and the rest of phases in each group, **** $p < 0.0001$, N=6.

Table 4. Percentage of cells in each phase of the cell cycle in the monolayer culture and spheroids.

Culture	Sub-G1 (%)	G0/G1-phase (%)	S-phase (%)	G2/M-phase (%)
Monolayer (0 h)	4.92 ± 2.11	74.65 ± 3.08	13.03 ± 5.60	7.15 ± 0.68
Day 4	12.50 ± 4.22	75.08 ± 3.23	4.63 ± 1.05	7.55 ± 1.73
Day 7	10.48 ± 3.04	77.12 ± 3.36	4.82 ± 1.02	7.75 ± 0.89
Day 10	20.55 ± 5.11	68.90 ± 5.26	4.17 ± 1.24	6.37 ± 1.13

3.2. Comparison of the effect of doxorubicin in the monolayer and spheroid culture models

3.2.1. Doxorubicin reduced monolayer cell density

The cytotoxicity of doxorubicin was determined in monolayer cultures by SRB staining. There was no significant difference between the negative and vehicle control, while the positive control (saponin) decreased cell density significantly ($p < 0.001$) (Figure 21A). Doxorubicin displayed an IC_{25} , IC_{50} and IC_{75} of 1.4 μM , 3.6 μM and 11.75 μM after 72 h exposure in monolayers, respectively (Figure 21B). Doxorubicin gradually induced cytotoxicity between 0.4 μM and 12.8 μM . A maximum reduction 89.12% cell density occurred at 32 μM .

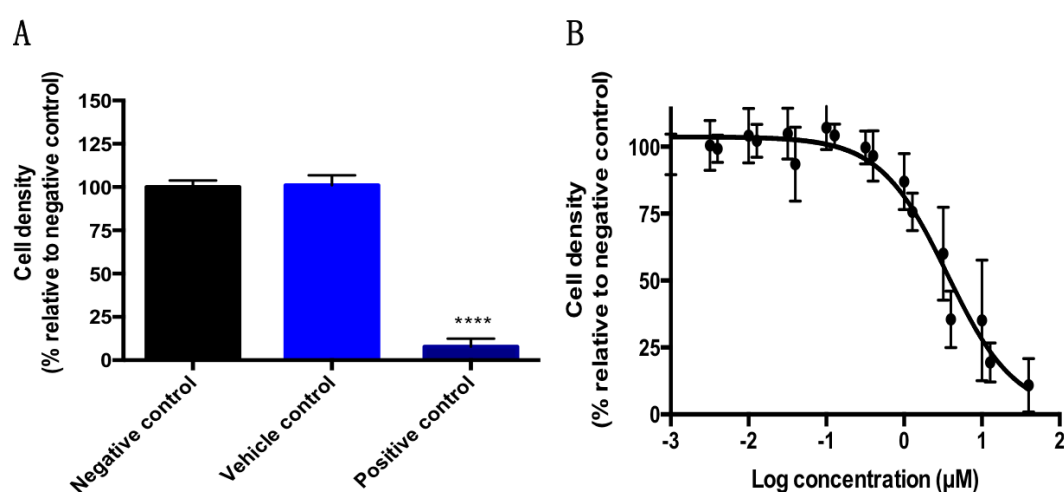


Figure 21. The effect of doxorubicin on cell density of cells grown in a monolayer culture after 72 h. A) Controls used during the assay, and B) dose-response curve of doxorubicin over a range of concentrations; Significant difference relative to the cell density of the negative control. **** $p < 0.0001$. $N = 6$.

3.2.2. Doxorubicin incurs cytotoxic morphological changes in monolayers at low concentrations, but requires higher concentrations in spheroids

Micrographs indicate that doxorubicin treatment at the IC_{25} , IC_{50} and IC_{75} in monolayer cultures were highly cytotoxic, with cells detached, floating or displaying elements of apoptosis (Figure 22). Spheroids treated with the IC_{25} and IC_{50} of doxorubicin were larger than the negative control, however, an increase in detached cells and/or cellular debris were observed (Figure 23). The volume of spheroids treated at the IC_{25} (0.32 mm^3) and IC_{50} (0.27 mm^3) were higher than the (147)negative control (0.15 mm^3) (Figure 24). Only spheroids treated with the IC_{75} displayed loss of integrity and shape, with slightly decreased volume (0.14 mm^3), and an increase in cellular debris.

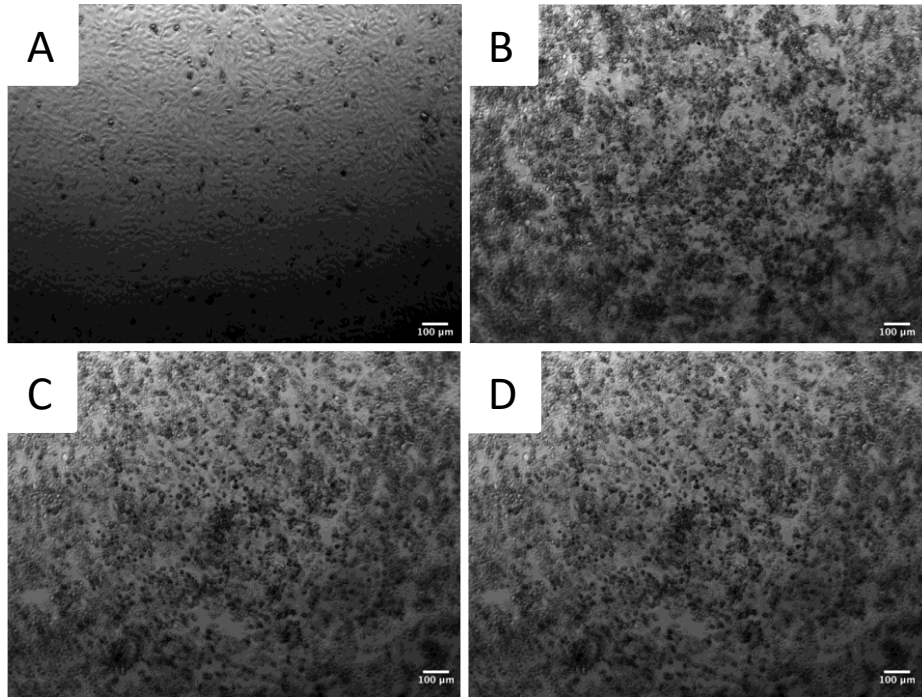


Figure 22. Representative images about morphology of monolayer cells treated by doxorubicin for 72 h and negative control (5X objective). A) Negative control; spheroids treated at B) IC₂₅, C) IC₅₀ and D) IC₇₅ concentration. All images were taken through the light microscope.

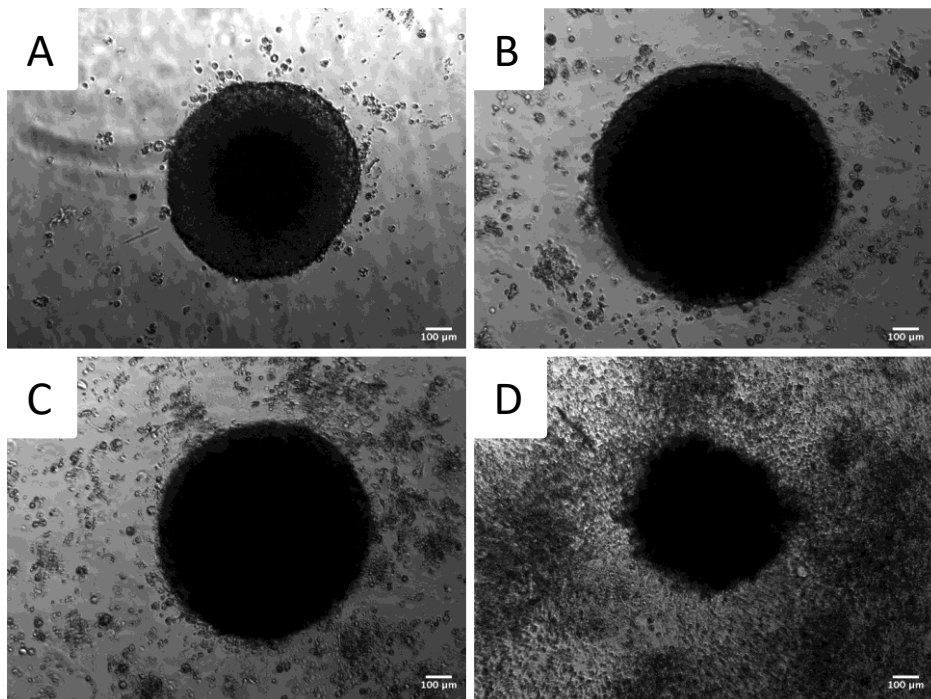


Figure 23. Representative images about morphology of spheroids treated by doxorubicin for 72 h and negative control (5X objective). A) Negative control; spheroids treated at B) IC₂₅, C) IC₅₀ and D) IC₇₅ concentration. All images were taken through the light microscope.

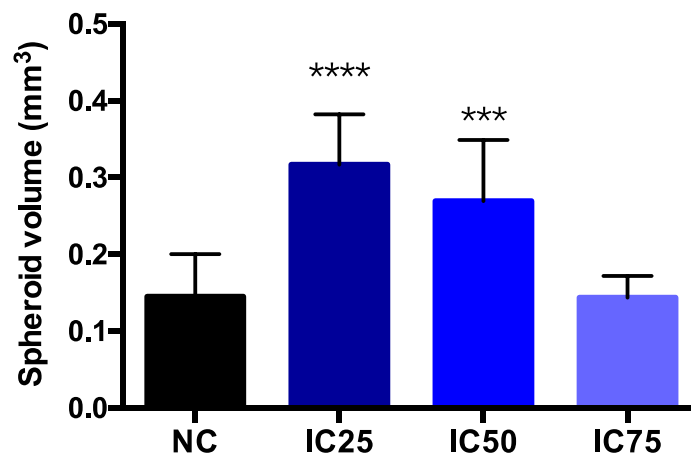


Figure 24. Volume of spheroids treated with doxorubicin after 72 h. Negative control (NC) = $0.15 \pm 0.06 \text{ mm}^3$; IC₂₅ = $0.32 \pm 0.07 \text{ mm}^3$, IC₅₀ = $0.27 \pm 0.08 \text{ mm}^3$, IC₇₅ = $0.14 \pm 0.03 \text{ mm}^3$; N=6; *** p<0.001 and **** p<0.0001.

3.2.3. Doxorubicin visibly decreases cell viability in spheroids and permeates the spheroid

Due to suspected interference from doxorubicin in live-dead staining, unstained spheroids were assessed for their ability to fluoresce in the same region of PI. Spheroids treated with doxorubicin displayed prominent fluorescence throughout the spheroid, however, fluorescence was less intense in the central core (Figure 25B). Doxorubicin thus does permeate the spheroid. Unfortunately, due to their fluorescence in a similar region of the electromagnetic spectrum, PI could thus not be used to determine the presence of compromised membranes. However, based on poor fluorescein diacetate cleavage, less viable cells were present suggesting cytotoxicity (Figure 25A).

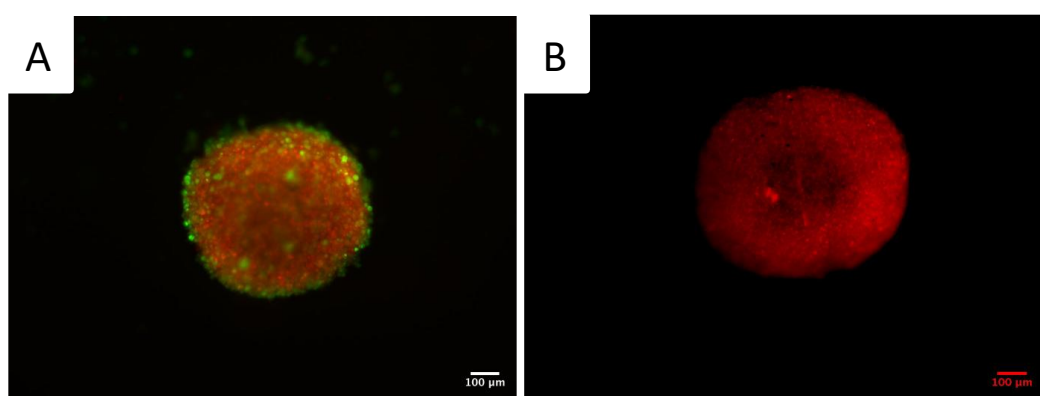


Figure 25. Representative images of spheroids exposed to doxorubicin at IC₂₅ for 72 h (5X objective). A) Spheroid stained by FDA-PI; B) unstained spheroid displaying doxorubicin fluorescence.

3.2.4. Doxorubicin reduces protein content at higher concentrations

Cells grown in monolayer culture displayed a significant decrease in protein content after treatment with doxorubicin: 28.38 $\mu\text{g}/\text{well}$, 5.51 $\mu\text{g}/\text{well}$ and 3.68 $\mu\text{g}/\text{well}$ for the IC₂₅, IC₅₀ and IC₇₅, respectively (Figure 26, Table 5). Protein content of the spheroids paralleled what was seen in micrographs (Figure 23), which did not differ significantly at the IC₂₅ (9.81 $\mu\text{g}/\text{spheroid}$) and IC₅₀ (8.03 $\mu\text{g}/\text{spheroid}$) compared to the negative control (8.98 $\mu\text{g}/\text{spheroid}$) (Figure 26, Table 5). However, exposure to the IC₇₅ decreased protein content significantly ($p < 0.0001$) by 6.51 $\mu\text{g}/\text{spheroid}$ (Figure 25, Table 5).

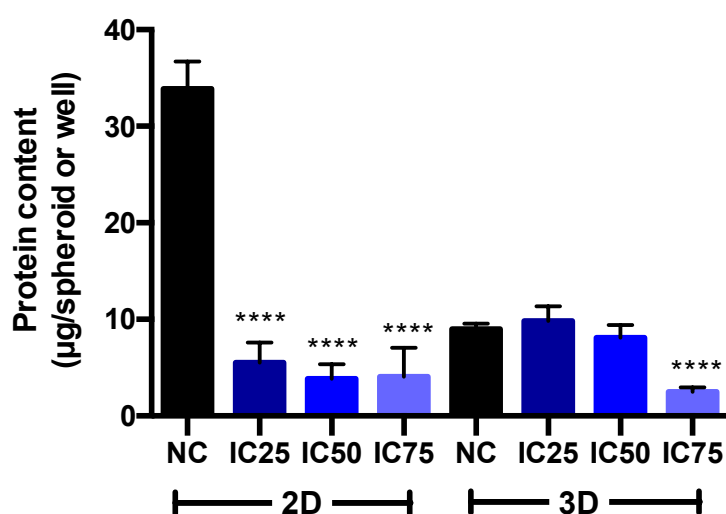


Figure 26. Protein content of cells cultured as a monolayer and spheroids after exposure to doxorubicin for 72 h. Significant difference relative to the protein content of the negative control in monolayer culture and spheroids. **** $p < 0.0001$. N=18.

Table 5. Protein content of cells after exposure to doxorubicin at IC₂₅, IC₅₀ and IC₇₅ in the monolayer culture and spheroids.

Sample	Monolayer culture ($\mu\text{g}/\text{well}$)	Spheroids ($\mu\text{g}/\text{spheroid}$)
Negative control	33.89 \pm 2.81	8.98 \pm 0.57
IC ₂₅	5.51 \pm 2.06	9.81 \pm 1.56
IC ₅₀	3.86 \pm 1.5	8.03 \pm 1.34
IC ₇₅	4.03 \pm 3.01	2.47 \pm 0.49

3.2.5. Doxorubicin decreases acid phosphatase activity at higher concentrations

Doxorubicin significantly decreased APH activity in monolayer cultures by 82.40%, 97.00% and 97.77% for the IC₂₅, IC₅₀ and IC₇₅, respectively (Figure 27). As with previous assays, spheroids were not significantly perturbed at the IC₂₅

and IC₅₀, with an increase of 10.70% and decrease of 0.73%, respectively, compared to the negative control. Treatment with the IC₇₅ significantly reduced APH activity by 76.28% compared to negative control (Figure 27).

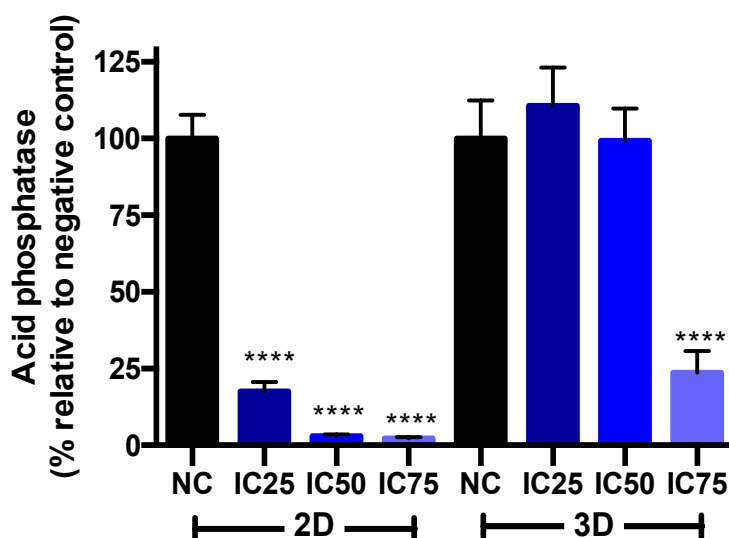


Figure 27. Acid phosphatase activity of monolayer culture and after 72 h exposure. **** $p < 0.0001$. N=9.

Table 6. Acid phosphatase activity of cells after exposure to doxorubicin at IC₂₅, IC₅₀ and IC₇₅ in the monolayer culture and spheroids.

Samples	Monolayer culture (%)	Spheroids (%)
NC	100.00 ± 7.781	100.00 ± 12.37
IC ₂₅	17.60 ± 3.07	110.70 ± 12.41
IC ₅₀	3.00 ± 0.48	99.27 ± 10.49
IC ₇₅	2.23 ± 0.40	23.72 ± 6.96

3.2.6 Doxorubicin blocks cells in the G2/M-phase in spheroid cultures, with associated DNA damage, due to p53-mediated activity

Due to the large increase of cells in the sub-G1-phase after exposure to doxorubicin in the monolayer culture, the sub-G1-phase was analysed separately. Cells in the sub-G1 phase increased significantly ($p < 0.0001$) in comparison to the negative control in the monolayer culture. After 72 h exposure to doxorubicin, a 59.01%, 69.79% and 68.33% increase was noted for exposure to the IC₂₅, IC₅₀ and IC₇₅, respectively (Figure 28A and Table 7). In spheroids, the percentage of cells in the sub-G1 phase increased by 12.32%, 17.54% and 36.04% in comparison to the negative control after exposure to doxorubicin at the IC₂₅, IC₅₀ and IC₇₅, respectively (Figure 29A and Table 9).

In the monolayer culture, doxorubicin treatment increased the amount of cells in

the S- and G2/M-phase similarly by 8.95% and 9.32%, respectively, for all concentrations (Figure 28B and Table 8). A similar trend was seen in spheroids, where exposure resulted in an increase on 2.32% and 9.42%, respectively, at all concentrations (Figure 29B and Table 10). These increases in both models were paralleled by a decrease of cells in the G0/G1-phase.

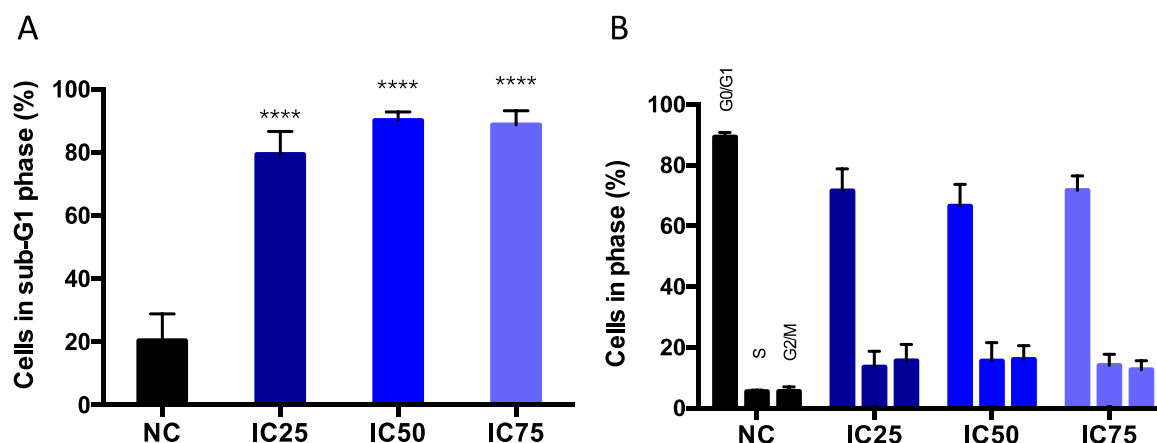


Figure 28. Cell cycle phases of cells exposed to doxorubicin at IC₂₅, IC₅₀ and IC₇₅ in monolayer culture. Significance in figure A is based on comparisons between negative control and each treatment group, **** p<0.0001, N=6. A) Sub-G1 phase; B) G0/G1-, S- and G2/M-phase.

Table 7. Percentage of cells in the sub-G1 phase of the monolayer culture after exposure to doxorubicin for 72 h.

Sample	Sub-G1(%)
Negative control	20.35 ± 8.50
IC ₂₅	79.36 ± 7.26
IC ₅₀	90.14 ± 2.67
IC ₇₅	88.68 ± 4.54

Table 8. Percentage of cells in the G0/G1-, S- and G2/M-phases of the monolayer culture after exposure to doxorubicin for 72 h.

Sample	G0/G1-phase (%)	S-phase (%)	G2/M-phase (%)
Negative control	89.18 ± 1.55	5.40 ± 0.48	5.48 ± 1.36
IC ₂₅	71.54 ± 7.22	13.54 ± 5.14	15.64 ± 5.35
IC ₅₀	66.52 ± 7.21	15.50 ± 6.01	16.02 ± 4.55
IC ₇₅	71.68 ± 4.79	14.02 ± 3.66	12.74 ± 2.91

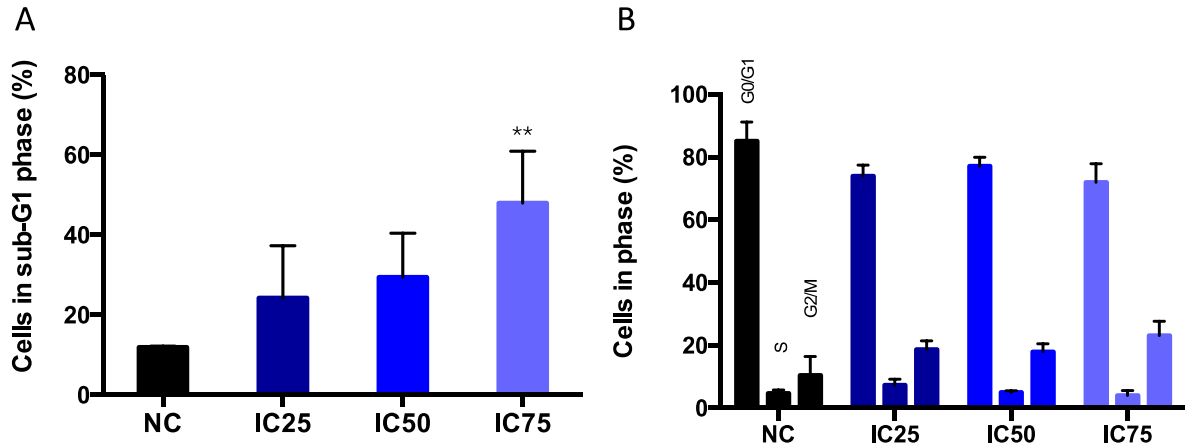


Figure 29. Cell cycle phases of cells exposed to doxorubicin at IC₂₅, IC₅₀ and IC₇₅ in spheroids. Significance in figure A is based on comparisons between negative control and each treatment group, ** p<0.01, N=5. A) Sub-G1 phase; B) G0/G1-, S- and G2/M-phase.

Table 9. Percentage of cells in the sub-G1 phase of the spheroid after exposure to doxorubicin for 72 h.

Sample	Sub-G1(%)
NC	11.90 ± 0.36
IC ₂₅	24.22 ± 13.06
IC ₅₀	29.44 ± 10.96
IC ₇₅	47.94 ± 13.03

Table 10. Percentage of cells in the G0/G1-, S- and G2/M-phases of the spheroid after exposure to doxorubicin for 72 h.

Sample	G0/G1-phase (%)	S-phase (%)	G2/M-phase (%)
NC	85.10 ± 6.15	4.70 ± 1.11	10.50 ± 5.98
IC ₂₅	73.94 ± 3.49	7.36 ± 1.82	18.68 ± 2.75
IC ₅₀	77.12 ± 2.84	5.00 ± 0.57	17.96 ± 2.62
IC ₇₅	71.92 ± 5.96	4.06 ± 1.57	23.12 ± 4.60

As doxorubicin was highly cytotoxic at the IC₅₀ and IC₇₅, reproducible and accurate results could not be obtained for p53 expression at these concentrations. The p53 expression was normalized to β-actin expression (as loading control). Compared to the negative control, the IC₂₅ of doxorubicin increased p53 expression by 2.6- and 1.5-fold in monolayer and spheroid cultures, respectively. (Figures 30 and 31, and Table 11).

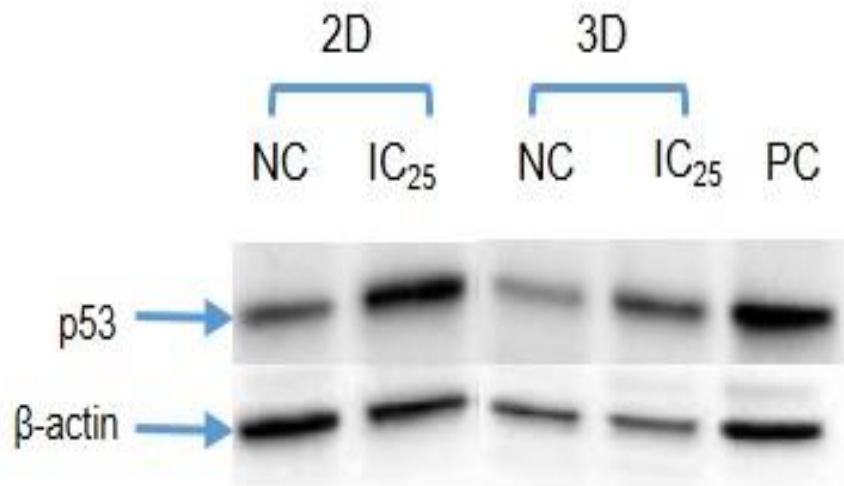


Figure 30. A representative image about expression of p53 in monolayer and spheroid cultures as measured by western blot.

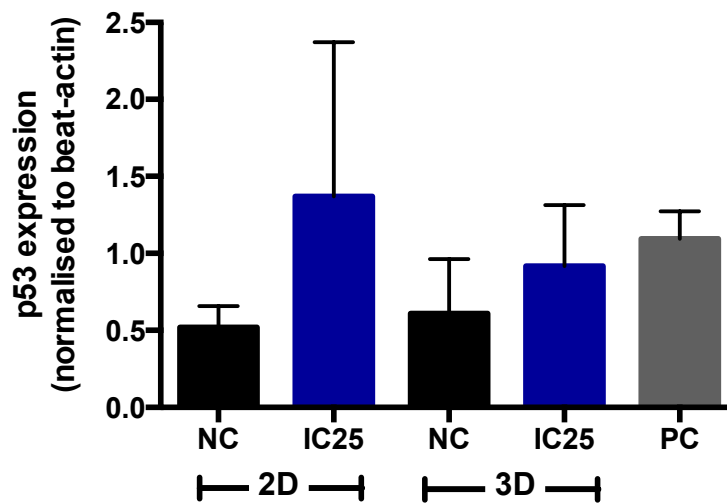


Figure 31. Expression of p53 in monolayer and spheroid cultures after exposure to doxorubicin for 72 h as measured by quantitation. Values were normalised to the β -actin loading control. N=6.

Table 11. Expression of p53 in monolayer and spheroid cultures after exposure to doxorubicin at IC₂₅ for 72 h. Values were normalised to the β -actin loading control.

Samples	Monolayer culture	Spheroids
NC	0.52±0.14	0.61±0.35
IC ₂₅	1.37±1	0.92±0.4
PC	1.1±0.18	

Chapter 4

Discussion

Three-dimensional spheroid culture models have been suggested as developmental tools for the evaluation of biological reactions in an environment that more closely represents the *in vivo* setting. Using spheroids, cancer-related studies may yield more accurate results during the investigation of anticancer drugs or molecular pathways that influence dormancy, resistance and recurrence. Compared to the traditional monolayer culture, MCTS offer physiological context which more closely represents the native tumour microenvironment.(148-151)

In monolayer cultures, cells are seeded onto the bottom of the well plate and thus typically grow with little overlap onto one another; this allows cells to be exposed to the same environment throughout.(152) All cells thus receive the same concentration of nutrients and oxygen, are rid of toxic metabolites at the same rate, lack different characteristics and are exposed to the same drug concentration.(153) This is not the reality within any organism, as cells form complex 3D structures that allow for gradients to be established. Cells in a low-attachment environment cannot adhere to the plate surface, and aggregate onto one another to form MCTS.(117) Thus, gradients of nutrient delivery, oxygen transfer, waste removal, drug exposure and proliferation are established as cells appear in different layers.(34, 85) Although spheroid cultures are more time-consuming and laborious than monolayer cultures, they are advantageous in their representation of the *in vivo* environment.

Using agarose, a low-attachment surface was created which facilitated the formation of reproducible, uniform spheroids four days after seeding. The BT-20 spheroids were circular, with a rounded, compact, dense appearance that did not permit light transmission. As seeding allowed for an edge of water within the 96-well plate, up to 60 spheroids could be formed from one seeding plate. Given their individual placement in the well, each spheroid could be individually assessed. Due to the robust nature of the spheroid, transferal between vessels was convenient and did not alter the morphology of spheroids. The liquid overlay method thus provided a simple way to generate large quantities of reproducible spheroids. Agarose was used due to its high water content and biocompatibility with downstream applications. The surface of agarose resists cellular adhesion, thus cells are forced to aggregate with one another instead.(128, 129) Adherent cells attach to each other via long-chain ECM fibres with multiple arginyglycylaspartic acid (RGD) motifs, which can combine with integrin on the

cell membrane.(118) The integrins, a family of cell-surface proteins, are receptors for cell adhesion molecules. Integrin interaction with the RGD motif allows for interaction of cells with the substratum and other cells.(154) Due to cell-to-cell interactions, membrane cadherin expression increases. As interactive forces increase, cells aggregates to multicellular tumor spheroids because of homotypic cadherin-cadherin binding.(118)

The resazurin assay was selected to determined metabolic capacity of viable cells as a surrogate for cell viability,(155, 156) however, spheroids did not produce noteworthy resorufin fluorescence. Fluorescent microscopy proved that resazurin did permeate the spheroid and successfully become converted to resorufin. During standard assays, resorufin is effluxed into the surrounding medium where it can then be detected by measurement of fluorescence.(157) As no efflux occurred, the assay is thus not suitable for BT-20 spheroid assessment with plate-reader measurement. Some compact spheroids have been shown to display poor resorufin release due to tight junctions formation, which was confirmed by the addition of the chelator, ethylene glycol-bis(2-aminoethylether)-N,N,N',N'-tetraacetic acid (EGTA), which destabilizes cell-cell interactions due to the exhaustion of calcium.(158, 159) As such, live-dead staining and APH activity was used to determine cytotoxicity effects.

In the present study, live-dead staining provided evidence of different zones of proliferation and viability. The data in this assay suggest that early after spheroid formation a necrotic zone with PI-positive and FDA-negative cells is present. However, after further culturing this zone is usurped by viable cells. At least early on, spheroids do display different zones including a viable outer zone and a necrotic central zone. Fluorescein release requires metabolically-active, viable cells, supporting the differential cellular activity observed throughout the spheroid. The size of spheroids is one of the critical parameters affecting the distribution of oxygen and nutrients to the inner regions of the spheroids.(125) Numerous spheroid models have shown that an increase in spheroid size decreases cell viability,(160) enlarges the necrotic core,(161, 162) induces quiescence (162) and reduces nutrient distribution.(163) As the size of the spheroid decreased from day four onwards, the reduced PI fluorescence could be a result of improved nutritional and oxygen status in the core of the spheroid. Literature supports this, where a 4% decrease in spheroid diameter reduced the total necrotic and quiescent zone by 39.8%.(125)

During the ten days of culturing, the size and volume of spheroids decreased, however, protein content and the overall shape remained stable. Lu *et al.* reported similar effects on protein content, where hepatocyte spheroids displayed relatively constant levels between four to eight days of culturing.(56) Given the stable protein content, it is suggested that compaction has occurred. Lin *et al.* monitored E-cadherin expression levels every 8 h during HepG2

spheroid formation, which showed an increase in expression.(118) Increased expression of such membrane proteins assist with the interaction of cells with one another, decreasing the size of a spheroid as distance reduces between them. As support to the compaction observed, fluorescence of fluorescein decreased with the passage of time in the centre of spheroids, which would suggest establishment of different zones of proliferation. Such factors are characteristic of compact spheroids.

Acid phosphatase activity of spheroids did not change significantly during the culturing period, which suggested that the number of viable cells in spheroids were stable during the culturing period. When APH activity was normalised to protein content, it was shown that a similar activity spectrum was produced, suggesting that viability was similar between both models.

Given the different zones formed within MCTS,(36, 82) the duration of cellular cycling will be different throughout the spheroid. The longest phase of the cell cycle is the G1 phase. During this phase, diploid cells synthesize protein required proteins required for DNA synthesis.(25) Nutrient, oxygen and ATP availability impacts on the cell cycle. In low nutrient conditions, cells proliferate slower and are arrested in the G0/G1-phase.(164) Analysis of the monolayer culture at 0 h showed that most cells were within the G0/G1 phase. Spheroid cultures displayed a similar circumstance, where the majority of cells were within the G0/G1-phase. As the PI assay cannot differentiate between cells in the quiescent G0-phase, it is expected that a percentage of these cells will form part of the dormant inner region of the spheroid.(165) Spheroids also displayed an increase in sub-G1-phase cells, suggesting increased DNA degradation, which would be indicative of cells undergoing cell death.(166) Cells in the inner regions of the spheroid are exposed to lower concentrations of nutrients and higher levels of metabolic waste, thus leading to an inhospitable environment for viable cells, leading to apoptosis or necrosis.(34, 85) Although the G0/G1-phase was higher in spheroids, the percentage of cells within the S-phase was non-significantly lower, with a slight trend for non-significant higher G2/M-phase cells. This suggests that cells have reduced proliferative capacity, which concurs with literature. It may further propose that quiescent cells are present within the spheroid. Antiproliferative drugs may have reduced efficacy within such a space as activity is directed towards fast-proliferating cells, and not slowly proliferating or quiescent cells, or those within a hypoxic environment.(167, 168) Compared to monolayer cultures, a low level of proliferation was observed as cells gradually moved from the S-phase and G2/M-phase to G0/G1-phase. It may suggest that quiescent cells were exhibited in the spheroids. Appearance of quiescent cells in the spheroids is associated with a decrease in cellular metabolism, which are typically not targeted by chemotherapeutic drugs. As such, spheroid viability may be increased as it is not susceptible to treatment. Gong *et al.* reported similar results, which indicated that the higher percentage of G0/G1-phase cells

represented quiescent cells in MCF-7 spheroids, with low proliferation due to decrease S- and G2/M-phase cells.(169) Given the results presented, spheroids remain viable through the course of the culturing period, and while presenting with reduced proliferative capacity, they do compact. Such characteristics are in line with that presented in *in vivo* settings, and as such should present with a greater representation than monolayer cultures.

As the BT-20 cell line displays a doubling time of 51 h, doxorubicin cytotoxicity was assessed after 72 h exposure to allow for a proliferative phase to occur. The cytotoxicity of doxorubicin in the present study is lower than that reported in literature. Doxorubicin displayed an IC₅₀ of 3.6 μ M, which is 2.1-fold higher (1.74 μ M) than data obtained from the *Institute of Microbial Technology, India* and 7.8-fold higher (0.459 μ M) than results reported by Campiglio *et al.* in the same cell line.(170),(171) The lower cytotoxicity observed in the present study may be a factor of phenotypic differences due to different growth conditions between laboratories.

As discussed in the literature review, doxorubicin binds to topoisomerase enzymes I and II, which can intercalate the base pairs of the DNA double helix and relax supercoils in DNA for transcription. Doxorubicin stabilizes the topoisomerase II complex after it has relaxed the DNA chain for replication, which inhibits the DNA double helix to be resealed and thus stops the process of replication.(103) As chromosomes replicate during the S-phase.(25) Even if doxorubicin is non-specific to the cell cycle, it is most active in the S-phase.(50) As the majority of cells assayed were present in the G0/G1-phase of the cell cycle, it is possible that a reduced cytotoxic effect was observed due to a short incubation period. Most anticancer drugs target rapidly-proliferating cells, and thus if not in the S-phase, will not be effective. Longer exposure may have incurred a greater effect as cellular cycling was achieved.

Based on micrographs, the morphology of doxorubicin-exposed monolayer cultures displayed high levels of cell death, detached cells and cellular debris throughout all three concentrations tested. However, spheroids were less susceptible to doxorubicin exposure. Spheroid integrity was maintained at the IC₂₅ and IC₅₀, with few dead or detached cells surrounding the spheroid. At these concentrations, spheroid size increased slightly, which may suggest either an adaptive response towards doxorubicin, or partial disassembly of spheroids due to weakened cadherin interactions.(157) Chen *et al.* reported that E-cadherin was downregulated in BT-20 cells through doxorubicin at concentrations between 0.15 and 0.62 μ M after 48 h treatment.(172) As such, reduced expression of such markers may have weakened cell-to-cell forces and promotes loosening of the 3D structure. At the IC₇₅, spheroids reduced in size, gained less defined margins, and were associated with a larger degree of detached or dead cells, thus, doxorubicin appears that have reached a threshold effect after which cytotoxicity could successfully be achieved.

Due to doxorubicin's fluorescence in the same region of the spectrum as PI, which is supported by literature,(173) it was not possible to confirm necrosis via such fluorescence staining. Given the fluorescent properties of doxorubicin, it is evident that the drug successfully permeated the spheroid, and thus the spheroid architecture did not prevent the drug from entering its core. Doxorubicin is known to permeate cells via passive diffusion(102) and disrupt E-cadherin.(172) However, it cannot be assumed that the concentration of doxorubicin within the spheroid is at an optimal cytotoxic concentration, thus it may contribute to the reduced toxicity observed. Further investigation is needed to determine the exposure level achieved within the spheroid.

The decrease in protein content in monolayer cultures between the IC₂₅, IC₅₀ and IC₇₅ was relatively constant. Taking the micrographs into consideration, such a decrease is indicative of loss of cellular material and cell death.(174) The binding of doxorubicin to nuclear and mitochondrial DNA may inhibit DNA, RNA and protein synthesis.(175) In the spheroid culture, protein contents of the spheroids were not decreased after treatment with lower concentrations (IC₂₅ and IC₅₀), which suggests that little cytotoxicity was observed in spheroids at these concentrations. However, at the IC₇₅, a prominent decrease was noted, indicative of cell death. Xu *et al.* reported similar effects, where four drugs (galactosamine, propranolol, diclofenac and paracetamol) only induced significant protein content reductions in HepG2 spheroids at high concentrations.(169)

During the screening of doxorubicin cytotoxicity, the decreased APH activity suggests high levels of cytotoxicity in monolayer cultures, which parallels the effects seen in other assays. However, this was only achieved at high concentrations in spheroids. Friedrich *et al.* reported similar results, in which HT20 and HCT-116 cells were treated with 5-fluorouracil and iriontecan in monolayer culture and spheroids. Cytotoxicity was observed in the monolayer and spheroid culture, however, a longer incubation time was needed to achieve this effect in the latter.(144) In comparison to the protein content assay, the APH assay displayed greater sensitivity towards cytotoxicity. Such an effect may showcase a membrane damaging effect of doxorubicin prior to alterations to protein content.(176)

Most antineoplastic drugs target proliferative cells and exhibit lower levels of cytotoxicity in hypoxic and acidic microenvironments. Thus, cancerous cells that remain in the dormant status are not targeted, and thus survive treatment. Furthermore, once sufficient factors (such as the expression/activation of cyclin D/cdk4,6 complex, which is regulated by the presence of mitotic growth factor and triggers the re-entry of G₀ cells into the G₁-phase) are released, cells re-enter the cell cycle and exit quiescence, thus proliferation may occur once again. (34, 83-85) The sub-G₁ phase significantly increased after exposure to doxorubicin, however, the increase was much more prominent in the monolayer cultures, which supports the decreased susceptibility of the spheroids to drug

treatment. Cellular debris observed during microscopy would corroborate the high levels of cytotoxicity noted in the cellular kinetics assay. The amount of cells in the G0/G1-phase during monolayer culture also decreased, suggesting blockage of later phases of the cell cycle. Supporting this, the G2/M-phase was non-significantly higher, suggesting that doxorubicin may have started incurring a G2-block. Given that p53 functions as an inhibitor of proliferation in the G2/M-transition, p53 expression was assessed.

Following the Western blot results, doxorubicin increased p53 expression, however, expression was lower in spheroids than in monolayers. This suggests that the 3D structure decreased chemosensitivity to doxorubicin by weaker p53 induction. He *et al.* reported increased expression of p53 by platinum in both monolayer and spheroid culture using HCT116 and LoVo cell lines, however, expression was lower in spheroids than that in monolayer cells due to decreased chemosensitivity in spheroids.(177) The p53 protein induces growth arrest by inhibiting the G2/M transition,(178) as was seen in the results. Doxorubicin increased the expression of p53 in the cells, regardless of whether the cells were in 2D or 3D cultures.

Cells are arrested for DNA damage repair, however, severe DNA damage leads to permanent cell cycle arrest.(147) Cell cycle arrest derived from doxorubicin mediation can appear either at G0/G1 or G2 checkpoints and is considered to be mediated by p53.(178) The cyclin-dependent kinase inhibitor p21 is known to function as a mediator of doxorubicin-induced cell cycle arrest in these phases, thus doxorubicin is expected to increase p53 and p21 expression.(179-181) When DNA gets damaged, p53 can activate expression of genes encoding for p21. The p21 protein inhibits the activity of cyclin-Cdk complexes to arrest cells for DNA repair proteins to rectify damage. If DNA damage is irreparable, p53 will initiate apoptosis.(39)

Apoptosis activated by p53 can be induced by the binding of caspase-9 to cytochrome C and Bax protein, which can be translocated by p53 from the cytoplasm into mitochondria, with consequent release of cytochrome C.(182) The response to DNA damage for cells is activating cell cycle checkpoints, which induce the temporary arrest at specific time point in the cell cycle to allow cells to correct possible defects.(183) There are two checkpoints available to check the DNA damage: one at the G1/S transition and the other one at the G2/M transition. The G1 checkpoint inhibits replication of damaged DNA and G2/M transition is prevented by incompletely replicated DNA.(184) p53 activates the transcription of downstream effector genes to encode for p21. The p21 protein inhibits kinase activity of various cyclin/cyclin-dependent kinase complexes (Cdk2 and Cdc2) to induce G1 or G2 arrest. (185-187)

The key component to regulate expression of p53 is murine double minute 2 (Mdm2) protein. The p53 protein can stimulate the expression of Mdm2 via

binding to two adjacent p53 binding sites (p53BS) in the *mdm2* gene.(188) On the one hand, binding of p53 by Mdm2 can physically block the transcriptional activates of p53 and promote p53 ubiquitnation and subsequent proteasomal degradation. On the other hand, p53 can locate to p53 binding site with the promoter of the *mdm2* gene and activate the expression of p53.(189-192) In normal cells, the combination between p53 and Mdm2 relies on three residues (Ser15, Thr18 and Ser20). The DNA damage activates the protein kinase to phosphorylate p53 at one of these three residues, thus disrupting its binding and increasing the p53 level. Although the increase of p53 promotes the expression of Mdm2, there is no effect from phosphorylated p53. The protein kinase can lose the function after DNA damage is repaired; p53 can then be dephosphorylated and degraded by the accelerated Mdm2. (193)

When the cells receive the p53-activating signal due to DNA damage, cells will be directed to either cell death via apoptosis, or growth arrest. The main factor is the cellular context, which is defined by the balance of intracellular and extracellular signalling events. The key component in the cellular context is the availability of survival signals, which includes the secreted molecules as well as those deriving from cell-cell and cell-matrix interactions. When survival signals are available, p53 activation prefers growth arrest than apoptosis. p53 will more like to activate apoptosis in the absence of adequate survival factors.(188)

Chapter 5

Conclusion

5.1. Summarisation

The aim of the study was to assess the potential of the BT-20 TNBC spheroid model to be used as a drug development platform for anti-neoplastic agents in comparison to a traditional culture system. By assessing the growth characteristics prior to and after exposure to doxorubicin, the reduced susceptibility and altered response to drug treatment was highlighted for more complex cellular systems (i.e. spheroids).

Various antineoplastic drugs have displayed high efficacy against cancer cells using traditional anticancer screening methods, such as monolayer culturing.(112) However, the findings in *in vitro* assays do not induce the same function and effect as in *in vivo* and clinical studies, which disrupts and delays drug development processes. As traditionally-used cytostatic drugs mainly target proliferating cells, tumor cell dormancy could be a reason for the limited response to these compounds. Thus, it's desirable to develop cell culture models that can accurately represent tumors in a laboratory setting. Multicellular tumor spheroids have the potential to rebuild the bridge between the *in vivo* and *in vitro* transition.

The TNBC BT-20 cell line formed compact spheroids that remained viable throughout the ten days of culturing. Spheroids were easily manipulated, allowing for downstream applications. The liquid overlay method allowed for production of large quantities of spheroids that can be used for individual treatments or end-point assessments. These spheroids displayed differential zones of viability and metabolic activity, as shown by live-dead staining, which suggests that a differential response may be incurred after treatment with chemotherapeutic drugs. Furthermore, cellular kinetics suggests high levels of cells within the early growth phase of proliferation, or potential entrapment within quiescence.

Spheroids displayed lower chemosensitivity to doxorubicin in comparison to monolayer cultures. Several reasons may exist for this, however, further assessment will be needed to ascertain the underlying process. Given the fluorescence microscopy data, doxorubicin does permeate the spheroid, however, it is unknown whether the exposure level is decreased. Given that proliferation is altered across the spheroid structure, as shown by live-dead staining and cellular

kinetic analysis, mechanistic actions may also be perturbed due to doxorubicin's need for active replication. Damage to DNA was seen after doxorubicin exposure (as shown by increased sub-G1-phase cells), which supports the increase in p53 expression, which in turn will promote cell cycle arrest to allow for DNA repair. In comparison to monolayer cultures, this was reduced in spheroid cultures, which further supports the reduced chemosensitivity of the 3D architecture.

In conclusion, using doxorubicin as a model antiproliferative chemotherapeutic drug, spheroid cultures were shown to be less susceptible to cytotoxicity than monolayer cultures. These may be a result of reduced spheroid permeability and altered proliferative status. Such 3D models may result in a greater representation of the *in vivo* environment, and thus assist with reducing the complications involved in drug development processes. Although improvements can be made to the model, it provides a foundation for further development.

5.2. Limitations and recommendations of the study

Although the BT-20 spheroid model was characterized using surrogate markers of growth and viability, more evidence is needed across the full spectrum of culturing to determine where dynamic equilibrium is achieved. As a static model, perfusion characteristics are not entirely representative of the *in vivo* environment, although it is an improvement on traditional systems. Further characterization of the model across a longer period will ascertain where treatment would be most appropriate. Different culturing conditions will need to be assessed, such as dynamic culturing environments using bio-reactors, to determine the best possible method for generation of spheroids.

The resazurin reduction assay failed to determine the metabolic capacity of spheroids due to the lack of resorufin release, however, use of agents such as EGTA may allow for a greater understanding on the cell-to-cell interactions in the spheroid.

Given the compactness of the spheroids, cell-to-cell interactions are increased, however, upon trypsinisation, the structure was easily perturbed. This may suggest that greater incubation times are needed to allow for full expression of membrane proteins associated with adhesion. Western blotting over the culture period will provide evidence of when such expression takes place.

Given the whole lysate nature of the experiments, it is unsure how diverse the distribution of cellular characteristics across the different zones of the spheroid is. Shedding of specific layers and further downstream analysis will provide data on how the proliferative capacity of the spheroid differs depending on depth, as well as the cellular viability thereof. Proteomic assessment of these layers will further indicate the upregulation or downregulation of prominent pathways involved with chemoresistance or chemosensitivity, such as those associated

with proliferation. This will provide further elucidation of the chemoresistance towards doxorubicin. Expression of drug-efflux transporters, such as P-glycoprotein and multi-drug resistance protein, will also further indicate whether doxorubicin permeation is occurring adequately to achieve pharmacodynamic effects.

Only doxorubicin was used as a candidate antineoplastic drug. Further investigation can be done across a range of cytotoxic or cytostatic drugs to ascertain the appropriateness and representation of the spheroid model.

References

1. Lowry OH, Rosebrough NJ, Farr AL, Randall RJ. Protein measurement with the Folin phenol reagent. *Journal of Biological Chemistry*. 1951;193(1):265-75.
2. Wiechelman KJ, Braun RD, Fitzpatrick JD. Investigation of the bicinchoninic acid protein assay: identification of the groups responsible for color formation. *Analytical Biochemistry*. 1988;175(1):231-7.
3. Bray F, Møller B. Predicting the future burden of cancer. *Nature Reviews Cancer*. 2006;6(1):63-74.
4. Jemal A, Siegel R, Ward E, Murray T, Xu J, Thun MJ. Cancer statistics, 2007. *CA: A Cancer Journal for Clinicians*. 2007;57(1):43-66.
5. Anand P, Kunnumakara AB, Sundaram C, Harikumar KB, Tharakan ST, Lai OS, Sung B, Aggarwal BB. Cancer is a preventable disease that requires major lifestyle changes. *Pharmaceutical Research*. 2008;25(9):2097-116.
6. World Cancer Report 2014. World Health Organization. 2014. pp. Chapter 1.1. ISBN 9283204298
7. World Cancer Report 2014. World Health Organization. 2014. pp. Chapter 1.1. ISBN 9283204298.
8. CANSA.org.za. Prevalence Cancer.2018. Accessed on 5 May 2018 from <https://www.cansa.org.za/south-african-cancer-statistics>
9. Hanahan D, Weinberg RA. Hallmarks of cancer: the next generation. *Cell*. 2011;144(5):646-74.
10. Lemmon MA, Schlessinger J. Cell signaling by receptor tyrosine kinases. *Cell*. 2010;141(7):1117-34.
11. Burkhart DL, Sage J. Cellular mechanisms of tumour suppression by the retinoblastoma gene. *Nature Reviews Cancer*. 2008;8(9):671-82.
12. Adams JM, Cory S. The Bcl-2 apoptotic switch in cancer development and therapy. *Oncogene*. 2007;26(9):1324-37.
13. Willis SN, Adams JM. Life in the balance: how BH3-only proteins induce apoptosis. *Current Opinion in Cell Biology*. 2005;17(6):617-25.
14. Junttila MR, Evan GI. p53—a Jack of all trades but master of none. *Nature Reviews Cancer*. 2009;9(11):821-9.
15. Lowe SW, Cepero E, Evan G. Intrinsic tumour suppression. *Nature*. 2004;432(7015):307-75.
16. Blasco MA. Telomeres and human disease: ageing, cancer and beyond. *Nature Reviews Genetics*. 2005;6(8):611-22.
17. Shay JW, Wright WE. Hayflick, his limit, and cellular ageing. *Nature Reviews Molecular Cell Biology*. 2000;1(1):72-6.
18. Hanahan D, Folkman J. Patterns and emerging mechanisms of the angiogenic switch during tumorigenesis. *Cell*. 1996;86(3):353-64.
19. Berx G, Van Roy F. Involvement of members of the cadherin superfamily in

- cancer. Cold Spring Harbor Perspectives in Biology. 2009:a003129.
20. Cabrita MA, Christofori G. Sprouty proteins, masterminds of receptor tyrosine kinase signaling. *Angiogenesis*. 2008;11(1):53-62.
 21. Talmadge JE, Fidler IJ. AACR centennial series: the biology of cancer metastasis: historical perspective. *Cancer Research*. 2010:0008-5472. CAN-10-1040.
 22. Fidler IJ. The pathogenesis of cancer metastasis: the 'seed and soil' hypothesis revisited. *Nature Reviews Cancer*. 2003;3(6):453-8.
 23. Coussens LM, Werb Z. Inflammation and cancer. *Nature*. 2002;420(6917):860-7.
 24. Minotti G, Menna P, Salvatorelli E, Cairo G, Gianni L. Anthracyclines: molecular advances and pharmacologic developments in antitumor activity and cardiotoxicity. *Pharmacological Reviews*. 2004;56(2):185-229.
 25. Arcamone FM. Fifty years of chemical research at farmitalia. *Chemistry–A European Journal*. 2009;15(32):7774-91.
 26. Misteli T, Soutoglou E. The emerging role of nuclear architecture in DNA repair and genome maintenance. *Nature Reviews Molecular Cell Biology*. 2009;10(4):243-54.
 27. University of Leicester. 2015. The Cell cycle, Mitosis and Meiosis. Accessed on 3 March 2018 from <https://www2.le.ac.uk/projects/vgec/highereducation/topics/cellcycle-mitosis-meiosis>
 28. Shanahan M. The brain's connective core and its role in animal cognition. *Philosophical Transactions of the Royal Society of London B: Biological Sciences*. 2012;367(1603):2704-14.
 29. Sutherland R, Freyer J, Mueller-Klieser W, Wilson R, Heacock C, Sciandra J, Sordat B. Cellular growth and metabolic adaptations to nutrient stress environments in tumor microregions. *International Journal of Radiation Oncology• Biology• Physics*. 1986;12(4):611-5.
 30. Freyer JP, Schor PL. Regrowth kinetics of cells from different regions of multicellular spheroids of four cell lines. *Journal of Cellular Physiology*. 1989;138(2):384-92.
 31. Kunz - Schughart LA, Kreutz M, Knuechel R. Multicellular spheroids: a three - dimensional in vitro culture system to study tumour biology. *International Journal of Experimental Pathology*. 1998;79(1):1-23.
 32. Trédan O, Galmarini CM, Patel K, Tannock IF. Drug resistance and the solid tumor microenvironment. *Journal of the National Cancer Institute*. 2007;99(19):1441-54.
 33. Baserga R. The cell cycle. *New England Journal of Medicine*. 1981;304(8):453-9.
 34. Hunter T, Pines J. Cyclins and cancer II: cyclin D and CDK inhibitors come of age. *Cell*. 1994;79(4):573-82.
 35. Sherr CJ, Roberts JM. CDK inhibitors: positive and negative regulators of G1-phase progression. *Genes & Development*. 1999;13(12):1501-12.

36. Lim S, Kaldis P. Cdks, cyclins and CKIs: roles beyond cell cycle regulation. *Development*. 2013;140(15):3079-93.
37. Strachan, T & Read, A. P. (Andrew P.) & National Library of Medicine (1999). *Human molecular genetics* (2nd ed). Wiley, Singapore ; New York
38. Chang C, Simmons DT, Martin MA, Mora PT. Identification and partial characterization of new antigens from simian virus 40-transformed mouse cells. *Journal of Virology*. 1979;31(2):463-71.
39. Vermeulen K, Van Bockstaele DR, Berneman ZN. The cell cycle: a review of regulation, deregulation and therapeutic targets in cancer. *Cell Proliferation*. 2003;36(3):131-49.
40. National Center for Biotechnology Information (US). Genes and Disease (Internet). Bethesda (MD): National Center for Biotechnology Information (US); The p53 tumor suppressor protein. Available from: <https://www.ncbi.nlm.nih.gov/books/NBK22268/>
41. Breast Cancer.NCI.Retrieved 29 June 2014.
42. Breast Cancer Treatment (PDQ®).NCI.23 May 2014.Retrieved 29 June 2014.
43. World Cancer Report.International Agency for Research on Cancer.2008. Retrieved 26 February 2011.
44. World Cancer Report 2014. World Health Organization. 2014. pp. Chapter 1.1. ISBN 9283204298.
45. Breast Cancer Treatment (PDQ®).NCI.23 May 2014.Retrieved 29 June 2014.
46. World Cancer Report (PDF).International Agency for Research on Cancer. 2008.Retrieved 26 February 2011.
47. Cancer survival in England:Patients Diagnosed 2007-2011 and followed up to 2012(PDF).Office for National Statistics.29 October 2013. Retrieved 29 June 2014.
48. MSD Manuals.com. Breast Cancer. 2018. Accessed on 12 June 2018 from http://www.merckmanuals.com/professional/gynecology_and_obstetrics/breast_disorders/breast_cancer.html
49. Elston E, Ellis I. Method for grading breast cancer. *Journal of Clinical Pathology*. 1993;46(2):189-90.
50. Wahl RL, Siegel BA, Coleman RE, Gatsonis CG. Prospective multicenter study of axillary nodal staging by positron emission tomography in breast cancer: a report of the staging breast cancer with PET Study Group. *Journal of Clinical Oncology*. 2004;22(2):277-85.
51. Foulkes WD, Smith IE, Reis-Filho JS. Triple-negative breast cancer. *New England Journal of Medicine*. 2010;363(20):1938-48.
52. Dahlman-Wright K, Cavailles V, Fuqua SA, Jordan VC, Katzenellenbogen JA, Korach KS, Maggi A, Muramatsu M, Parker MG, Gustafsson J-Å. International union of pharmacology. LXIV. Estrogen receptors. *Pharmacological Reviews*. 2006;58(4):773-81.
53. Murphy E, Steenbergen C. Estrogen regulation of protein expression and signaling pathways in the heart. *Biology of Sex Differences*. 2014;5(1):6.
54. Deroo BJ, Korach KS. Estrogen receptors and human disease. *The Journal of*

- Clinical Investigation. 2006;116(3):561-70.
55. Daniel AR, Hagan CR, Lange CA. Progesterone receptor action: defining a role in breast cancer. *Expert Review of Endocrinology & Metabolism*. 2011;6(3):359-69.
56. Lu H-F, Chua K-N, Zhang P-C, Lim W-S, Ramakrishna S, Leong KW, Mao H-Q. Three-dimensional co-culture of rat hepatocyte spheroids and NIH/3T3 fibroblasts enhances hepatocyte functional maintenance. *Acta Biomaterialia*. 2005;1(4):399-410.
57. Hudis CA, Gianni L. Triple-negative breast cancer: an unmet medical need. *The Oncologist*. 2011;16(Supplement 1):1-11.
58. Chobanyan NS. Re: Henderson, be and Feigelson, hs (2000) Hormonal carcinogenesis. *carcinogenesis*, 21, 427–433. *Carcinogenesis*. 2001;22(3):529.
59. Yue W, Wang J-P, Li Y, Bocchinfuso WP, Korach KS, Devanesan PD, Rogan E, Cavalieri E, Santen RJ. Tamoxifen versus aromatase inhibitors for breast cancer prevention. *Clinical Cancer Research*. 2005;11(2):925s-30s.
60. Grimm SL, Hartig SM, Edwards DP. Progesterone receptor signaling mechanisms. *Journal of Molecular Biology*. 2016;428(19):3831-49.
61. Muller WJ, Sinn E, Pattengale PK, Wallace R, Leder P. Single-step induction of mammary adenocarcinoma in transgenic mice bearing the activated c-neu oncogene. *Cell*. 1988;54(1):105-15.
62. Di Fiore PP, Pierce JH, Kraus MH, Segatto O, King CR, Aaronson SA. erbB-2 is a potent oncogene when overexpressed in NIH/3T3 cells. *Science*. 1987;237(4811):178-82.
63. Cho H-S, Mason K, Ramyar KX, Stanley AM, Gabelli SB, Denney Jr DW, Leahy DJ. Structure of the extracellular region of HER2 alone and in complex with the Herceptin Fab. *Nature*. 2003;421(6924):756-60.
64. Wieduwilt M, Moasser M. The epidermal growth factor receptor family: biology driving targeted therapeutics. *Cellular and Molecular Life Sciences*. 2008;65(10):1566-84.
65. Hynes NE, Stern DF. The biology of erbB-2/nue/HER-2 and its role in cancer. *Biochimica et Biophysica Acta (BBA)-Reviews on Cancer*. 1994;1198(2-3):165-84.
66. Saini K, Taylor C, Ramirez A-J, Palmieri C, Gunnarsson U, Schmoll H-J, Dolci S, Ghene C, Metzger-Filho O, Skrzypski M. Role of the multidisciplinary team in breast cancer management: results from a large international survey involving 39 countries. *Annals of Oncology*. 2011;23(4):853-9.
67. Bao T, Rudek MA. The clinical pharmacology of anastrozole. *European Oncology&Haematology*. 2011;7:106-8.
68. Group EBCTC. Aromatase inhibitors versus tamoxifen in early breast cancer: patient-level meta-analysis of the randomised trials. *The Lancet*. 2015;386(10001):1341-52.
69. Fisher B, Brown AM, Dimitrov NV, Poisson R, Redmond C, Margolese RG, Bowman D, Wolmark N, Wickerham DL, Kardinal CG. Two months of doxorubicin-cyclophosphamide with and without interval reinduction therapy

compared with 6 months of cyclophosphamide, methotrexate, and fluorouracil in positive-node breast cancer patients with tamoxifen-nonresponsive tumors: results from the National Surgical Adjuvant Breast and Bowel Project B-15. *Journal of Clinical Oncology*. 1990;8(9):1483-96.

70. Perez EA, Suman VJ, Davidson NE, Sledge GW, Kaufman PA, Hudis CA, Martino S, Gralow JR, Dakhil SR, Ingle JN. Cardiac safety analysis of doxorubicin and cyclophosphamide followed by paclitaxel with or without trastuzumab in the North Central Cancer Treatment Group N9831 adjuvant breast cancer trial. *Journal of Clinical Oncology: official journal of the American Society of Clinical Oncology*. 2008;26(8):1231-8.

71. Slamon D, Eiermann W, Robert N, Pienkowski T, Martin M, Press M, Mackey J, Glaspy J, Chan A, Pawlicki M. Adjuvant trastuzumab in HER2-positive breast cancer. *New England Journal of Medicine*. 2011;365(14):1273-83.

72. Lehmann BD, Bauer JA, Chen X, Sanders ME, Chakravarthy AB, Shyr Y, Pietenpol JA. Identification of human triple-negative breast cancer subtypes and preclinical models for selection of targeted therapies. *The Journal of Clinical Investigation*. 2011;121(7):2750-67.

73. Sørlie T, Tibshirani R, Parker J, Hastie T, Marron JS, Nobel A, Deng S, Johnsen H, Pesich R, Geisler S. Repeated observation of breast tumor subtypes in independent gene expression data sets. *Proceedings of the National Academy of Sciences*. 2003;100(14):8418-23.

74. Yuan N, Meng M, Liu C, Feng L, Hou L, Ning Q, Xin G, Pei L, Gu S, Li X. Clinical characteristics and prognostic analysis of triple-negative breast cancer patients. *Molecular and Clinical Oncology*. 2014;2(2):245-51.

75. Koeneman KS, Yeung F, Chung LW. Osteomimetic properties of prostate cancer cells: a hypothesis supporting the predilection of prostate cancer metastasis and growth in the bone environment. *The Prostate*. 1999;39(4):246-61.

76. Sihto H, Lundin J, Lundin M, Lehtimäki T, Ristimäki A, Holli K, Sailas L, Kataja V, Turpeenniemi-Hujanen T, Isola J. Breast cancer biological subtypes and protein expression predict for the preferential distant metastasis sites: a nationwide cohort study. *Breast Cancer Research*. 2011;13(5):R87.

77. Lin NU, Claus E, Sohl J, Razzak AR, Arnaout A, Winer EP. Sites of distant recurrence and clinical outcomes in patients with metastatic triple - negative breast cancer: high incidence of central nervous system metastases. *Cancer*. 2008;113(10):2638-45.

78. Anders CK, Carey LA. Biology, metastatic patterns, and treatment of patients with triple-negative breast cancer. *Clinical Breast Cancer*. 2009;9:S73-S81.

79. Dawood S. Triple-negative breast cancer. *Drugs*. 2010;70(17):2247-58.

80. Nofech-Mozes S, Trudeau M, Kahn HK, Dent R, Rawlinson E, Sun P, Narod SA, Hanna WM. Patterns of recurrence in the basal and non-basal subtypes of triple-negative breast cancers. *Breast Cancer Research and Treatment*. 2009;118(1):131-7.

81. Ismail-Khan R, Bui MM. A review of triple-negative breast cancer. *Cancer*

- Control. 2010;17(3):173-6.
82. McCarty MF. Cytostatic and reverse-transforming therapies of cancer—A brief review and future prospects. *Medical Hypotheses*. 1982;8(6):589-612.
83. Hande KR. Clinical applications of anticancer drugs targeted to topoisomerase II. *Biochimica et Biophysica Acta (BBA)-Gene Structure and Expression*. 1998;1400(1-3):173-84.
84. Pines J. Cyclins and cyclin-dependent kinases: theme and variations. *Advances in Cancer Research*. 661995. p. 181-212.
85. Planas-Silva MD, Weinberg RA. The restriction point and control of cell proliferation. *Current Opinion in Cell Biology*. 1997;9(6):768-72.
86. Sielecki TM, Boylan JF, Benfield PA, Trainor GL. Cyclin-dependent kinase inhibitors: useful targets in cell cycle regulation. *Journal of Medicinal Chemistry*. 2000;43(1):1-18.
87. Yao H, He G, Yan S, Chen C, Song L, Rosol TJ, Deng X. Triple-negative breast cancer: is there a treatment on the horizon? *Oncotarget*. 2017;8(1):1913.
88. Martín M, Rodríguez-Lescure Á, Ruiz A, Alba E, Calvo L, Ruiz-Borrego M, Santaballa A, Rodríguez CA, Crespo C, Abad M. Molecular predictors of efficacy of adjuvant weekly paclitaxel in early breast cancer. *Breast Cancer Research and Treatment*. 2010;123(1):149-57.
89. Pang B, Qiao X, Janssen L, Velds A, Groothuis T, Kerkhoven R, Nieuwland M, Ovaa H, Rottenberg S, Van Tellingen O. Drug-induced histone eviction from open chromatin contributes to the chemotherapeutic effects of doxorubicin. *Nature Communications*. 2013;4:1908.
90. Hamilton G. Multicellular spheroids as an in vitro tumor model. *Cancer Letters*. 1998;131(1):29-34.
91. Marusyk A, Almendro V, Polyak K. Intra-tumour heterogeneity: a looking glass for cancer? *Nature Reviews Cancer*. 2012;12(5):323-34.
92. Minchinton AI, Tannock IF. Drug penetration in solid tumours. *Nature Reviews Cancer*. 2006;6(8):583-92.
93. Viale G, Rotmensz N, Maisonneuve P, Bottiglieri L, Montagna E, Luini A, Veronesi P, Intra M, Torrisi R, Cardillo A. Invasive ductal carcinoma of the breast with the “triple-negative” phenotype: prognostic implications of EGFR immunoreactivity. *Breast Cancer Research and Treatment*. 2009;116(2):317-28.
94. Banerjee S, Reis-Filho JS, Ashley S, Steele D, Ashworth A, Lakhani SR, Smith IE. Basal-like breast carcinomas: clinical outcome and response to chemotherapy. *Journal of Clinical Pathology*. 2006;59(7):729-35.
95. Nogi H, Kobayashi T, Suzuki M, Tabei I, Kawase K, Toriumi Y, Fukushima H, Uchida K. EGFR as paradoxical predictor of chemosensitivity and outcome among triple-negative breast cancer. *Oncology Reports*. 2009;21(2):413-7.
96. Orlando UD, Castillo AF, Dattilo MA, Solano AR, Maloberti PM, Podesta EJ. Acyl-CoA synthetase-4, a new regulator of mTOR and a potential therapeutic target for enhanced estrogen receptor function in receptor-positive and-negative breast cancer. *Oncotarget*. 2015;6(40):42632-50.
97. Nicolini A, Ferrari P, Kotlarova L, Rossi G, M Biava P. The PI3K-Akt-mTOR

- pathway and new tools to prevent acquired hormone resistance in breast cancer. *Current Pharmaceutical Biotechnology*. 2015;16(9):804-15.
98. Trebunova M, Laputkova G, Slaba E, Lacjakova K, Verebova A. Effects of docetaxel, doxorubicin and cyclophosphamide on human breast cancer cell line MCF-7. *Anticancer Research*. 2012;32(7):2849-54.
99. Carvalho C, Santos RX, Cardoso S, Correia S, Oliveira PJ, Santos MS, Moreira PI. Doxorubicin: the good, the bad and the ugly effect. *Current Medicinal Chemistry*. 2009;16(25):3267-85.
100. Minotti G, Recalcati S, Menna P, Salvatorelli E, Corna G, Cairo G. Doxorubicin cardiotoxicity and the control of iron metabolism: quinone-dependent and independent mechanisms. *Methods in Enzymology*. 3782004. p. 340-61.
101. Tacar O, Sriamornsak P, Dass CR. Doxorubicin: an update on anticancer molecular action, toxicity and novel drug delivery systems. *Journal of Pharmacy and Pharmacology*. 2013;65(2):157-70.
102. Skovsgaard T, Nissen NI. Membrane transport of anthracyclines. *Pharmacology & Therapeutics*. 1982;18(3):293-311.
103. Gewirtz D. A critical evaluation of the mechanisms of action proposed for the antitumor effects of the anthracycline antibiotics adriamycin and daunorubicin. *Biochemical Pharmacology*. 1999;57(7):727-41.
104. Hilmer SN, Cogger VC, Muller M, Le Couteur DG. The hepatic pharmacokinetics of doxorubicin and liposomal doxorubicin. *Drug Metabolism and Disposition*. 2004;32(8):794-9.
105. Tewey K, Rowe T, Yang L, Halligan B, Liu L. Adriamycin-induced DNA damage mediated by mammalian DNA topoisomerase II. *Science*. 1984;226(4673):466-8.
106. Doroshow JH. Role of hydrogen peroxide and hydroxyl radical formation in the killing of Ehrlich tumor cells by anticancer quinones. *Proceedings of the National Academy of Sciences*. 1986;83(12):4514-8.
107. Fogli S, Nieri P, Breschi MC. The role of nitric oxide in anthracycline toxicity and prospects for pharmacologic prevention of cardiac damage. *The FASEB Journal*. 2004;18(6):664-75.
108. Pawłowska J, Tarasiuk J, Wolf CR, Paine MJ, Borowski E. Differential ability of cytostatics from anthraquinone group to generate free radicals in three enzymatic systems: NADH dehydrogenase, NADPH cytochrome P450 reductase, and xanthine oxidase. *Oncology Research Featuring Preclinical and Clinical Cancer Therapeutics*. 2003;13(5):245-52.
109. Thorn CF, Oshiro C, Marsh S, Hernandez-Boussard T, McLeod H, Klein TE, Altman RB. Doxorubicin pathways: pharmacodynamics and adverse effects. *Pharmacogenetics and Genomics*. 2011;21(7):440-6.
110. Valentovic MA. Evaluation of Resveratrol in Cancer Patients and Experimental Models. *Advances in Cancer Research*. 1372018. p. 171-88.
111. Colotta F, Allavena P, Sica A, Garlanda C, Mantovani A. Cancer-related inflammation, the seventh hallmark of cancer: links to genetic instability.

- Carcinogenesis. 2009;30(7):1073-81.
112. Wenzel C, Riefke B, Gründemann S, Krebs A, Christian S, Prinz F, Osterland M, Golfier S, Räse S, Ansari N. 3D high-content screening for the identification of compounds that target cells in dormant tumor spheroid regions. *Experimental Cell Research*. 2014;323(1):131-43.
 113. DiMasi JA, Grabowski HG. Economics of new oncology drug development. *Journal of Clinical Oncology*. 2007.
 114. Breslin S, O'Driscoll L. Three-dimensional cell culture: the missing link in drug discovery. *Drug Discovery Today*. 2013;18(5-6):240-9.
 115. Nath S, Devi GR. Three-dimensional culture systems in cancer research: Focus on tumor spheroid model. *Pharmacology & Therapeutics*. 2016;163:94-108.
 116. Cui X, Hartanto Y, Zhang H. Advances in multicellular spheroids formation. *Journal of The Royal Society Interface*. 2017;14(127):2016.0877.
 117. Dolezalova D, Mraz M, Barta T, Plevova K, Vinarsky V, Holubcova Z, Jaros J, Dvorak P, Pospisilova S, Hampl A. MicroRNAs regulate p21Waf1/Cip1 protein expression and the DNA damage response in human embryonic stem cells. *Stem Cells*. 2012;30(7):1362-72.
 118. Lin R-Z, Chou L-F, Chien C-CM, Chang H-Y. Dynamic analysis of hepatoma spheroid formation: roles of E-cadherin and β 1-integrin. *Cell and Tissue Research*. 2006;324(3):411-22.
 119. Adam G, Duncan H. Development of a sensitive and rapid method for the measurement of total microbial activity using fluorescein diacetate (FDA) in a range of soils. *Soil Biology and Biochemistry*. 2001;33(7-8):943-51.
 120. Aguirre-Ghiso JA. Models, mechanisms and clinical evidence for cancer dormancy. *Nature Reviews Cancer*. 2007;7(11):834-46.
 121. Kyle AH, Baker JH, Minchinton AI. Targeting quiescent tumor cells via oxygen and IGF-I supplementation. *Cancer Research*. 2011.
 122. Nagelkerke A, Bussink J, Sweep FC, Span PN. Generation of multicellular tumor spheroids of breast cancer cells: how to go three-dimensional. *Analytical Biochemistry*. 2013;437(1):17-9.
 123. Goodman TT, Ng CP, Pun SH. 3-D tissue culture systems for the evaluation and optimization of nanoparticle-based drug carriers. *Bioconjugate Chemistry*. 2008;19(10):1951-9.
 124. Ivascu A, Kubbies M. Rapid generation of single-tumor spheroids for high-throughput cell function and toxicity analysis. *Journal of Biomolecular Screening*. 2006;11(8):922-32.
 125. Hirschhaeuser F, Menne H, Dittfeld C, West J, Mueller-Klieser W, Kunz-Schughart LA. Multicellular tumor spheroids: an underestimated tool is catching up again. *Journal of Biotechnology*. 2010;148(1):3-15.
 126. Clejan S, O'connor K, Rosensweig N. Tri - dimensional prostate cell cultures in simulated microgravity and induced changes in lipid second messengers and signal transduction. *Journal of Cellular and Molecular Medicine*. 2001;5(1):60-73.

127. Hedlund TE, Duke RC, Miller GJ. Three - dimensional spheroid cultures of human prostate cancer cell lines. *The Prostate*. 1999;41(3):154-65.
128. Freyer JP, Sutherland RM. Selective dissociation and characterization of cells from different regions of multicell tumor spheroids. *Cancer Research*. 1980;40(11):3956-65.
129. Kwok T, Twentyman P. The relationship between tumour geometry and the response of tumour cells to cytotoxic drugs—an in vitro study using EMT6 multicellular spheroids. *International Journal of Cancer*. 1985;35(5):675-82.
130. Freyer JP, Schor PL. Automated selective dissociation of cells from different regions of multicellular spheroids. *In Vitro Cellular & Developmental Biology*. 1989;25(1):9-19.
131. Collins TJ. ImageJ for microscopy. *Biotechniques*. 2007;43(S1):S25-S30.
132. Steinhaus H. *Mathematical Snapshots*. (Third American Edition, Revised and Enlarged.): Oxford University Press; 1969.
133. Graff CP, Wittrup KD. Theoretical analysis of antibody targeting of tumor spheroids: importance of dosage for penetration, and affinity for retention. *Cancer Research*. 2003;63(6):1288-96.
134. Csepregi R, Lemli B, Kunsági-Máté S, Szente L, Kőszegi T, Németi B, Poór M. Complex Formation of Resorufin and Resazurin with B-Cyclodextrins: Can Cyclodextrins Interfere with a Resazurin Cell Viability Assay? *Molecules*. 2018;23(2):382.
135. Oudar O. Spheroids: relation between tumour and endothelial cells. *Critical Reviews in Oncology/Hematology*. 2000;36(2-3):99-106.
136. Furbert-Harris PM, Laniyan I, Harris D, Dunston GM, Vaughn T, Abdelnaby A, Parish-Gause D, Oredipe OA. Activated eosinophils infiltrate MCF-7 breast multicellular tumor spheroids. *Anticancer Research*. 2003;23(1A):71-8.
137. Heimdal JH, Aarstad H, Olsnes C, Olofsson J. Human Autologous Monocytes and Monocyte - Derived Macrophages in Co - Culture with Carcinoma F - Spheroids Secrete IL - 6 by aNon - CD14 - Dependent Pathway. *Scandinavian Journal of Immunology*. 2001;53(2):162-70.
138. Fennema E, Rivron N, Rouwkema J, van Blitterswijk C, de Boer J. Spheroid culture as a tool for creating 3D complex tissues. *Trends in Biotechnology*. 2013;31(2):108-15.
139. Netzer P, Domek M, Pai R, Halter F, Tarnawski A. Inhibition of human colon cancer cell growth by antisense oligodeoxynucleotides targeted at basic fibroblast growth factor. *Alimentary Pharmacology & Therapeutics*. 2001;15(10):1673-9.
140. Höpfner M, Maaser K, Barthel B, Von Lampe B, Hanski C, Riecken E-O, Zeitz M, Scherübl H. Growth inhibition and apoptosis induced by P2Y₂ receptors in human colorectal carcinoma cells: involvement of intracellular calcium and cyclic adenosine monophosphate. *International Journal of Colorectal Disease*. 2001;16(3):154-66.
141. Chang YH, Chao Y, Hsieh SL, Lin WW. Mechanism of LIGHT/interferon - γ - induced cell death in HT - 29 cells. *Journal of Cellular Biochemistry*.

2004;93(6):1188-202.

142. Cholody WM, Kosakowska-Cholody T, Hollingshead MG, Hariprakash HK, Michejda CJ. A new synthetic agent with potent but selective cytotoxic activity against cancer. *Journal of Medicinal Chemistry*. 2005;48(13):4474-81.

143. Yang T-T, Sinai P, Kain SR. An acid phosphatase assay for quantifying the growth of adherent and nonadherent cells. *Analytical Biochemistry*. 1996;241(1):103-8.

144. Friedrich J, Eder W, Castaneda J, Doss M, Huber E, Ebner R, Kunz-Schughart LA. A reliable tool to determine cell viability in complex 3-D culture: the acid phosphatase assay. *Journal of Biomolecular Screening*. 2007;12(7):925-37.

145. Mahmood T, Yang P-C. Western blot: technique, theory, and trouble shooting. *North American Journal of Medical Sciences*. 2012;4(9):429-34.

146. Netherlands Translational Research Center.com. Oncoline. 2016. Accessed on 18 June 2018 from <https://www.ntrc.nl/wp-content/uploads/2016/04/Oncolines-2.0-BT-20-data-sheet.pdf>

147. Siu WY, Yam CH, Poon RY. G1 versus G2 cell cycle arrest after adriamycin - induced damage in mouse Swiss3T3 cells. *FEBS Letters*. 1999;461(3):299-305.

148. Hutmacher DW. Biomaterials offer cancer research the third dimension. *Nature Materials*. 2010;9(2):90-3.

149. Pampaloni F, Reynaud EG, Stelzer EH. The third dimension bridges the gap between cell culture and live tissue. *Nature Reviews Molecular Cell Biology*. 2007;8(10):839-45.

150. Abbott A. Cell culture: biology's new dimension. Nature Publishing Group; 2003.

151. Schmeichel KL, Bissell MJ. Modeling tissue-specific signaling and organ function in three dimensions. *Journal of Cell Science*. 2003;116(12):2377-88.

152. Duval K, Grover H, Han L-H, Mou Y, Pegoraro AF, Fredberg J, Chen Z. Modeling physiological events in 2D vs. 3D cell culture. *Physiology*. 2017;32(4):266-77.

153. Edmondson R, Broglie JJ, Adcock AF, Yang L. Three-dimensional cell culture systems and their applications in drug discovery and cell-based biosensors. *Assay and Drug Development Technologies*. 2014;12(4):207-18.

154. D'Souza SE, Ginsberg MH, Plow EF. Arginyl-glycyl-aspartic acid (RGD): a cell adhesion motif. *Trends in Biochemical Sciences*. 1991;16:246-50.

155. Ahmed SA, Gogal Jr RM, Walsh JE. A new rapid and simple non-radioactive assay to monitor and determine the proliferation of lymphocytes: an alternative to [³H] thymidine incorporation assay. *Journal of Immunological Methods*. 1994;170(2):211-24.

156. Nakayama GR. Assessment of the Alamar Blue assay for cellular growth and viability in vitro. *J Immunol Methods*. 1997;204:205-8.

157. Walzl A, Unger C, Kramer N, Unterleuthner D, Scherzer M,

- Hengstschläger M, Schwanzer-Pfeiffer D, Dolznig H. The resazurin reduction assay can distinguish cytotoxic from cytostatic compounds in spheroid screening assays. *Journal of Biomolecular Screening*. 2014;19(7):1047-59.
158. Volberg T, Geiger B, Kartenbeck J, Franke WW. Changes in membrane-microfilament interaction in intercellular adherens junctions upon removal of extracellular Ca^{2+} ions. *The Journal of Cell Biology*. 1986;102(5):1832-42.
159. Laprise P, Langlois MJ, Boucher MJ, Jobin C, Rivard N. Down - regulation of MEK/ERK signaling by E - cadherin - dependent PI3K/Akt pathway in differentiating intestinal epithelial cells. *Journal of Cellular Physiology*. 2004;199(1):32-9.
160. Curcio E, Salerno S, Barbieri G, De Bartolo L, Drioli E, Bader A. Mass transfer and metabolic reactions in hepatocyte spheroids cultured in rotating wall gas-permeable membrane system. *Biomaterials*. 2007;28(36):5487-97.
161. Grimes DR, Kelly C, Bloch K, Partridge M. A method for estimating the oxygen consumption rate in multicellular tumour spheroids. *Journal of The Royal Society Interface*. 2014;11(92):2013.1124.
162. Däster S, Amatruda N, Calabrese D, Ivanek R, Turrini E, Drosner RA, Zajac P, Fimognari C, Spagnoli GC, Iezzi G. Induction of hypoxia and necrosis in multicellular tumor spheroids is associated with resistance to chemotherapy treatment. *Oncotarget*. 2017;8(1):1725-36.
163. Hu G, Li D. Three-dimensional modeling of transport of nutrients for multicellular tumor spheroid culture in a microchannel. *Biomedical Microdevices*. 2007;9(3):315-23.
164. Haass NK, Beaumont KA, Hill DS, Anfosso A, Mrass P, Munoz MA, Kinjyo I, Weninger W. Real - time cell cycle imaging during melanoma growth, invasion, and drug response. *Pigment Cell & Melanoma Research*. 2014;27(5):764-76.
165. Kim KH, Sederstrom JM. Assaying cell cycle status using flow cytometry. *Current Protocols in Molecular Biology*. 2015;111(1):28.6. 1-.6. 11.
166. Kajstura M, Halicka HD, Pryjma J, Darzynkiewicz Z. Discontinuous fragmentation of nuclear DNA during apoptosis revealed by discrete “sub - G1” peaks on DNA content histograms. *Cytometry Part A: the Journal of the International Society for Analytical Cytology*. 2007;71(3):125-31.
167. Kim JW, Ho WJ, Wu BM. The role of the 3D environment in hypoxia-induced drug and apoptosis resistance. *Anticancer Research*. 2011;31(10):3237-45.
168. Vaupel P, Mayer A. Hypoxia in cancer: significance and impact on clinical outcome. *Cancer and Metastasis Reviews*. 2007;26(2):225-39.
169. Xu J, Ma M, Purcell WM. Characterisation of some cytotoxic endpoints using rat liver and HepG2 spheroids as in vitro models and their application in hepatotoxicity studies. I. Glucose metabolism and enzyme release as cytotoxic markers. *Toxicology and Applied Pharmacology*. 2003;189(2):100-11.
170. Campiglio M, Somenzi G, Olgiate C, Beretta G, Balsari A, Zaffaroni N, Valagussa P, Ménard S. Role of proliferation in HER2 status predicted response to

- doxorubicin. *International Journal of Cancer*. 2003;105(4):568-73.
171. CancerDR: Cancer Drug Resistance Database. BT-20. 2012. Accessed on 6 June 2018 from http://crdd.osdd.net/raghava/cancerdr/submitkey_r.php?ran=1494
172. Chen W-C, Lai Y-A, Lin Y-C, Ma J-W, Huang L-F, Yang N-S, Ho C-T, Kuo S-C, Way T-D. Curcumin suppresses doxorubicin-induced epithelial–mesenchymal transition via the inhibition of TGF- β and PI3K/AKT signaling pathways in triple-negative breast cancer cells. *Journal of Agricultural and Food Chemistry*. 2013;61(48):11817-24.
173. De Lange J, Schipper N, Schuurhuis G, Ten Kate T, Van Heijningen TH, Pinedo H, Lankelma J, Baak J. Quantification by laser scan microscopy of intracellular doxorubicin distribution. *Cytometry: The Journal of the International Society for Analytical Cytology*. 1992;13(6):571-6.
174. Elmore S. Apoptosis: a review of programmed cell death. *Toxicologic Pathology*. 2007;35(4):495-516.
175. Schwede M, Richter O, Alef M, Theuß T, Loderstedt S. Vascular surgery of aortic thrombosis in a dog using Fogarty maneuver–technical feasibility. *Clinical Case Reports*. 2018;6(1):214-9.
176. Alves AC, Magarkar A, Horta M, Lima JL, Bunker A, Nunes C, Reis S. Influence of doxorubicin on model cell membrane properties: insights from in vitro and in silico studies. *Scientific Reports*. 2017;7(1):6343.
177. He J, Liang X, Luo F, Chen X, Xu X, Wang F, Zhang Z. P53 is involved in a three-dimensional architecture-mediated decrease in chemosensitivity in colon cancer. *Journal of Cancer*. 2016;7(8):900-9.
178. Lowe SW, Lin AW. Apoptosis in cancer. *Carcinogenesis*. 2000;21(3):485-95.
179. Arima Y, Hirota T, Bronner C, Mousli M, Fujiwara T, Niwa Si, Ishikawa H, Saya H. Down - regulation of nuclear protein ICBP90 by p53/p21Cip1/WAF1 - dependent DNA - damage checkpoint signals contributes to cell cycle arrest at G1/S transition. *Genes to Cells*. 2004;9(2):131-42.
180. Attardi LD, de Vries A, Jacks T. Activation of the p53-dependent G1 checkpoint response in mouse embryo fibroblasts depends on the specific DNA damage inducer. *Oncogene*. 2004;23(4):973-80.
181. Venkatakrisnan C, Dunsmore K, Wong H, Roy S, Sen CK, Wani A, Zweier JL, Ilangovan G. HSP27 regulates p53 transcriptional activity in doxorubicin-treated fibroblasts and cardiac H9c2 cells: p21 upregulation and G2/M phase cell cycle arrest. *American Journal of Physiology-Heart and Circulatory Physiology*. 2008;294(4):H1736-H44.
182. Schuler M, Bossy-Wetzel E, Goldstein JC, Fitzgerald P, Green DR. p53 induces apoptosis by caspase activation through mitochondrial cytochrome c release. *Journal of Biological Chemistry*. 2000;275(10):7337-42.
183. Hartwell LH, Weinert TA. Checkpoints: controls that ensure the order of cell cycle events. *Science*. 1989;246(4930):629-34.
184. Hartwell LH, Kastan MB. Cell cycle control and cancer. *Science*.

- 1994;266(5192):1821-8.
185. Harper JW, Adami GR, Wei N, Keyomarsi K, Elledge SJ. The p21 Cdk-interacting protein Cip1 is a potent inhibitor of G1 cyclin-dependent kinases. *Cell*. 1993;75(4):805-16.
186. Xiong Y, Hannon GJ, Zhang H, Casso D, Kobayashi R, Beach D. p21 is a universal inhibitor of cyclin kinases. *Nature*. 1993;366(6456):701-14.
187. Gu Y, Turck CW, Morgan DO. Inhibition of CDK2 activity in vivo by an associated 20K regulatory subunit. *Nature*. 1993;366(6456):707-10.
188. Pellegata NS, Antoniono RJ, Redpath JL, Stanbridge EJ. DNA damage and p53-mediated cell cycle arrest: a reevaluation. *Proceedings of the National Academy of Sciences*. 1996;93(26):15209-14.
189. Asher G, Lotem J, Kama R, Sachs L, Shaul Y. NQO1 stabilizes p53 through a distinct pathway. *Proceedings of the National Academy of Sciences*. 2002;99(5):3099-104.
190. Benetti R, Del Sal G, Monte M, Paroni G, Brancolini C, Schneider C. The death substrate Gas2 binds m-calpain and increases susceptibility to p53-dependent apoptosis. *The EMBO Journal*. 2001;20(11):2702-14.
191. Fuchs SY, Adler V, Buschmann T, Yin Z, Wu X, Jones SN, Ronai Ze. JNK targets p53 ubiquitination and degradation in nonstressed cells. *Genes & Development*. 1998;12(17):2658-63.
192. Kubbutat M, Vousden KH. Proteolytic cleavage of human p53 by calpain: a potential regulator of protein stability. *Molecular and Cellular Biology*. 1997;17(1):460-8.
193. Vazquez A, Bond EE, Levine AJ, Bond GL. The genetics of the p53 pathway, apoptosis and cancer therapy. *Nature Reviews Drug Discovery*. 2008;7(12):979-87.

Appendix I: Ethical approvals

The Research Ethics Committee, Faculty Health Sciences, University of Pretoria complies with ICH-GCP guidelines and has US Federal wide Assurance.

- FWA 00002567, Approved dd 22 May 2002 and Expires 03/20/2022.
- IRB 0000 2235 IORG0001762 Approved dd 22/04/2014 and Expires 03/14/2020.



UNIVERSITEIT VAN PRETORIA
UNIVERSITY OF PRETORIA
YUNIBESITHI YA PRETORIA

Faculty of Health Sciences Research Ethics Committee

1/06/2017

Approval Certificate New Application

Ethics Reference No.: 214/2017

Title: Comparative analysis of a two-dimensional and three-dimensional model of BT-20 triple negative breast carcinoma cells in response to an antiproliferative agent

Dear Mr Jie Wang

The **New Application** as supported by documents specified in your cover letter dated 22/05/2017 for your research received on the 22/05/2017, was approved by the Faculty of Health Sciences Research Ethics Committee on its quorate meeting of 31/05/2017.

Please note the following about your ethics approval:

- Ethics Approval is valid for 1 year
- Please remember to use your protocol number (**214/2017**) on any documents or correspondence with the Research Ethics Committee regarding your research.
- Please note that the Research Ethics Committee may ask further questions, seek additional information, require further modification, or monitor the conduct of your research.

Ethics approval is subject to the following:

- The ethics approval is conditional on the receipt of **6 monthly written Progress Reports**, and
- The ethics approval is conditional on the research being conducted as stipulated by the details of all documents submitted to the Committee. In the event that a further need arises to change who the investigators are, the methods or any other aspect, such changes must be submitted as an Amendment for approval by the Committee.

We wish you the best with your research.

Yours sincerely

Dr R Sommers; MBChB; MMed (Int); MPharMed, PhD

Deputy Chairperson of the Faculty of Health Sciences Research Ethics Committee, University of Pretoria

The Faculty of Health Sciences Research Ethics Committee complies with the SA National Act 61 of 2003 as it pertains to health research and the United States Code of Federal Regulations Title 45 and 46. This committee abides by the ethical norms and principles for research, established by the Declaration of Helsinki, the South African Medical Research Council Guidelines as well as the Guidelines for Ethical Research: Principles Structures and Processes, Second Edition 2015 (Department of Health).

☎ 012 356 3084 ✉ deepeka.behari@up.ac.za / fhsethics@up.ac.za 🌐 <http://www.up.ac.za/healthethics>
✉ Private Bag X323, Arcadia, 0007 - Tswelopele Building, Level 4, Room 60, Gezina, Pretoria



UNIVERSITEIT VAN PRETORIA
UNIVERSITY OF PRETORIA
YUNIBESITHI YA PRETORIA

Faculty of Health Sciences

DATE: 13/09/2018

Mr Jie Wang
Department of Pharmacology
University of Pretoria

Dear Mr Jie Wang

RE.: 214/2017 ~ Letter dated 7 August 2018

214/2017 Wang	
Protocol Title	Comparative analysis of a two-dimensional and three-dimensional model of BT-20 triple negative breast carcinoma cells in response to an antiproliferative agent
Principal Investigator	Mr Jie Wang, Tel: 0768056296 Email: wangjiegideon@gmail.com Dept: Pharmacology

We hereby acknowledge receipt of the following document:

- Renewal of ethics approval of study granted for 1 year until end of 12 September 2019.

which has been approved at 12 September 2018 meeting.

With regards

Dr R Sommers; MBChB; MMed (Int); MPharMed; PhD
Deputy Chairperson of the Faculty of Health Sciences Research Ethics Committee, University of Pretoria

Research Ethics Committee
Room 4-59, Level 4, Tswelopele Building
University of Pretoria, Private Bag X323
Arcadia 0007, South Africa
Tel +27 (0)12 356 3085
Email manda.smith@up.ac.za
www.up.ac.za

Fakulteit Gesondheidswetenskappe
Lefapha la Disaense tša Maphele

Appendix II: Reagent preparation

Acetic acid

Glacial acetic acid was purchased from Merck Chemicals (South Africa) and used undiluted. A 1% v/v acetic acid solution was prepared by diluting 1 mL acetic acid per 99 mL distilled water. The solution was stored at room temperature.

Agarose

Agarose (low electroendosmosis and low melting) was purchased from Sigma-Aldrich (St. Louis, USA) as a purified powder and stored at room temperature. A 1% solution was made by diluting 1 g per 100 mL DMEM and Ham F12 (1:1) mixture.

Anti-p53 antibody

Mouse anti-p53 (100 μ L) antibody, which was monoclonal, was purchased from Celtic Diagnostics (South Africa), and was stored at -20°C . The antibody was diluted in blocking buffer (see Bovine serum albumin) at 1:1000.

Anti-mouse secondary antibody

Goat anti-mouse antibody (0.5 mL) conjugated to horseradish peroxidase was purchased from Celtic Diagnostics (South Africa). The antibody was dissolved in 2 mL distilled water and stored at 4°C . The antibody was further diluted in blocking buffer at 1:5000 prior to experimentation.

Bicinchoninic acid reagent

Sodium bicarbonate, sodium bicinchoninate, sodium carbonate decahydrate, sodium hydroxide, sodium tartrate dehydrate and copper sulfate pentahydrate were purchased from Merck Chemicals (South Africa). Reagent A was prepared by dissolving 475 mg sodium bicarbonate, 500 mg sodium bicinchoninate, 1 g sodium carbonate decahydrate, 200 mg sodium hydroxide and 80 mg sodium tartrate dehydrate per 50 mL distilled water, and adjusting the pH to 11.25 using sodium hydroxide. Reagent B was prepared by dissolving 1.2 mg copper sulfate pentahydrate in 3 mL distilled water. Both solutions were stored at 4°C . A working dilution was prepared by mixing both reagents at 1:50.

Blocking buffer

Blocking buffer was prepared by dissolving 3 g BSA in 100 TBST solution, which

was stored at 4 °C for one week.

Bovine serum albumin

Bovine serum albumin was purchased from Sigma-Aldrich (St. Louis, USA) as a lyophilized powder and stored at 4 °C. A 2 mg/mL working dilution was prepared by dissolving 2 mg per 1 mL PBS to use as the protein concentration standard in the BCA assay.

A 3% blocking buffer (for Western blot analysis) was prepared by dissolving 3 g BSA per 100 mL Tris-buffered saline buffer.

Dimethyl sulfoxide (DMSO)

Dimethyl sulfoxide was purchased from Merck Chemicals (South Africa) and used undiluted.

Dulbecco's Modified Eagle Medium (DMEM)

Powdered DMEM was purchased from Sigma-Aldrich (St. Louis, USA). A 1.04% solution was prepared in autoclaved, ultra-pure, pyrogen-free, deionized water and adjusted to pH 7.4 using sodium hydrogen carbonate obtained from Merck Chemicals (Darmstadt, Germany) in powder form. The solution was filtered *in vacuo* thrice (Sartorius, 0.22 µm), and supplemented with 1% penicillin/streptomycin. Medium was stored at 4 °C.

Doxorubicin

Doxorubicin was purchased from Sigma-Aldrich (St. Louis, USA) as a powder. A 10 mM stock solution was prepared by dissolving 5.44 mg in 1 mL DMSO. Aliquots (4 µL) of the stock solution was stored at -80 °C.

Enhanced chemiluminescence (ECL) mix

Clarity™ Western ECL substrate mix was purchased from Bio-Rad (California, USA) and contained two prepared solutions. The working dilution was prepared prior to the assay by mixing solution A and B at a ratio of 1:1. Solution A consisted of 250 mM luminol, 90 mM p-coumaric acid and 100 mM Tris (pH 8.6), while solution B consisted of 30% v/v hydrogen peroxide and 100 mM Tris (pH 8.6). Both solutions were stored at room temperature.

Ethanol solution

Ethanol was purchased from Merck Chemicals (South Africa) and used diluted. A 70% v/v solution was prepared by mixing 70 mL ethanol with distilled water up to 100 mL. The solution was stored at room temperature.

Fluorescein diacetate solution

Fluorescein diacetate solution was purchased from Sigma-Aldrich (St. Louis, USA) as a powder. 1 mL solution was prepared by dissolving 4 µg FDA fluorescein diacetate in 1 mL acetone. The solution was stored at 4 °C.

Foetal calf serum (FCS)

Foetal calf serum was purchased from The Scientific Group (Gauteng, RSA) and stored at 4 °C. The solution was used undiluted.

Ham's F12 nutrient medium

Ham's F12 medium was purchased from Sigma Aldrich (St Louis, USA) in powder form. A 0.96% solution was prepared in autoclaved, ultra-pure, pyrogen-free, deionized water and adjusted to pH 7.4 using sodium hydrogen carbonate obtained from Merck Chemicals (Darmstadt, Germany) in powder form. The solution was filtered *in vacuo* thrice (Sartorius, 0.22 µm), and supplemented with 1% penicillin/streptomycin. Medium was stored at 4 °C.

Laemmli buffer

A concentrated Laemmli buffer (2X) was purchased from Bio-Rad (California, USA) and contained 2.1% sodium dodecyl sulfate, 26.3% (w/v) glycerol, 0.01% bromphenol blue and 65.8 mM Tris hydrochloride (pH 6.8). The solution was stored at room temperature.

Phosphate buffered saline (PBS)

Phosphate-buffered saline was obtained from BD Biosciences (France) as FTA haemagglutination powder. A 0.923% w/v solution was prepared by dissolving 9.23 g per 1 L. The solution was stored at 4 °C.

Propidium iodide solution

Propidium iodide was purchased from Sigma Aldrich (St Louis, USA) as a powder. For live-dead staining, a 2 mg/mL stock solution was made by dissolving 2 mg PI in 1 mL distilled water.

The PI staining solution used for determining cellular kinetics was prepared by dissolving 4 mg propidium iodide, 10 mg DNA-free RNase and 100 µL Triton X-100 per 100 mL distilled water. Triton X-100 and DNA-free RNase were purchased from Sigma-Aldrich (St Louis, USA). DNA-free RNase was added prior to experimentation. The solutions were stored at 4°C.

Radio-immunoprecipitation assay (RIPA) buffer

Sodium chloride, sodium deoxycholate, sodium dodecyl sulfate (SDS) and Tris-base were purchased from Merck Chemicals (South Africa). Triton X-100 and the protease inhibitor cocktail were purchased from Sigma-Aldrich (St. Louis, USA). A solution of 150 mM sodium chloride, 1% (v/v) Triton X-100, 0.5 (w/v) sodium deoxycholate, 0.1% (w/v) SDS and 50 mM Tris-base was prepared by dissolving 438.3 mg sodium chloride, 0.5 mL Triton X-100, 250 mg sodium deoxycholate, 50 mg SDS and 302.9 mg Tris-base in 45.5 mL distilled water. The pH was adjusted to 8 using sodium hydroxide and hydrochloric acid. The solution was stored at 4 °C. The protease inhibitor cocktail was added at a ratio of 1:10.

Resazurin

Resazurin was purchased from Sigma-Aldrich (St. Louis, USA). A 10 mM resazurin solution was prepared by dissolving 2.99 mg in 1 mL DMSO. Aliquots (20 µL) were stored at -80 °C.

10x Running buffer

Running buffer was purchased from Bio-Rad (California, USA) and contained 25 mM Tris-base, 190 mM glycine and 0.1% (w/v) sodium dodecyl sulfate. The pH was checked and adjusted to 8.3 if necessary. To make 1 L of working buffer, 100 mL buffer was added to 900 mL deionized water and mixed thoroughly. The buffer was stored at room temperature.

Sulforhodamine B solution

Sulforhodamine B was purchased from Sigma-Aldrich (St. Louis, USA). A 0.057% solution was prepared by dissolving 57 mg per 100 mL aqueous acetic acid (1%). The solution was stored at 4°C.

Trichloroacetic acid (TCA)

Trichloroacetic acid was purchased from Merck Chemicals (South Africa). A 50% (w/v) solution was prepared by dissolving 50 g crystals per 100 mL distilled water, and stored at 4 °C.

Tris-base buffer

Tris-base powder was purchased from Sigma-Aldrich (St. Louis, USA). A 10 mM solution was prepared by dissolving 121.1 mg per 100 mL distilled water. The pH was adjusted to 10.5 using sodium hydroxide.

10x Tris-buffered saline (TBS)

A Tris-buffered saline (TBS) solution was prepared by dissolving 24 g Tris-hydrochloride, 5.6 g Tris-base and 88 g sodium chloride per 900 mL distilled water. The solution was adjusted pH 7.6 using hydrochloric acid. The solution was stored at room temperature.

Trypsin/Versene

Trypsin/Versene solution was purchased from The Scientific Group (Gauteng, RSA) and used undiluted. The solution was stored at 4 °C.